

T H E U N I V E R S I T Y O F M I C H I G A N
COLLEGE OF ENGINEERING
Department of Mechanical Engineering
Heat Transfer Laboratory

Technical Report No. 4

FINITE DIFFERENCE SOLUTION OF STRATIFICATION
AND PRESSURE RISE IN CONTAINERS

Herman Merte, Jr.
John A. Clark
Hussein Z. Barakat

ORA Project 07461

under contract with:

NATIONAL AERONAUTICS AND SPACE ADMINISTRATION
GEORGE C. MARSHALL SPACE FLIGHT CENTER
CONTRACT NO. Nas-8-20228
HUNTSVILLE, ALABAMA

administered through:

OFFICE OF RESEARCH ADMINISTRATION ANN ARBOR

January 1968

TABLE OF CONTENTS

	Page
LIST OF FIGURES	v
NOMENCLATURE	vi
ABSTRACT	ix
I. INTRODUCTION	1
II. FORMULATION	5
A. LIQUID REGION	8
B. VAPOR REGION	10
C. LIQUID-VAPOR COUPLING AT INTERFACE	13
D. SUMMARY OF FORMULATION	14
III. TRANSFORMATION OF THE PARTIAL DIFFERENTIAL EQUATIONS	16
A. LIQUID REGION	16
B. VAPOR REGION	17
IV. DIMENSIONLESS FORM OF THE EQUATIONS	25
A. WALL TEMPERATURE	25
B. LIQUID REGION	26
C. VAPOR REGION	28
V. METHOD OF SOLUTION	30
A. FINITE-DIFFERENCE FORMS	30
B. STABILITY OF FINITE-DIFFERENCE EQUATIONS	32
C. COMPUTATIONAL PROCEDURES	33
D. COMPUTER PROGRAM	39
VI. COMPUTATIONS	41
A. GENERAL ASSUMPTIONS	41
B. VARIATIONS POSSIBLE IN PROGRAM	41
C. VARIABLES	42
D. RESULTS	43
APPENDIX A. COMPUTER PROGRAM LISTING	59
APPENDIX B. FLOW CHART	71
APPENDIX C. PROGRAM NOTATION AND NOMENCLATURE	73

TABLE OF CONTENTS (Concluded)

	Page
APPENDIX D. DATA INPUTS	83
APPENDIX E. TYPICAL OUTPUT	85
REFERENCES	97

LIST OF FIGURES

Figure	Page
1. Container configuration and coordinate system.	6
2. Container wall section.	7
3. Control volume of vapor region.	21
4. Effect of grid size on computed interfacial velocity.	35
5. Effect of grid size on computed condensed mass.	36
6. Effect of grid size on computed temperature distribution.	37
7. Total mass evaporated and pressure rise under high heat flux.	44
8. Total mass evaporated and pressure rise under low heat flux.	45
9. Effect of heat flux on pressure rise and mass evaporated.	46
10. Effect of heat flux on pressure rise.	47
11. Effect of initial ullage on pressure rise and mass evaporated.	49
12. Effect of initial ullage on pressure rise and mass evaporated.	50
13. Effect of acceleration on pressure rise and mass evaporated.	51
14. Axial temperature distribution.	52

NOMENCLATURE

- A - Area, Ft²
- a - Cylindrical tank radius, Ft, Acceleration, Ft/Sec²
- b - Total tank height, Ft
- C_p, C_v - Specific heats BTU/LB_m-°F
- $\frac{Df}{Dt}$ - Substantial derivative of function f
- e - Specific internal energy, BTU/Lb_m
- E - Total internal energy, BTU
- g - Acceleration due to local gravity, Ft/Sec²
- h - Heat transfer coefficient, BTU/HR-Ft²-°F, Enthalpy, BTU/Lb_m
- h_{fg} - Latent heat, BTU/Lb_m
- k - Thermal conductivity, BTU/HR-Ft-°F
- P - Pressure, psia
- q - Heat flux, BTU/HR-Ft²
- r - Radial coordinate direction, Ft
- R - Gas constant, $\frac{Lb_f}{Lb_m} \cdot \frac{Ft}{°R}$
- t - Time, Hour
- T - Temperature, °F, °R
- $\Delta T_w = T_w - T_{sat}$, °F
- ΔT_{wmax} - Specified maximum value of ΔT_w , °F
- u - Axial component of velocity, Ft/Sec
- U - Dimensionless Axial velocity - Eq. (85)
- v - Radial component of velocity, Ft/Sec

NOMENCLATURE (Continued)

V - Volume, Ft³; Dimensionless radial velocity - Eq. (85)

w - Mass flow rate, Lb_m/Sec

x - Axial coordinate direction, Ft.

X - Liquid height in container, Ft

Δx - Finite-difference grid spacing, Ft

Z - Compressibility factor, [1]

Greek Letters

α - Thermal diffusivity, Ft²/Hour

β - Coefficient of thermal expansion, °F⁻¹

γ - Ratio of specific heats C_p/C_v, [1]

δ - Tank wall thickness, Ft

η - Dimensionless radius, [1] - Eq. (85)

θ - Dimensionless temperature - Eq. (85)

ζ - Dimensionless axial distance, [1] - Eq. (85)

ψ - Dimensionless stream function - Eq. (85)

ψ', ψ'' - Liquid and vapor stream functions, Equations (50) and (56) [1]

τ - Dimensionless time - Eq. (85)

μ - Kinematic viscosity, Ft²/Hour

ν - Dynamic viscosity, Lb_m/Ft-Hour

ρ - Density, Lb_m/Ft³

ω' - Vorticity, Equation (49) [Ft-Sec]⁻¹

ω - Dimensionless vorticity - Eq. (85)

NOMENCLATURE (Concluded)

Subscripts

d - discharge

f - liquid or fluid

g - gas or vapor

i - liquid-vapor interface

l - liquid

o - initial state

p - pressurization

r - reduced

s - saturation

w - wall

ABSTRACT

The processes of heat and mass transfer interactions between the gas and liquid phases of a single component in cylindrical containers with axial symmetry are considered. In the general formulation attention is given to the cases of external pressurization with and without liquid discharge as well as to the nonvented condition. The governing equations are cast into finite-difference form and numerical computations are carried out for the case of a non-vented container having an imposed head flux, using ideal gas relations for the vapor properties. Of specific interest is the calculation of the pressure-time history of the container under these conditions.

I. INTRODUCTION

A number of space missions of current interest will require the storage of liquid propellants for long periods of time, varying from hours to months. The ultimate goal is to maximize the quantity of useful propellant remaining at the end of this period of time. In the limit this maximum corresponds to the non-vented condition in which the original mass of propellant is retained. Whether or not non-venting is practical depends on the maximum internal pressure which results as a consequence of the thermal interaction between the storage container and its ambient.

Higher pressures require increased structural weight of the container, and a trade-off may become necessary between tank weight and propellant loss due to venting in order to maximize the mass of propellant remaining. Each case must be evaluated for the specific mission, storage time, environment and propellant. An additional factor is the method of discharge from the tank. Where the propellant discharges to the suction of a pump, some degree of sub-cooling is necessary to avoid cavitation and, depending on the fluid, may require additional external pressurization just prior to discharge. The pressure at which venting might take place would thus be less than the tank design pressure.

The pressure in a tank containing two phase, liquid and vapor, is related directly to the temperature at the liquid-vapor interface for a single component system. For a binary system, the pressure depends not only on the temperature at the interface but the relative liquid-vapor concentration of the two components as well. Pressure changes take place owing to heat and mass transfer interactions between the vapor, liquid and container walls.

The processes of heat and mass transfer interactions between the gas and liquid phases of a single component in cylindrical containers with axial symmetry are considered in this study. In the general formulation presented first attention is given to the cases of external pressurization with and without liquid discharge as well as to the non-vented case. Solutions are then presented, utilizing numerical finite-difference procedures for the non-vented case.

The initial conditions of the liquid and vapor are considered to be those at equilibrium, with uniform pressure P_0 and saturation temperature T_0 . From these initial conditions, the walls of the container undergo a thermal perturbation, such as a change in temperature or an exposure to an external heat flux, either of which may be an arbitrary function of time and axial location. The perturbations in the boundary conditions lead to a series of non-equilibrium phenomena within the container. Natural convection currents are set up in the liquid and in the vapor spaces. The liquid-vapor system

tends to adjust to the new non-equilibrium conditions within the container by transferring mass and energy across the interface by either evaporation or condensation. The conditions at the liquid-vapor interface couple simultaneous transport processes in the liquid and gas phases. In the case of self-pressurization of non-vented tanks the rate of pressure rise within the tank is governed by the rate of heat and mass transfer from the walls and the liquid phase to the gas phase. The interfacial temperature is essentially that of equilibrium (saturation) conditions corresponding to the system pressure. At the same time, the temperature of the liquid-vapor interface affects both the interfacial mass and heat transfer, as well as the convective processes in both phases. These latter processes influence the temperature gradients within both phases and in turn will have an effect on the rate of pressure rise in the ullage space. Indeed, all the processes of heat transfer from the ambient to both phases, the natural convection within the container, the interfacial phenomena and the rate of ullage pressure rise are all mutually coupled. Such interactions have been the subject of many experimental investigations.

Any analytical approach that would adequately describe the phenomena taking place in propellant tanks must take into account these interactions. This requires the calculation of the transient velocity and temperature profiles in both the gas and liquid phases, as well as the corresponding concentration distributions in the case of multicomponent systems. Owing to the complexity of these phenomena, no analytical studies have been presented which consider their simultaneous interaction. The problem may be complicated further with the presence of turbulence or boiling of the liquid near the tank walls, as their nature is not yet fully understood nor adequately described. It is evident that some assumptions are necessary for the construction of models which reasonably represent the practical situations.

A review which covered much of the available literature on pressurization, stratification and interfacial phenomena in propellant tanks is given in Ref. (1). Therefore no further survey of the literature will be presented here. However, several studies which are pertinent to the present one will be mentioned. Thomas and Morse (2) and Knuth (3) have considered the phase change of suddenly pressurized single-component liquid-vapor system. Yang, *et al.*, (4,5,6), have solved the phase change in a suddenly pressurized single-component and binary liquid-vapor system. The model adopted in these cases was one-dimensional, with the origin of the x-axis at the initial position of the liquid vapor interface. Initially, the gas and the liquid regions are at the same temperature T_0 . The conditions in the gas space are suddenly changed to a pressure P_∞ and temperature T_∞ . The differential equations describing the temperature and velocity transients in both phases are:

$$\frac{\partial T_g}{\partial t} + u \frac{\partial T_g}{\partial x} = \alpha_g \frac{\partial^2 T_g}{\partial x^2} \quad (1)$$

$$\frac{\partial T_l}{\partial t} = \alpha_l \frac{\partial^2 T_l}{\partial x^2} \quad (2)$$

These are coupled at the interface by the condition

$$\rho_l h_{fg} u_i = k_l \frac{\partial T_l}{\partial x} - k_g \frac{\partial T_g}{\partial x} \quad (3)$$

Thermodynamic equilibrium is assumed at the interface, i.e., the interfacial temperature is always at the saturation temperature corresponding to the ullage pressure. Experience shows that this is a reasonable assumption (1). The details of the solution as well as the differential equations describing the concentration distribution for the binary case are given in Ref. (1).

The effect of the changes in the properties of the fluids with temperature on the accuracy of the results was investigated by O'Loughlin and Glenn (7). The same one-dimensional single component model was employed to study the case of interfacial phase change with variable ullage pressure. Finite-differences were used to solve Eqs. (1) through (3). The pressure in the ullage volume was either constant or a specified function of time. For the case in which the pressure decreases with time, the interfacial temperature also is reduced with time. In this case the liquid layers which may exist at a temperature higher than the interfacial temperature are made equal to the saturation temperature. The excess energy of this liquid over that of the saturated liquid is used to evaporate some liquid into the vapor region. Likewise any supersaturated vapor that may be present is allowed to condense a fraction of the vapor, thus providing the energy required to heat the supersaturated vapor to the saturation temperature. This supersaturation is a result of the expansion of the gas during the pressure decrease process, which is assumed to be isentropic. The results show that the variation in the thermal conductivity with temperature has very little effect. This one-dimensional model does not account for the effect of wall heat transfer.

Epstein, et al., (8), used finite-differences for the calculation of the pressurization process. In this model, the axial variation of temperature is considered while the radial variation is neglected. The wall to fluid heat transfer was accounted for by introducing an effective heat transfer coefficient between the fluid and the wall. Also, effective thermal conductivities and mass diffusivities between the adjacent fluid layers were used to simulate the effects of random fluid motion. Provisions for variable tank cross-section as well as variable heat transfer coefficients were made in the program. The effect of boiling near the walls was not considered, and momentum effects were neglected. The principal advantage of this program is its simplicity and the relatively small amount of machine time required to advance the solution to a particular time level. However, the determination of the effective thermal conductivities and heat transfer coefficients and their variation with location require the determination of a large number of empirical constants, which require considerable experimental experience with a particular system.

Although some analytical models have been used to study liquid stratification in self-pressurized propellant containers, none has considered the simultaneous interactions between the liquid and the vapor phases. Most of the available studies of the pressure and temperature transients in the vapor space are experimental in nature and have served to identify some factors influencing the rate of pressure rise within the containers. The studies of Huntley (9) show that liquid stratification causes the pressure to rise at a higher rate than that calculated using the average or mixed mean liquid temperature. These also showed that stirring the liquid causes a smaller rate of pressure rise, while stirring the vapor resulted in a substantial increase in pressure. Higher rates of pressure rise were obtained with smaller ullage volumes. Liebenberg and Edescuty have shown similar results (10).

II. FORMULATION

As mentioned earlier, the formulation of the most general case will be given first. This involves external pressurization, liquid discharge and the consideration of the vented and nonvented container. The heat capacity of the container side wall is also included in the formulation. The heat capacity of the end walls of the cylindrical container is neglected. The assumptions and limitations will be mentioned as appropriate and the results and problems encountered in the solution of the unvented, non-discharge case will be given.

A cylindrical container of diameter $2a$, height b and with wall thickness δ , is partially filled with a liquid as shown in Figure 1. The initial height of the liquid is X_0 , and that of the vapor is $b-X_0$. The origin of the coordinate system is taken at the center of the container base with x -positive in the direction of the liquid. At any time t , the location of the liquid-vapor interface is given by $X = X(t)$. The fluid in both phases is initially at rest in an equilibrium state at a uniform temperature T_0 and pressure P_0 . From these initial conditions the tank side walls are subjected to an arbitrary heat flux, $q_w(x,t)$. The tank ends are assumed adiabatic but this restriction can be removed if desired. The differential equation describing the temperature-time history of the tank wall obtained by lumping the wall radially, but not axially, is, Figure (2),

$$\begin{aligned}
 (\rho c_p \delta \frac{\partial T}{\partial t})_w &= -(k \frac{\partial T}{\partial r})_f + (\delta k \frac{\partial^2 T}{\partial x^2})_w \\
 &+ q_w(x,t), \tag{4}
 \end{aligned}$$

where the subscripts w and f refer to the wall and the fluid, respectively. The first term on the right-hand side of Eq. (4) is the rate of heat flow from the wall to the fluid, while the second term accounts for the net axial conduction. It is usual to calculate the heat flow from the wall to the liquid by introducing the heat transfer coefficient h according to;

$$(k \frac{\partial T}{\partial r})_f = h(T_w - T_f) . \tag{5}$$

However, the determination of the heat transfer coefficient for these cases is difficult and subject to many uncertainties. Furthermore, its a priori use in studies of this kind is not relevant. The numerical procedure used in this study allows the direct evaluation of the rate of heat flow from the wall to the liquid, thus making the use of a heat transfer coefficient unnecessary.

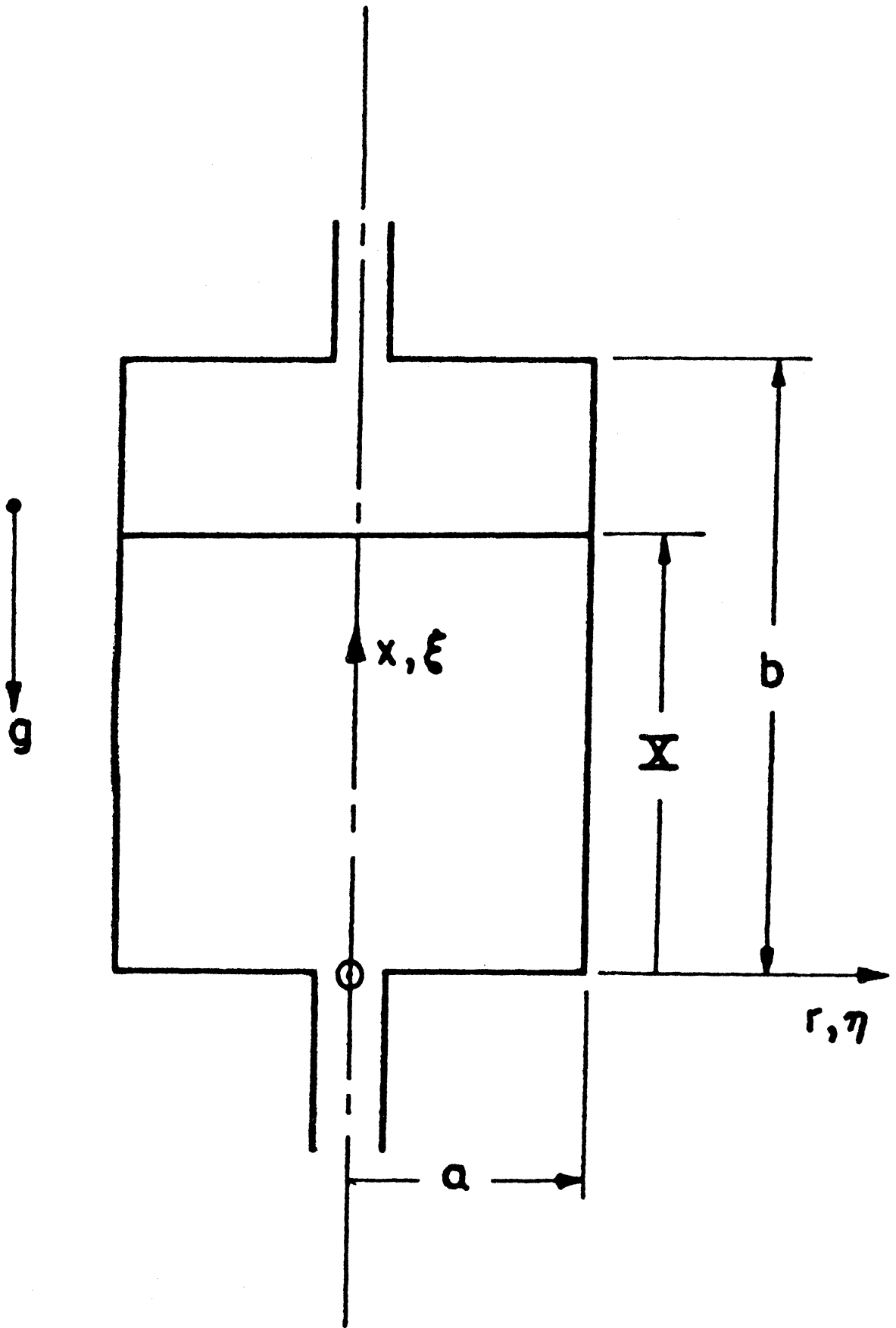


Figure 1. Container configuration and coordinate system.

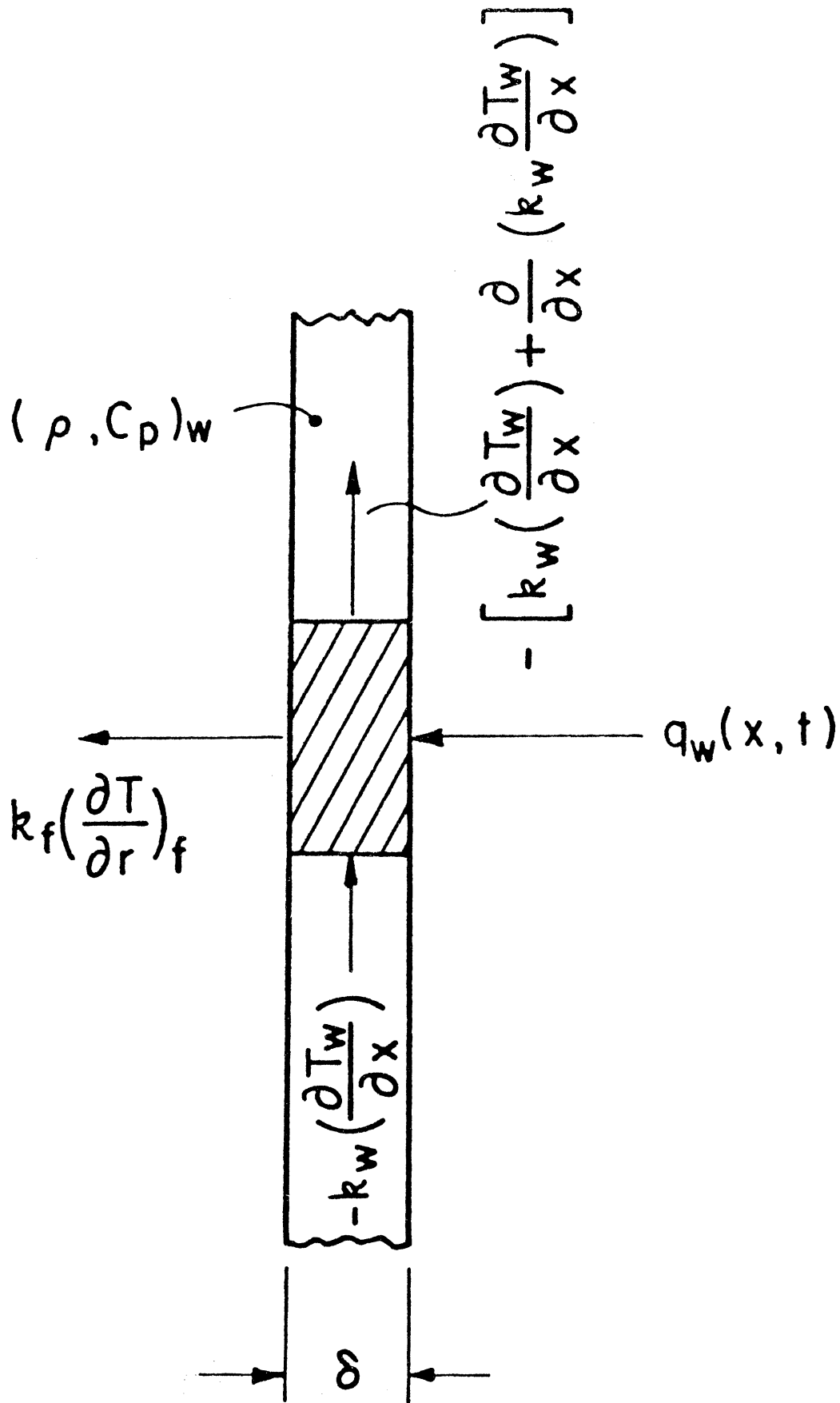


Figure 2. Container wall section.

A reversed process may be used, however, to determine a value for the heat transfer coefficient under these transient conditions. From the rate of heat flow from the wall to the fluid in the container as determined by Eq. (5), the transient heat transfer coefficient h may be computed. This procedure permits the determination of the variation of the heat transfer coefficient with time and space during this transient process.

The differential equations governing the velocity and temperature distribution in both phases are developed as follows.

A. LIQUID REGION

The following assumptions are made:

1. Constant thermal conductivity and viscosity.
2. Incompressible fluid. Density variations are introduced only in the body force term of the momentum equation. These variations are described by

$$\rho = \rho_0[1 + \beta(T_0 - T)] \quad (6)$$

3. The influence of viscous dissipation is neglected.

Governing Equations

(i) x-momentum

$$\rho \left(\frac{\partial u}{\partial t} + u \frac{\partial u}{\partial x} + v \frac{\partial u}{\partial r} \right) = -\rho g - \frac{\partial P}{\partial x} + \mu \left(\frac{\partial^2 u}{\partial x^2} + \frac{1}{r} \frac{\partial u}{\partial r} + \frac{\partial^2 u}{\partial r^2} \right) \quad (7)$$

(ii) radial momentum

$$\rho \left(\frac{\partial v}{\partial t} + u \frac{\partial v}{\partial x} + v \frac{\partial v}{\partial r} \right) = - \frac{\partial P}{\partial r} + \mu \left(\frac{\partial^2 v}{\partial x^2} - \frac{v}{r^2} + \frac{1}{r} \frac{\partial v}{\partial r} + \frac{\partial^2 v}{\partial r^2} \right) \quad (8)$$

(iii) continuity

$$\frac{\partial u}{\partial x} + \frac{\partial v}{\partial r} + \frac{v}{r} = 0 \quad (9)$$

(iv) energy

$$\frac{\partial T}{\partial t} + u \frac{\partial T}{\partial x} + v \frac{\partial T}{\partial r} = \alpha \left(\frac{\partial^2 T}{\partial x^2} + \frac{1}{r} \frac{\partial T}{\partial r} + \frac{\partial^2 T}{\partial r^2} \right) \quad (10)$$

Initial Conditions

$$T(x,r,0) = T_0, \quad u(x,r,0) = 0, \quad v(x,r,0) = 0 \quad (11)$$

Boundary Conditions

Velocity

$$u(0,r,t) = 0 \quad (12)$$

$$u(X_0,r,t) = - \frac{w_{ld}}{\rho_l \pi a^2} \quad (13)$$

where w_{ld} is the rate of liquid discharge.

$$u(x,a,t) = 0 \quad (14)$$

$$\frac{\partial u(x,0,t)}{\partial r} = 0 \quad (15)$$

$$v(x,a,t) = 0 \quad (16)$$

$$v(x,0,t) = 0 \quad (17)$$

$$v(0,r,t) = 0 \quad (18)$$

$$\frac{\partial v(X,r,t)}{\partial x} = 0 \quad (19)$$

Temperature

$$T(X,r,t) = T_s(t) \quad (20)$$

$$T(x,a,t) = T_w(x,t) \quad (21)$$

$$\frac{\partial T(o,r,t)}{\partial x} = 0 \quad (22)$$

$$\frac{\partial T(x,o,t)}{\partial r} = 0 \quad (23)$$

where $T_s(t)$ is the saturation temperature corresponding to the system pressure and T_w is the wall temperature, Eq. (4).

B. VAPOR REGION

The differential equations for the vapor region are obtained assuming negligible changes in the viscosity and thermal conductivity within the vapor phase. The compressibility of the vapor is considered.

Governing Equations

(i) x-momentum

$$\begin{aligned} \rho \left(\frac{\partial u}{\partial t} + u \frac{\partial u}{\partial x} + v \frac{\partial u}{\partial r} \right) &= -pg - \frac{\partial P}{\partial x} \\ &+ \mu \left(\frac{\partial^2 u}{\partial x^2} + \frac{1}{r} \frac{\partial u}{\partial r} + \frac{\partial^2 u}{\partial r^2} \right) \\ &+ \frac{1}{3} \mu \frac{\partial}{\partial x} \left(\frac{\partial u}{\partial x} + \frac{\partial v}{\partial r} + \frac{v}{r} \right) \end{aligned} \quad (24)$$

(ii) radial momentum

$$\begin{aligned} \rho \left(\frac{\partial v}{\partial t} + u \frac{\partial v}{\partial x} + v \frac{\partial v}{\partial r} \right) &= - \frac{\partial P}{\partial r} \\ &+ \mu \left(\frac{\partial^2 v}{\partial x^2} - \frac{v}{r^2} + \frac{1}{r} \frac{\partial v}{\partial r} + \frac{\partial^2 v}{\partial r^2} \right) + \frac{1}{3} \mu \frac{\partial}{\partial r} \left(\frac{\partial u}{\partial x} + \frac{\partial v}{\partial r} + \frac{v}{r} \right) \end{aligned} \quad (25)$$

(iii) continuity

$$\frac{D\rho}{Dt} + \rho \left(\frac{\partial u}{\partial x} + \frac{\partial v}{\partial r} + \frac{v}{r} \right) = 0, \quad (26)$$

(iv) energy

$$\begin{aligned} \rho c_v \left(\frac{\partial T}{\partial t} + u \frac{\partial T}{\partial x} + v \frac{\partial T}{\partial r} \right) + \rho \frac{D(P/\rho)}{Dt} \\ = \frac{DP}{Dt} + k \left(\frac{\partial^2 T}{\partial x^2} + \frac{1}{r} \frac{\partial T}{\partial r} \frac{\partial^2 T}{\partial r^2} \right). \end{aligned} \quad (27)$$

(v) equation of state

$$P = z\rho RT \quad (28)$$

where z is the compressibility factor which can be evaluated from P , V , T , data or by using an equation of state which accounts for real gas effects. Using the Van der Waal equation of state the following equation relating z to the reduced pressure and temperature is obtained.

$$z^3 - \left(\frac{Pr}{8Tr} + 1 \right) z^2 + \frac{27}{64} \frac{Pr}{Tr^2} z - \frac{27}{512} \frac{Pr^2}{Tr^3} = 0, \quad (29)$$

where P_r and T_r are the reduced pressure and temperature, respectively.

The value of z obtained from Eq. (29) is quite accurate for engineering applications (11). Other equations describing z or tabulated values of z can also be employed. However, calculation of z using an equation of the form of (29) offers less difficulties from the programming standpoint.

Initial Conditions

$$\begin{aligned} T(x,r,0) &= T_0 \\ \rho(x,r,0) &= \rho_0 \\ u(x,r,0) &= 0 \\ v(x,r,0) &= 0 \end{aligned} \quad (30)$$

Boundary Conditions

Velocity

$$u(b,r,t) = 0 \quad (31-a)$$

or

$$u(b,r,t) = u_{gp} = - \frac{w_{gp}}{\rho_{gp} \pi a^2} , \quad \chi \quad (31-b)$$

where w_{gp} is the rate of mass flow of the pressurant and ρ_{gp} is its density. Equation (31-b) is written for the case of uniform velocity at the inlet diffuser of the tank as in Fig. 3.

$$u(X_0,r,t) = u_{gi} \quad (32)$$

$$\frac{\partial u(x,0,t)}{\partial r} = 0 \quad (33)$$

$$u(x,a,t) = 0 \quad (34)$$

$$v(b,r,t) = 0 \quad (35)$$

$$v(x,a,t) = 0 \quad (36)$$

$$u(x,0,t) = 0 \quad (37)$$

$$\frac{\partial v(X,r,t)}{\partial x} = 0 \quad (38)$$

where u_{gi} is the velocity of the vapor at the interface caused by simultaneous phase change and liquid discharge, Eq. (47). The boundary conditions given by Eqs. (19) and (38) assume a zero shear stress in both the liquid and vapor at the interface. These are reasonable and are made for the sake of simplification. Another approximation would be to take the vapor velocity at the interface equal to that of the liquid at that point. The interfacial shear stress would then be determined by the analysis. For flows with large radial gas velocities at the interface, this latter boundary condition becomes more realistic.

Temperature

$$T(X,r,t) = T_s(t) \quad (39)$$

$$T(x,a,t) = T_w(x,t) \quad (40)$$

$$\frac{\partial T(x,o,t)}{\partial r} = 0 \quad (41)$$

$$\frac{\partial T(b,r,t)}{\partial x} = 0 \quad (42-a)$$

or

$$T(b,r,t) = T_{gp}(r,t) \quad (42-b) \quad \times$$

Equation (42-a) applies for the case with no external pressurization, and Eq. (42-b) for arbitrary external pressurization.

C. LIQUID-VAPOR COUPLING AT INTERFACE

The processes in the liquid and vapor regions are coupled by T_s in Eqs. (20) and (39) and by u_{gi} in Eq. (32), which is related to the rate of mass transfer at the interface.

The rate of mass transfer by evaporation or condensation across the liquid-vapor interface depends on the relative rates of heat transfer by diffusion from each phase at the interphase. Conservation of energy at the interface determines the rate of phase change as well as the interfacial displacement, according to;

$$h_{fg}w_i = \int_0^a \left\{ \left[k \frac{\partial T(X,r,t)}{\partial x} \right]_l - \left[k \frac{\partial T(X,r,t)}{\partial x} \right]_v \right\} 2\pi r dr, \quad (43)$$

where w_i is the rate of interfacial phase change. According to Eq. (43), w_i will be positive if condensation takes place. The interfacial displacement with no liquid discharge is then given by:

$$\rho_l \pi a^2 \frac{dX_i}{dt} = w_i \quad (44)$$

Should it be desirable to include the process of liquid discharge, Eq. (44) would be written

$$\rho_l \pi a^2 \frac{dX_d}{dt} = -w_d \quad (45)$$

and

$$u_i = \frac{dX}{dt} = \frac{dX_i}{dt} + \frac{dX_d}{dt} \quad (46)$$

where

$\frac{dX_i}{dt}$ = rate of interfacial displacement due to phase change,

$\frac{dX_d}{dt}$ = rate of interfacial displacement due to liquid discharge,

$\frac{dX}{dt}$ = combined rate of interfacial displacement due to phase change and liquid discharge.

Equation (46) is obtained assuming that the liquid surface remains flat during the discharge process. This is an approximation which neglects the influence of viscosity near the walls and surface tension effects. Such effects are negligible except for very low gravity levels and small Bond numbers.

The vapor velocity u_{gi} at the interface is related to the rate of interfacial displacement due to phase change and discharge by,

$$u_{gi} = -\left(\frac{\rho_l - \rho_{gs}}{\rho_{gs}}\right) \frac{dX_i}{dt} + \frac{dX_d}{dt} \quad (47)$$

D. SUMMARY OF FORMULATION

Taking a broad perspective of the foregoing formulation the following observations might be made. For convenience the liquid and vapor regions are considered separately, recognizing that they are coupled at the liquid-vapor interface.

1. Liquid Region

Four unknowns exist: u, v, T, P , each of which are functions of x, r, t . The four Eqs. (7)-(10), together with the boundary conditions, are available for the solution of these unknowns. The solution of this system of equations

by finite-difference procedures has been attempted with no success. The reason for this is believed due to the extremely small variations in pressure within the domain, $P(x,r,t)$, compared to the level of pressure. With the assumption of an incompressible fluid (except for changes in density due to temperatures in the body force term of the momentum equation) the pressure terms occur only in the x-and r-momentum equations. The pressure distribution is not of particular interest except that it is a factor in the fluid motion. This motion is influenced by the system pressure level only indirectly in that it establishes the temperature boundary condition at the liquid-vapor interface.

It is, however, possible to eliminate the pressure term by cross-differentiating and combining the two momentum equations. Introducing the definitions of vorticity and stream function, the system of 4 equations with 4 unknowns is reduced to a system of 3 equations in 3 unknowns, temperature $T(x,r,t)$, vorticity $\omega'(x,r,t)$, and stream function $\psi'(x,r,t)$. This procedure will be outlined below, and has been successfully applied to a single uncoupled domain (12,16).

2. Vapor Region

Since the assumption of an incompressible fluid is not a valid approximation in the vapor region, five unknowns exist: u , v , T , P , ρ , each of which are functions of x,r,t . The five Eqs. (24-28), together with the boundary conditions, are available for the solution of these unknowns. As in the case with the liquid region, the pressure distribution is of interest only insofar as it gives rise to the fluid motion. The influence of the spatial pressure variation within the vapor space on other properties can reasonably be neglected. Thus, the pressure term can be eliminated from the two momentum equations by combining them, and introducing the vorticity and stream function. The temporal variation of pressure, however, still remains in the energy equation. As will be demonstrated, the system is now described by 4 equations with 5 unknowns, i.e., $T(x,r,t)$, $\omega'(x,r,t)$, $\psi''(x,r,t)$, $\rho(x,r,t)$, $P(t)$. The additional needed relation is furnished by the energy equation written for the entire vapor space as a control volume. These procedures will now be described.

III. TRANSFORMATION OF THE PARTIAL DIFFERENTIAL EQUATIONS

The momentum and the continuity equations are combined to obtain the vorticity equation and an elliptic equation relating the vorticity and the stream function. This is accomplished in the same manner as described in Ref. (12). The x-momentum is differentiated with respect to r, the r-momentum equation is differentiated with respect to x and the two combined to eliminate the pressure terms.

A. LIQUID REGION

Equations (7) and (8) reduce to:

$$\frac{\partial \omega'}{\partial t} + u \frac{\partial \omega'}{\partial x} + v \frac{\partial \omega'}{\partial r} = -\frac{1}{\rho r} g \frac{\partial \rho}{\partial r} + \nu \left[\frac{\partial^2 \omega'}{\partial x^2} + \frac{3}{r} \frac{\partial \omega'}{\partial r} + \frac{\partial^2 \omega'}{\partial r^2} \right] \quad (48)$$

where ω' is given by:

$$\omega' = \frac{1}{r} \left(\frac{\partial u}{\partial r} - \frac{\partial v}{\partial x} \right) \quad (49)$$

Introducing the stream function ψ' , defined by

$$u = \frac{1}{r} \frac{\partial \psi'}{\partial r}; \quad v = -\frac{1}{r} \frac{\partial \psi'}{\partial x} \quad (50)$$

Equations (10), (48), and (9) are transformed respectively to:

$$\frac{\partial T}{\partial t} + \frac{1}{r} \frac{\partial \psi'}{\partial r} \frac{\partial T}{\partial x} - \frac{1}{r} \frac{\partial \psi'}{\partial x} \frac{\partial T}{\partial r} = \alpha \left(\frac{\partial^2 T}{\partial x^2} + \frac{1}{r} \frac{\partial T}{\partial r} + \frac{\partial^2 T}{\partial r^2} \right), \quad (51)$$

$$\frac{\partial \omega'}{\partial t} + \frac{1}{r} \frac{\partial \psi'}{\partial r} \frac{\partial \omega'}{\partial x} - \frac{1}{r} \frac{\partial \psi'}{\partial x} \frac{\partial \omega'}{\partial r} = \frac{g\beta}{r} \frac{\partial T}{\partial r} + \nu \left(\frac{\partial^2 \omega'}{\partial x^2} + \frac{3}{r} \frac{\partial \omega'}{\partial r} + \frac{\partial^2 \omega'}{\partial r^2} \right), \quad (52)$$

$$\frac{\partial^2 \psi'}{\partial x^2} - \frac{1}{r} \frac{\partial \psi'}{\partial r} + \frac{\partial^2 \psi'}{\partial r^2} = \omega' r^2 \quad (53)$$

The initial and boundary conditions must also be transformed appropriately. Equations (51), (52), and (53) are solved numerically by finite differences to obtain the temperature, vorticity and stream function distributions. From

Eq. (50) the velocity distributions can then be computed.

B. VAPOR REGION

Combining the momentum Eqs. (24) and (25) in the manner described above, the following is obtained:

$$\begin{aligned} \frac{\partial \omega'}{\partial t} + u \frac{\partial \omega'}{\partial x} + v \frac{\partial \omega'}{\partial r} = & \left[\frac{\omega'}{\rho} \frac{D\rho}{Dt} - \frac{1}{\rho r} \frac{Du}{Dt} \frac{\partial \rho}{\partial r} + \frac{1}{\rho r} \frac{Dv}{Dt} \frac{\partial \rho}{\partial x} \right] \\ & - \frac{g}{\rho r} \frac{\partial \rho}{\partial r} + \nu \left[\frac{\partial^2 \omega'}{\partial x^2} + \frac{3}{r} \frac{\partial \omega'}{\partial r} \frac{\partial^2 \omega'}{\partial r^2} \right] \end{aligned} \quad (54)$$

where ω' is given by Eq. (49).

Equation (54) is the vorticity equation for this case. The first terms within the brackets on the right-hand side of this equation account for the compressibility effects due to density variation. Should the compressibility effects be neglected, Eq. (54) will reduce to Eq. (52). It should be noted that the presence of these terms does not introduce any additional difficulties as far as the solution of the vorticity equation is concerned. The difficulty will be in combining the continuity Eq. (26) and Eq. (49), in order to obtain an equation similar to Eq. (53). However, this difficulty can be overcome if the term $\partial \rho / \partial t$ is neglected in combining the continuity Eq. (26) with the definition of vorticity. The rigorous justification for this approximation has not yet been established. In this case Eq. (26) will be rewritten as:

$$\frac{\partial(\rho u)}{\partial x} + \frac{1}{r} \frac{\partial(\rho r v)}{\partial r} = 0. \quad (55)$$

The continuity Eq. (55) is combined with Eq. (49) by introducing the stream function ψ'' , which satisfies (55). This stream function ψ'' is defined by:

$$u = \frac{1}{\rho r} \frac{\partial \psi''}{\partial r}; \quad v = - \frac{1}{\rho r} \frac{\partial \psi''}{\partial x} \quad (56)$$

Substituting (56) and (49) into (55), the following equation which relates ψ'' to ω' , is obtained,

$$\frac{\partial^2 \psi''}{\partial r^2} - \frac{1}{r} \frac{\partial \psi''}{\partial x} + \frac{\partial^2 \psi''}{\partial x^2} = \rho \omega' r^2 + r \left[u \frac{\partial \rho}{\partial r} - v \frac{\partial \rho}{\partial x} \right] \quad (57)$$

The last terms within the brackets in Eq. (57) account for the density changes in the vapor region. The terms $\partial\rho/\partial r$ and $\partial\rho/\partial x$ are calculated in the finite-difference procedure using the equation of state and the temperature distribution from the previous time step. The coefficients u and v in $u \partial\rho/\partial r$ and $v \partial\rho/\partial x$ will be taken equal to their values at the previous time step, which is the same procedure used in calculating the non-linear terms $u \partial T/\partial x$, $v \partial T/\partial r$, $u \partial\omega'/\partial x$, and $v \partial\omega'/\partial r$, thus in effect linearizing these terms.

The spatial variation of pressure in the vapor region can be neglected. Hence,

$$\frac{DP}{Dt} = \frac{dP}{dt} \quad (58)$$

The density terms in Eqs. (54) and (57) are evaluated using the equation of state (28), and the derivatives given by:

$$\frac{\partial\rho}{\partial r} = - \frac{P}{RZ^2T^2} \left(\frac{\partial(ZT)}{\partial T} \right)_p \frac{\partial T}{\partial r} \quad (59)$$

$$\frac{\partial\rho}{\partial x} = - \frac{P}{RZ^2T^2} \left(\frac{\partial(ZT)}{\partial T} \right)_p \frac{\partial T}{\partial x} \quad (60)$$

Substitution in Eq. (54) gives:

$$\begin{aligned} & \frac{D\omega'}{Dt} - \frac{\omega'}{P} \frac{dP}{dt} + \frac{\omega'}{ZT} \left(\frac{\partial(ZT)}{\partial T} \right)_p \frac{DT}{Dt} \\ & = - \frac{g}{rZT} \left(\frac{\partial(ZT)}{\partial T} \right)_p \frac{\partial T}{\partial r} + \frac{1}{rZT} \frac{\partial T}{\partial r} \left(\frac{\partial(ZT)}{\partial T} \right)_p \\ & \cdot \frac{Du}{Dt} - \frac{1}{rZT} \left(\frac{\partial(ZT)}{\partial T} \right)_p \frac{\partial T}{\partial x} \frac{Dv}{Dt} \\ & + v \left[\frac{\partial^2\omega'}{\partial x^2} + \frac{3}{r} \frac{\partial\omega'}{\partial r} \frac{\partial^2\omega'}{\partial r^2} \right] \end{aligned} \quad (61)$$

Substitution of Eqs. (28), (59), and (60) into Eq. (57) gives:

$$\begin{aligned} & \frac{\partial^2\psi''}{\partial r^2} - \frac{1}{r} \frac{\partial\psi''}{\partial r} + \frac{\partial^2\psi''}{\partial x^2} = \frac{P}{RZT} \omega' r^2 \\ & - \frac{P r}{RZ^2T^2} \left(\frac{\partial(ZT)}{\partial T} \right)_p \left[u \frac{\partial T}{\partial r} - v \frac{\partial T}{\partial x} \right] \end{aligned} \quad (62)$$

The terms u and v in Eqs. (61) and (62) could also be expressed in terms of ψ'' by Eq. (56). Substitution of the equation of state (28) into the energy Eq. (27) gives:

$$\rho \left[C_V + R \left(\frac{\partial(ZT)}{\partial T} \right)_p \right] \frac{DT}{dt} = \frac{dP}{dt} + k\nabla^2 T \quad (63)$$

Taking the thermodynamic relation

$$C_p - C_V = T \left(\frac{\partial v}{\partial T} \right)_p \left(\frac{\partial p}{\partial T} \right)_v \quad (64)$$

and the ratio of specific heats

$$\frac{C_p}{C_V} = \gamma \quad (65)$$

and substituting into Eq. (63) and rearranging, another form of the energy equation is:

$$\frac{DT}{Dt} = \frac{1}{1 + \frac{(\gamma-1)Z}{\left(\frac{\partial(ZT)}{\partial T} \right)_v}} \cdot \frac{RZT}{C_V P} \frac{dP}{dt} + \frac{\gamma}{1 + \frac{(\gamma-1)Z}{\left(\frac{\partial(ZT)}{\partial T} \right)_v}} \alpha \nabla^2 T \quad (66)$$

It might be noted that the body force term in Eq. (61) could also be expressed as:

$$\frac{g}{rZT} \left(\frac{\partial(ZT)}{\partial T} \right)_p \frac{\partial T}{\partial r} = \frac{g}{r} \beta \frac{\partial T}{\partial r} \quad (67)$$

Since the assumption of ideal gas behavior is adequate for the vapor,* Eqs. (61), (62), and (66) reduce, respectively, to:

$$\begin{aligned} \frac{D\omega'}{Dt} - \frac{\omega'}{P} \frac{dP}{dt} + \frac{\omega'}{T} \frac{DT}{Dt} &= -\frac{g}{rT} \frac{\partial T}{\partial r} + \frac{1}{rT} \frac{\partial T}{\partial r} \frac{Du}{Dt} \\ &- \frac{1}{rT} \frac{\partial T}{\partial x} \frac{Dv}{Dt} + v \left[\frac{\partial^2 \omega'}{\partial x^2} + \frac{3}{r} \frac{\partial \omega'}{\partial r} + \frac{\partial^2 \omega'}{\partial r^2} \right] \end{aligned} \quad (68)$$

*For saturated O_2 vapor at atmospheric pressure, $Z = 0.97$, and $[\partial(ZT)/\partial T]_p = 1.015$. For an ideal gas, $Z = 1.00$, and $\partial(ZT)/\partial T = 1.00$.

$$\frac{\partial^2 \psi''}{\partial r^2} - \frac{1}{r} \frac{\partial \psi''}{\partial r} + \frac{\partial^2 \psi''}{\partial x^2} = \frac{P}{RT} \omega' r^2 - \frac{Pr}{RT^2} \left[u \frac{\partial T}{\partial r} - v \frac{\partial T}{\partial x} \right] \quad (69)$$

$$\frac{DT}{Dt} = \frac{\gamma - 1}{\gamma} \frac{T}{P} \frac{dP}{dt} + \alpha \nabla^2 T \quad (70)$$

Equations (61), (62) and (66) (or (68)-(70) for ideal gases) together with the transformed boundary conditions constitute the system of 3 equations with 4 unknowns for the vapor space, $\omega'(x,r,t)$, $\psi''(x,r,t)$, $T(x,r,t)$, and $P(t)$ referred to earlier. The finite-difference solution of Eqs. (61), (62), and (66) for ω' , ψ'' and T requires that a function for dP/dt be available. This is obtained from the First Law of Thermodynamics written as an instantaneous rate equation, taking the vapor space as the control volume. Referring to Figure 3 this formulation is written:

$$\begin{aligned} \frac{d}{dt} \int_{V_g(t)} (\rho_g e_g) dV - \int_{A_i} h_{gs} \rho_{gs} (u_{gi} - u_i) dA \\ + \int_{A_p} h_{gp} \rho_{gp} u_{gp} dA = \int_{A_{c.s.}} q dA - P \frac{dV_g}{dt} \end{aligned} \quad (71)$$

This formulation includes the following generalized variation:

$$e_g = e(x,r,t)$$

$$\rho_g = \rho(x,r,t)$$

$$u_{gi} = u(r,t)$$

h_{gs}, ρ_{gs} are uniform over the liquid-vapor interface

u_i is uniform for a flat interface

$h_{gp}, \rho_{gp}, u_{gp}$ are specified by the particular pressurization process.

q is the local heat flux on the control surface, and its integral includes that from the tank wall and through the liquid-vapor interface.

Given property information on $e_g = f_1(P,T)$, $\rho_g = f_2(P,T)$, $h_{gs} = f_3(P)$, $\rho_{gs} = f_4(P)$, the desired term dP/dt can be extracted from the first term of Eq. (71). The necessary properties can come either from specific heat data plus an equation of state, or from tabulated values. It may be anticipated that different computational procedures would be required for each of these.

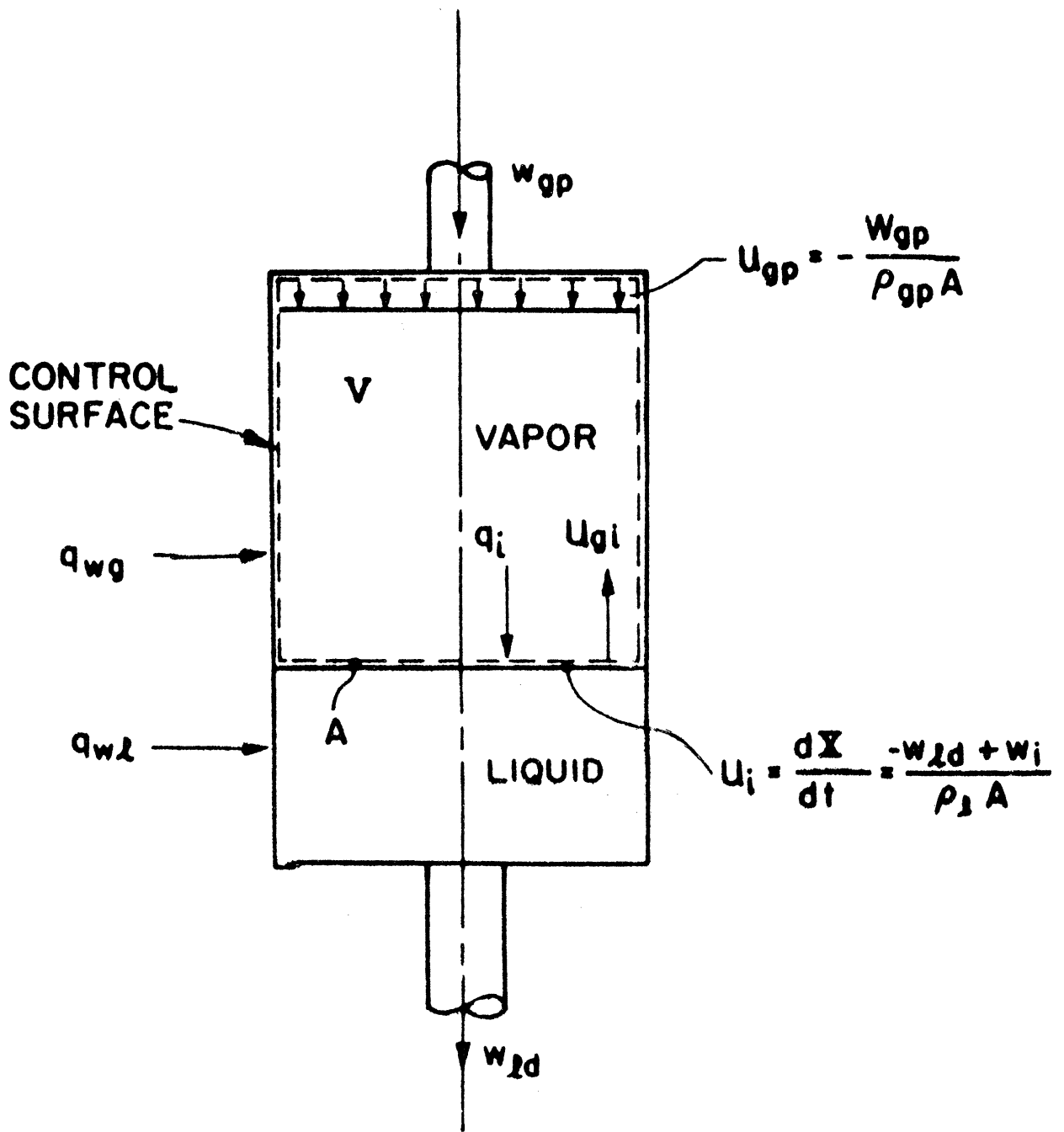


Figure 3. Control volume of vapor region.

The procedure will be demonstrated for the case of self-pressurization, that is with no liquid discharge, no external pressurization, and a flat interface. Thus, $w_d = 0$, $w_p = 0$, and $u_{gp} = 0$. Then,

$$\frac{dX}{dt} = u_i = \frac{dX_i}{dt} \quad (72)$$

and from Eq. (47), assuming a uniform vapor velocity across the interface

$$u_{gi} - u_i = \frac{\rho_l}{\rho_l - \rho_{gs}} u_{gi} \quad (73)$$

For the coordinate frame selected

$$\frac{dV_g}{dt} = - A_i \frac{dX}{dt} = - A_i u_i \quad (74)$$

For brevity

$$q_{tot} = \int_{A_{c.s.}} q \, dA \quad (75)$$

Substituting Eqs. (73)-(75) into Eq. (71)

$$\begin{aligned} \frac{d}{dt} \int_{V_g(t)} (\rho_g e_g) dV &= q_{tot} \\ &+ h_{gs} \rho_{gs} \frac{\rho_l}{\rho_l - \rho_{gs}} u_{gi} A_i + P A_i u_i \end{aligned} \quad (76)$$

Using Leibnitz's rule for differentiation of integrals having variable limits the first term of Eq. (76) can be written as

$$\begin{aligned} \frac{d}{dt} \int_{V_g(t)} (\rho_g e_g) dV &= \int_{V_g} \rho_g \frac{\partial e_g}{\partial t} dV \\ &+ \int_{V_g} e_g \frac{\partial \rho_g}{\partial t} dV - \rho_{gs} e_{gs} u_i A_i \end{aligned} \quad (77)$$

Substituting Eq. (77) in Eq. (76) and rearranging with the use of Eq. (47) gives,

$$\int_{V_g} \rho_g \frac{\partial e_g}{\partial t} dV + \int_{V_g} e_g \frac{\partial \rho_g}{\partial t} dV = q_{tot} + h_{gs} A_i u_i (\rho_{gs} - \rho_l) \quad (78)$$

For the case in which the use of an equation of state (28) is desired, the entire left-hand side of Eq. (78) can be expressed as the following by means of general thermodynamic property relations:

$$\begin{aligned} & \frac{C_V}{R} \frac{dP}{dt} \int_{V_g} \frac{dV}{\left[\frac{\partial(ZT)}{\partial T} \right]_V} + \int_{V_g} \left\{ \frac{PC_V}{R} \frac{1}{\left[\frac{\partial(ZT)}{\partial T} \right]_P} \right. \\ & \left. + \frac{T}{Z^2} \left(\frac{\partial P}{\partial T} \right)_V \right\} \frac{1}{ZT} \left[\frac{\partial(ZT)}{\partial T} \right] dV \\ & - \frac{P}{R} \int_{V_g} \frac{h_g}{Z^2 T^2} \left[\frac{\partial(ZT)}{\partial t} \right] dV \end{aligned} \quad (79)$$

The enthalpy terms in Eqs. (78) and (79) can be expressed by:

$$h - h_R = \int_{T_R}^T C_{pR} dT + \int_{P_R}^P \frac{RT}{P} \left\{ Z - \left[\frac{\partial(ZT)}{\partial T} \right]_P \right\} \frac{dp}{T} \quad (80)$$

where the subscript R refers to a low pressure reference condition.

For an ideal gas with constant specific heat expression (79) reduces to:

$$\frac{C_V}{R} \left(\frac{dP}{dt} \right)_{V_g} \quad (81)$$

Substituting expression (81) for the left-hand side of Eq. (78), writing the enthalpy by a specific heat term, and rearranging, Eq. (78) reduces to:

$$\frac{dP}{dt} = \frac{R}{C_V V_g} q_{tot} + \frac{RT_s \gamma}{V_g} A_i u_i (\rho_{gs} - \rho_l) \quad (82)$$

For the case far from the region of the critical state, such that $\rho_l \gg \rho_{gs}$, Eq. (82) can be written as

$$\frac{dP}{dt} = \frac{R}{C_V V_g} q_{tot} - \frac{w_i R \gamma T_s}{V_g} \quad (83)$$

where w_i is the rate of interfacial mass transfer (having a negative value for evaporation) and is given by

$$w_i = - \frac{\rho_l \rho_{gs}}{(\rho_l - \rho_{gs})} A_i u_{gi} \quad (84)$$

IV. DIMENSIONLESS FORM OF THE EQUATIONS

The governing equations for the wall, liquid and vapor regions (4), (51), (52), (53), (61), (62), and (66) are next made nondimensional, along with the boundary conditions.

The substitutions necessary to nondimensionalize the differential equations are:

$$\left. \begin{aligned} u &= \frac{\alpha_l b}{a^2} U; & v &= \frac{\alpha_l}{a} V; & T-T_0 &= \frac{\nu_l \alpha_l b}{\beta_l q a^4} \theta \\ t &= \frac{a^2}{\alpha_l} \tau; & x &= b\xi; & r &= a\eta \\ \omega'' &= \frac{\alpha_l b}{a^4} \omega; & \psi' &= \alpha b \psi \end{aligned} \right\} \quad (85)$$

The resulting dimensionless equations are given below.

A. WALL TEMPERATURE

The dimensionless equations describing the wall temperature, from Eq. (4), are given by:

$$\begin{aligned} \text{(i)} \quad 0 \leq \xi \leq \xi_i &= \frac{X(t)}{b} \\ \frac{\partial \theta_w}{\partial \tau} &= -\frac{a}{\delta_w} \cdot \frac{(\rho C_p)_l}{(\rho C_p)_w} \left(\frac{\partial \theta_l}{\partial \eta} \right)_{\eta=1} + \frac{a^2}{b^2} \cdot \frac{(\rho C_p)_l}{(\rho C_p)_w} \cdot \frac{k_w}{k_l} \frac{\partial^2 \theta_w}{\partial \xi^2} \\ &+ \frac{a}{b} \cdot \frac{a}{\delta_w} \cdot \frac{(\rho C_p)_l}{(\rho C_p)_w} \cdot Pr_l \cdot Gr_w^*(\xi, t) \end{aligned} \quad (86)$$

$$\begin{aligned} \text{(ii)} \quad \frac{X(t)}{b} \leq \xi \leq 1 \\ \frac{\partial \theta_w}{\partial \tau} &= -\frac{a}{\delta_w} \cdot \frac{(\rho C_p)_l}{(\rho C_p)_w} \cdot \frac{k_g}{k_l} \cdot \left(\frac{\partial \theta_g}{\partial \eta} \right)_{\eta=1} + \frac{a^2}{b^2} \cdot \frac{(\rho C_p)_l}{(\rho C_p)_w} \cdot \frac{k_w}{k_l} \cdot \frac{\partial^2 \theta_w}{\partial \xi^2} \\ &+ \frac{a}{b} \cdot \frac{a}{\delta_w} \cdot \frac{(\rho C_p)_l}{(\rho C_p)_w} \cdot Pr_l \cdot Gr_w^*(\xi, t) \end{aligned} \quad (87)$$

where $Gr_w^*(\zeta, t)$ is the modified Grashof number and is given by:

$$Gr_w^*(\zeta, t) = \frac{g\beta a^4}{k_l \nu_l^2} q_w(\zeta, t) \quad (88)$$

(iii) Boundary and Initial Conditions

$$\frac{\partial \theta_w(0, \tau)}{\partial \zeta} = \frac{\partial \theta_w(1, \tau)}{\partial \zeta} = 0 \quad (89)$$

$$\theta(\zeta, 0) = 0 \quad (90)$$

B. LIQUID REGION

(i) The energy equation, Eq. (51)

$$\frac{\partial \theta}{\partial \tau} + \frac{1}{\eta} \cdot \frac{\partial \psi}{\partial \eta} \cdot \frac{\partial \theta}{\partial \xi} - \frac{1}{\eta} \frac{\partial \psi}{\partial \xi} \cdot \frac{\partial \theta}{\partial \eta} = \frac{a^2}{b^2} \frac{\partial^2 \theta}{\partial \xi^2} + \frac{1}{\eta} \frac{\partial \theta}{\partial \eta} + \frac{\partial^2 \theta}{\partial \eta^2} \quad (91)$$

(ii) The vorticity equation, Eq. (52)

$$\frac{\partial \omega}{\partial \tau} + \frac{1}{\eta} \frac{\partial \psi}{\partial \eta} \frac{\partial \omega}{\partial \xi} - \frac{1}{\eta} \frac{\partial \psi}{\partial \xi} \frac{\partial \omega}{\partial \eta} = Pr_l \left[\frac{1}{\eta} \frac{\partial \theta}{\partial \eta} + \frac{a^2}{b^2} \frac{\partial^2 \omega}{\partial \xi^2} + \frac{3}{\eta} \frac{\partial \omega}{\partial \eta} + \frac{\partial^2 \omega}{\partial \eta^2} \right] \quad (92)$$

(iii) The vorticity-stream function equation, Eq. (53)

$$\frac{a^2}{b^2} \frac{\partial^2 \omega}{\partial \xi^2} - \frac{1}{\eta} \frac{\partial \psi}{\partial \eta} + \frac{\partial^2 \psi}{\partial \eta^2} = \omega \quad (93)$$

$$U = \frac{1}{\eta} \frac{\partial \psi}{\partial \eta} ; \quad V = - \frac{1}{\eta} \frac{\partial \psi}{\partial \xi} \quad (94)$$

(iv) The Boundary Conditions

(1) Stream function boundary conditions

$$\psi(0, \eta, \tau) = \frac{\partial \psi(0, \eta, \tau)}{\partial \xi} = 0 \quad (95)$$

$$\psi(\xi_1, \eta, \tau) = \frac{\partial^2 \psi(\xi_1, \eta, \tau)}{\partial \xi^2} = 0 \quad (96)$$

$$\psi(\xi, 0, \tau) = \frac{\partial}{\partial \eta} \left[\frac{1}{\eta} \frac{\partial \psi(\xi, 0, \tau)}{\partial \eta} \right] = 0 \quad (97)$$

$$\psi(\xi, 1, \tau) = \frac{\partial \psi(\xi, 1, \tau)}{\partial \eta} = 0 \quad (98)$$

(2) Vorticity boundary conditions

$$\omega(1, \eta, \tau) = 0 \quad (99)$$

$$\omega(\xi, 0, \tau) = 0 \quad (100)$$

Two additional vorticity boundary conditions are required at the tank wall and bottom. An explicit expression for the vorticity at any of these locations is difficult to obtain. The method of solution used in this work, which follows that of Ref. (16), overcomes this difficulty.

(3) Thermal boundary conditions

$$\theta(\xi, 1, \tau) = \theta_w(\xi, \tau) \quad (101)$$

$$\theta(\xi_i, \eta, \tau) = \theta_s(\tau) \quad (102)$$

$$\frac{\partial \theta(0, \eta, \tau)}{\partial \xi} = 0 \quad (103)$$

$$\frac{\partial \theta(\xi, 0, \tau)}{\partial \eta} = 0 \quad (104)$$

where θ_s is given by:

$$\theta_s(\tau) = \frac{a}{b} \text{Fr}_l \left[T_s(t) - T_0 \right] \frac{g\beta_l a^3}{\nu_l^2} \quad (105)$$

(4) Initial Conditions

$$\begin{aligned} \theta(\xi, \eta, 0) &= U(\xi, \eta, 0) = V(\xi, \eta, 0) \\ &= \omega(\xi, \eta, 0) = \psi(\xi, \eta, 0) = 0 \end{aligned} \quad (106)$$

C. VAPOR REGION

(i) The energy equation, Eq. (66)

$$\frac{\partial \theta}{\partial \tau} + \frac{1}{\rho \eta} \frac{\partial \psi}{\partial \eta} \frac{\partial \theta}{\partial \xi} - \frac{1}{\rho \eta} \frac{\partial \psi}{\partial \xi} \frac{\partial \theta}{\partial \eta} = \frac{1}{1 + (\gamma - 1)Z / \left(\frac{\partial(ZT)}{\partial T} \right)_v} \cdot \frac{RZ}{C_v} \cdot \frac{(\theta + \theta_0)}{P} \cdot \frac{\partial P}{\partial \tau}$$

$$+ \frac{\gamma}{1 + (\gamma - 1)Z / \left(\frac{\partial(ZT)}{\partial T} \right)_v} \frac{\alpha_g}{\alpha_l} \left[\frac{a^2}{b^2} \frac{\partial^2 \theta}{\partial \xi^2} + \frac{1}{\eta} \frac{\partial \theta}{\partial \eta} + \frac{\partial^2 \theta}{\partial \eta^2} \right] \quad (107)$$

where $\theta = \frac{g \beta_l a^4}{v_l \alpha_l b} T_0$ (108)

(ii) The vorticity equation, Eq. (61)

$$\frac{\partial \omega}{\partial \tau} + \frac{1}{\rho \eta} \frac{\partial \psi}{\partial \eta} \frac{\partial \omega}{\partial \xi} - \frac{1}{\rho \eta} \frac{\partial \psi}{\partial \xi} \frac{\partial \omega}{\partial \eta} = \text{Pr}_l \frac{v_g}{v_l} \left[\frac{a^2}{b^2} \frac{\partial^2 \omega}{\partial \xi^2} + \frac{1}{\eta} \frac{\partial \omega}{\partial \eta} + \frac{\partial^2 \omega}{\partial \eta^2} \right] + \frac{g a^4}{\alpha_l^2 b Z \eta (\theta + \theta_0)} \left(\frac{\partial(ZT)}{\partial T} \right)_P \frac{\partial \theta}{\partial \eta}$$

$$+ \frac{1}{\eta Z (\theta + \theta_0)} \left(\frac{\partial(ZT)}{\partial T} \right)_P \frac{\partial \theta}{\partial \eta} \frac{DU}{D\tau} - \frac{1}{\eta Z (\theta + \theta_0)} \left(\frac{\partial(ZT)}{\partial T} \right)_P \frac{\partial \theta}{\partial \xi} \frac{DV}{D\tau} + \frac{\omega}{P} \left(\frac{dP}{d\tau} \right) \quad (109)$$

where β is given by:

$$\beta_g = \frac{1}{ZT} \left(\frac{\partial(ZT)}{\partial T} \right)_P \quad (110)$$

(iii) The vorticity-stream function equation, Eq. (62)

$$\frac{a^2}{b^2} \frac{\partial^2 \psi}{\partial \xi^2} - \frac{1}{\eta} \frac{\partial \psi}{\partial \eta} + \frac{\partial^2 \psi}{\partial \eta^2} = \frac{P}{ZR(\theta + \theta_0)} \left(\frac{g \beta_l a^4}{v_l \alpha_l b} \right) \omega \eta^2$$

$$- \left(\frac{g \beta_l a^4}{v_l \alpha_l b} \right) \frac{P}{Z^2 R(\theta + \theta_0)} \left(\frac{\partial(ZT)}{\partial T} \right)_P \eta \left[U \frac{\partial \theta}{\partial \eta} - \frac{a^2}{b^2} v \frac{\partial \theta}{\partial \xi} \right] \quad (111)$$

(iv) Boundary Conditions

(1) Stream function boundary conditions

$$\psi(1, \eta, \tau) = \frac{2\psi(1, \eta, \tau)}{2\xi} = 0 \quad (112)$$

$$\psi(\xi_1, \eta, \tau) = (\rho_l - \rho_{g,s}) \frac{w_i}{\rho_l \alpha_l} \frac{\eta^2}{2\pi b} = \frac{\rho_{g,s} U_{g,i} \eta^2}{2} \quad (113)$$

$$\psi(\xi, 0, \tau) = \frac{\partial}{\partial \eta} \left(\frac{1}{\rho_{gi} \eta} \frac{2\psi(\xi, 0, \tau)}{2\eta} \right) = 0 \quad (114)$$

$$\psi(\xi, 1, \tau) = \frac{2\psi(\xi, 1, \tau)}{2\eta} = 0 \quad (115)$$

(2) Vorticity boundary conditions

$$\omega(\xi, 0, \tau) = 0 \quad (116)$$

$$\omega(\xi_i, \eta, \tau) = 0 \quad (117)$$

(3) Temperature boundary conditions

$$\theta(\xi_i, \eta, \tau) = \theta_s(\tau) \quad (118)$$

$$\frac{\partial \theta(1, \eta, \tau)}{\partial \xi} = 0 \quad (119)$$

$$\theta(\xi, 1, \tau) = \theta_w(\xi, \tau) \quad (120)$$

$$\frac{\partial \theta(\xi, 0, \tau)}{\partial \eta} = 0 \quad (121)$$

(4) Initial Conditions

$$\theta(\xi, \eta, 0) = U(\xi, \eta, 0) = V(\xi, \eta, 0) = \psi(\xi, \eta, 0) = \omega(\xi, \eta, 0) = 0 \quad (122)$$

From the above results, it is clear that the temperature, pressure and velocity within the container are functions of the parameters Gr_w^* , Pr , $(\rho C_p)_l / (\rho C_p)_w$, (k_w / k_l) , (α_g / α_l) , (ν_g / ν_l) , (β_g / β_l) , (a/b) and (a/δ) . Gr_w^* is defined in Eq. (88).

V. METHOD OF SOLUTION

A. FINITE-DIFFERENCE FORMS

The finite-difference method of solution used in Ref. (16) is adopted here. A complete discussion of the application of difference methods for the solution of the energy and vorticity equations is given in this reference, along with the problem of stability of the difference equations. A brief discussion of the method of solution will be made here.

The basic concept in the application of finite-difference methods for the solution of partial differential equations is the use of Taylor Series Expansion to approximate the derivatives at a point in terms of the value of the function at that point and/or at its neighboring points. This may be demonstrated as follows:

1. The time derivative is represented by

$$\frac{\partial f}{\partial \tau} = \frac{f(\tau + \Delta\tau) - f(\tau)}{\Delta\tau} + O(\Delta\tau) \quad (123)$$

2. The first order derivatives $\frac{\partial f}{\partial x}$ and $\frac{\partial f}{\partial R}$ can be approximated by

$$(i) \quad \frac{\partial f}{\partial x} = \frac{f(x + \Delta x, R, \tau) - f(x, R, \tau)}{\Delta x} + O(\Delta x) \quad (\text{forward differences}) \quad (124)$$

or

$$(ii) \quad \frac{\partial f}{\partial x} = \frac{f(x, R, \tau) - f(x - \Delta x, R, \tau)}{\Delta x} + O(\Delta x) \quad (\text{backward differences}) \quad (125)$$

or

$$(iii) \quad \frac{\partial f}{\partial x} = \frac{f(x + \Delta x, R, \tau) - f(x - \Delta x, R, \tau)}{2\Delta x} + O(\Delta x)^2 \quad (\text{central differences}) \quad (126)$$

3. The second order derivatives are replaced by finite-differences according to the formula.

$$\frac{\partial^2 f}{\partial x^2} = \frac{f(x+\Delta x, R, \tau) - 2f(x, R, \tau) + f(x-\Delta x, R, \tau)}{(\Delta x)^2} + O(\Delta x)^2 \quad (127)$$

The function f represents either θ or ω , and Δx is the spatial increment in the x -direction. The last term on the righthand side of Eqs. (123) through (127) indicates the order of the truncation error involved in replacing the derivatives by finite-differences. It is clear that the central differences offer a better representation of the first order derivative $\frac{\partial f}{\partial x}$ than the forward or backward differences. However, the form used to approximate the first order derivatives is usually determined by stability considerations. Similar formulations can be written for the derivatives $\frac{\partial f}{\partial R}$ and $\frac{\partial^2 f}{\partial R^2}$.

The substitution of the above formulae in the energy and vorticity equations produces a set of explicit difference equations. However, if the values of the function f in Eqs. (124) through (127) are taken at the time level $\tau+\Delta\tau$ instead of being taken at time level τ , the resulting finite-difference methods may require the use of small time increments and consequently large machine time. Certain implicit formulations may permit the use of large increments. The application of both explicit and implicit methods to the present problem has been extensively investigated in Ref. (16). It was concluded that the lack of explicit boundary conditions for the vorticity at the solid boundaries prevent the use of large time increments, i.e., implicit methods. Therefore, it was decided to employ explicit methods.

It is clear from Eqs. (124) through (126) that more than one explicit finite-difference formulation can be constructed for each of the vorticity and energy equations. The finite-difference formulation chosen for the solution of the present problem is dictated by stability, as well as practical considerations, which will be shown below in studying the stability of the finite-difference equations.

The method of solution used in the present problem can be summarized as follows:

1. The time derivatives $\frac{\partial \theta}{\partial \tau}$ and $\frac{\partial \omega}{\partial \tau}$ are approximated by Eq. (123).
2. The nonlinear terms $U \frac{\partial \theta}{\partial x}$, $V \frac{\partial \theta}{\partial R}$, $U \frac{\partial \omega}{\partial x}$ and $V \frac{\partial \omega}{\partial R}$ are linearized by considering the velocity components U and V to be known and are taken equal to their values at time level τ . The order of the error introduced by this linearization can be obtained from Taylor Series Expansion. If U_0 and U are the values of the axial velocity component at time levels τ_0 and $\tau_0+\Delta\tau_0$, respectively, then

$$U \frac{\partial \theta}{\partial x} = U_0 \frac{\partial \theta}{\partial x} + \Delta\tau \left(\frac{\partial U}{\partial \tau} \right)_{\tau_0} + \beta \frac{\partial \theta}{\partial x}, \quad (128)$$

where

$$0 \leq \beta \leq \Delta\tau.$$

The last term on the right side of Eq. (128) represents the linearization error and is of order $O(\Delta\tau)$.

3. The nonlinear terms $U \frac{\partial \theta}{\partial x}$ and $U \frac{\partial \omega}{\partial x}$ are approximated by backward differences, Eq. (125), if the coefficient velocity U is positive and by forward differences, Eq. (124), if U is negative. The same procedure is followed for approximating the terms $V \frac{\partial \theta}{\partial R}$ and $V \frac{\partial \omega}{\partial R}$ according to the sign of the velocity component V .

4. Central differences are used to approximate the first order terms $\frac{1}{R} \frac{\partial \theta}{\partial R}$, $\frac{3}{R} \frac{\partial \omega}{\partial R}$ and $\frac{1}{R} \frac{\partial \psi}{\partial R}$. No stability problems will be encountered in this case. At the centerline where both R and $\frac{\partial \theta}{\partial R}$ are zero, $\frac{1}{R} \frac{\partial \theta}{\partial R}$ is replaced by its limit according to

$$\text{Limit}_{R \rightarrow 0} \frac{1}{R} \frac{\partial \theta}{\partial R} = \frac{\partial^2 \theta}{\partial R^2} \Big|_{R=0} \quad (129)$$

5. The second order terms $\frac{\partial^2 \theta}{\partial x^2}$, $\frac{\partial^2 \theta}{\partial R^2}$, $\frac{\partial^2 \omega}{\partial x^2}$, $\frac{\partial^2 \omega}{\partial R^2}$, $\frac{\partial^2 \psi}{\partial x^2}$ and $\frac{\partial^2 \psi}{\partial R^2}$ are represented by Eq. (127).

6. Although the first order derivative $\frac{\partial \theta}{\partial \eta} \Big|_{\eta=1}$ in Eqs. (86) and (87) can be represented by any of Eqs. (124), (125) or (126), the following formula, which has a higher truncation error is used,

$$\frac{\partial \theta}{\partial \eta} \Big|_{\eta=1} = \frac{11\theta(\xi, 1) - 18\theta(\xi, \eta - \Delta\eta) + 9\theta(\xi, \eta - 2\Delta\eta) - 2\theta(\xi, \eta - 3\Delta\eta)}{6\Delta\eta} \quad (130)$$

Similarly

$$\frac{\partial \theta}{\partial \xi} \Big|_{\xi=\xi_i} = \frac{11\theta(\xi_i, \eta) - 18\theta(\xi_i - \Delta\xi, \eta) + 9\theta(\xi_i - 2\Delta\xi, \eta) - 2\theta(\xi_i - 3\Delta\xi, \eta)}{6\Delta\xi} \quad (131)$$

B. STABILITY OF FINITE-DIFFERENCE EQUATIONS

The stability of the finite-difference equations is an important consideration in establishing the size of the grid and the time steps, and the type of differencing used. The details are given in Ref. (16). As might be anticipated, the size of the grid and time steps will also be governed by the storage capacity of the machine and limitations of time and cost. The necessary requirements for stability are given by the following:

$$\Delta\tau \left(\frac{2a^2}{b^2(\Delta\xi)^2} + \frac{2}{(\Delta\eta)^2} + \frac{|U_{i,j}|}{\Delta\xi} + \frac{|V_{i,j}|}{\Delta\eta} \right) \leq 1 \quad (132)$$

$$\Delta\tau \left(\frac{2a^2\text{Pr}}{b^2(\Delta\xi)^2} + \frac{2\text{Pr}}{(\Delta\eta)^2} + \frac{|U_{i,j}|}{\Delta\xi} + \frac{|V_{i,j}|}{\Delta\eta} \right) \leq 1 \quad (133)$$

For Prandtl number less than unity, inequality (132) is more restrictive and therefore should be used. For Prandtl numbers greater than unity inequality (133) must be used.

C. COMPUTATIONAL PROCEDURES

The sequence of steps in establishing the numerical calculation is as follows:

- (1) A convenient grid size is selected, dictated by the machine storage capacity.
- (2) A suitable time increment is chosen. This may be altered during the course of computation as necessary to maintain numerical stability.
- (3) The temperature distribution is computed using velocities, temperatures and pressure from the previous time step.
- (4) These temperatures are used to compute the vorticity at the interior nodal points for the current time step.
- (5) The stream function is computed at the interior nodal points.
- (6) The vorticities at the solid boundaries are calculated.
- (7) The velocity components are calculated.
- (8) The rate of phase change at the interface is determined using the computed temperature distribution, with Eq. (43).
- (9) The pressure rise is computed with an equation such as (83) using the parameters from the previous time step.
- (10) The above procedures are repeated successively.

A problem inherent in the use of numerical methods is the accurate determination of temperature gradients. In the present application temperature gradients are computed in the liquid and vapor at the liquid-vapor interface to determine the rate of phase change, from Eq. (43), and in the liquid and vapor at the wall to determine the heat transfer to the bulk liquid and vapor, respectively.

The general problem of the effect of grid size on the interfacial heat and mass transfer is presented in some detail here.

The formulation with Eq. (43) was used by a number of investigators (2 through 8) to determine the rate of interfacial phase change for the case of a suddenly pressurized one-dimensional model. However, the determination of the temperature gradients by numerical differentiation of the calculated temperature distribution in the case of self-pressurized containers may be

difficult for two-dimensional problems. This would occur in cases in which the temperature gradients near the interface, that cause the phase change, are large. These large temperature gradients exist in a very thin layer near the interface, as has been shown by experimental measurements (13,14). This requires the use of a very small grid size in order to obtain an acceptable approximation for the temperature gradients near the interface.

Computations have shown that the spatial grid size has a considerable effect on the calculated rates of heat transfer at the interface. These calculations have been performed for the one-dimensional problem described by Eqs.(1), (2), (3), and the results are shown in Figures 4, 5, 6. Figure 4 gives the interfacial velocity and indicates that the effect of grid size is large at early times. As time progresses the interface velocity becomes less influenced by choice of grid size. This is also seen in Figure 5, which shows that for suitably small grid size the rate of condensation approaches a value independent of grid size. However, the influence on total mass condensed (or evaporated) is a cumulative one, as also noted in Figure 5, and can give rise to serious error in cases where the ratio of interfacial area to vapor volume is large or for small times. Figure 6 shows the influence of grid size on the computed temperatures for two different time periods of 10 and 100 seconds. As the grid size decreases the finite-difference calculations of the rate of interfacial phase change may be expected to approach the exact solution.

The example presented above dealt with an externally pressurized system, and the severity of the temperatures gradients at the interface will depend on the magnitudes of the pressure change and the superheat of the pressurant. In the case of self-pressurized containers the liquid is considered initially saturated. Any disturbances from these conditions such as imposed heat transfer from the ambient will cause the liquid to become superheated. This is an unstable nonequilibrium state, and the liquid will attempt to adjust to a new equilibrium condition by convection and evaporation. The evaporation of the liquid will cause the pressure in the ullage space to rise. The net effect will be to decrease the degree of superheat of the liquid, and increase the mass of the vapor in the ullage volume. If the rate of heating is low, the conditions in the liquid will be very close to equilibrium conditions. In this case the degree of superheat will be small. This condition may be expected to exist in high altitude flights with a well-insulated container. Under these circumstances evaporation takes place such that the pressure in the ullage volume rises at a rate which keeps the liquid near an equilibrium state. It thus might be anticipated that the temperature gradients in the liquid and vapor at the liquid-vapor interface will be relatively small, and the errors associated with reasonably sized grid spacing will be small. The only true test available is to vary the grid size for given conditions and compare the computed results.

In the case of the temperature gradients in the fluid adjacent to the wall two aspects must be considered when either the heat flux or the wall temperatures are imposed. One is similar to the liquid-vapor interface problem in that the grid spacing should again be small enough to permit sufficiently accurate representation of the temperature distribution in the

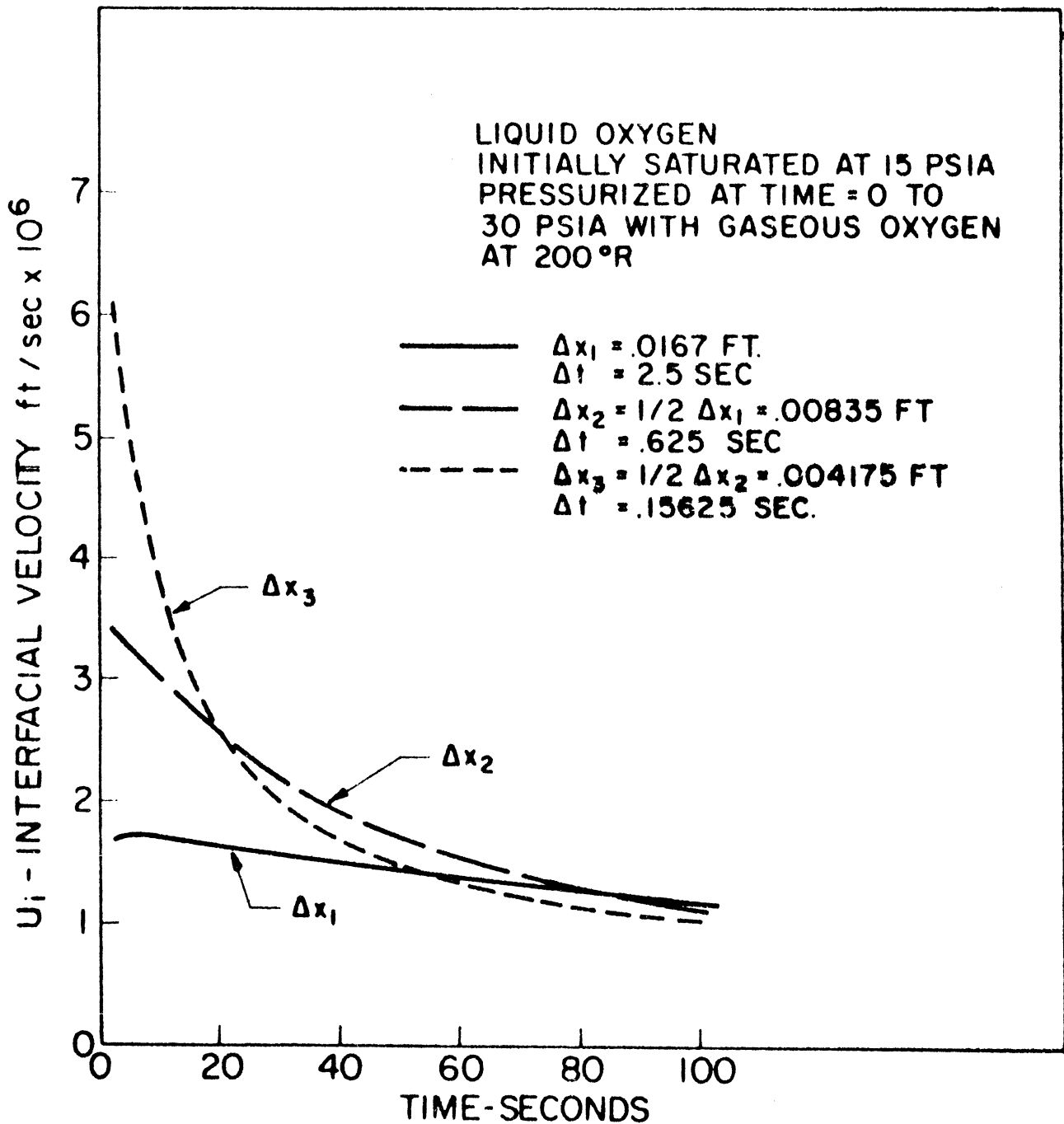


Figure 4. Effect of grid size on computed interfacial velocity.

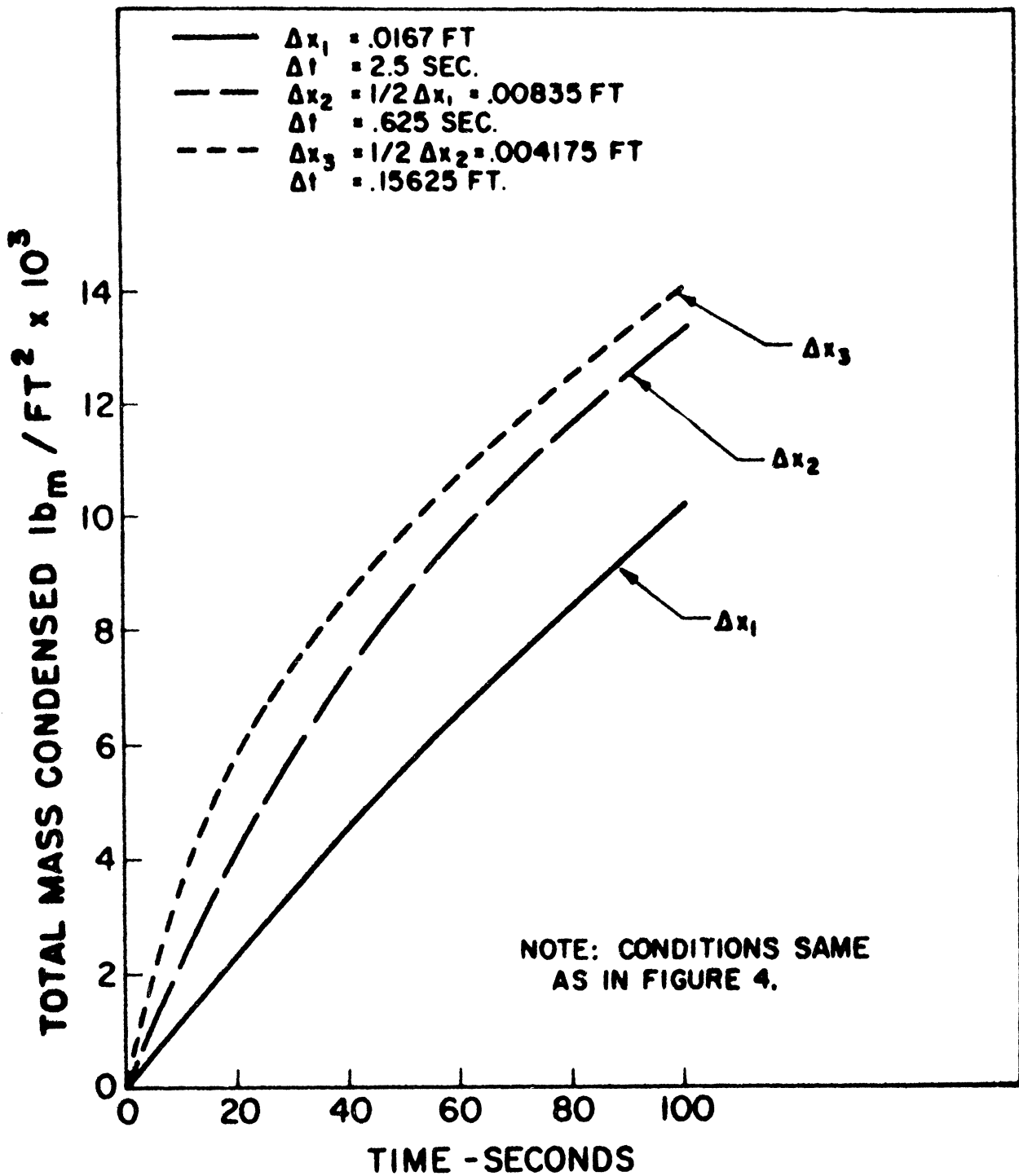


Figure 5. Effect of grid size on computed condensed mass.

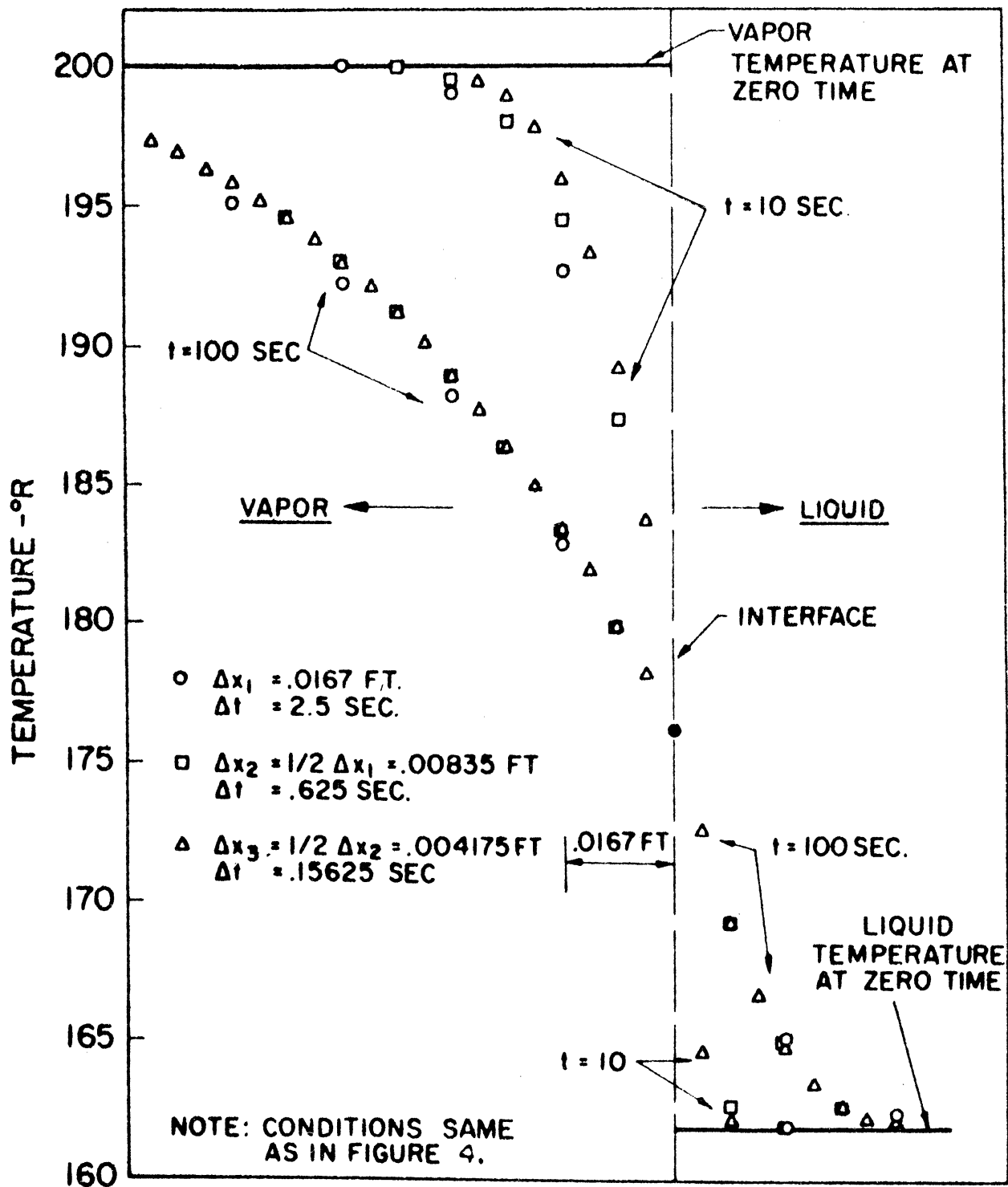


Figure 6. Effect of grid on computed temperature distribution.

fluid, either liquid or vapor, and in general dictates that the grid spacing be as small as possible. The degree of being sufficiently small will be dictated in part by the magnitude of the imposed heat flux or the imposed temperature, and the response of the transient convective process to these disturbances under the prevailing effective gravity level. Again, the only true test available is to vary the grid size for given conditions and compare the coupled results.

The other aspect to be considered is a physical one involving only the liquid, but is also related to the problem of grid spacing. If the temperature of the solid wall in contact with the liquid exceeds the saturation temperature by some amount, dependent upon various parameters including liquid and solid properties and the configuration, nucleate boiling will be initiated. This particular heating surface superheat might be called the incipient boiling point. If information on the incipient boiling point is available for the prevailing conditions, an imposed wall temperature below this point then represents no additional problem beyond that of having sufficiently small grid sizes, as discussed above. For the case of a heat flux imposed on the outer surface of the container, however, the resulting wall temperature is a variable dependent upon a number of parameters such as wall thickness and heat capacity, fluid properties, acceleration level and container geometry. Whether the wall temperature will exceed the incipient boiling point will not be known a priori since the wall temperature is computed during the course of the computations.

The procedure by which the possibility of nucleate boiling is taken into account is based on the following physical assumptions:

(1) should nucleate boiling begin, further increases in heat flux generally result in relatively small increases in surface temperature as compared to nonboiling convection. This has been observed widely (e.g., Ref. (15)).

(2) The vapor bubbles formed are transported by buoyant forces to the ullage volume quite rapidly. The extent to which this may occur is as yet uncertain, but may be anticipated to depend upon the degree of subcooling present, the pressure and the effective gravity level. These are implemented in the computational procedure by considering that should the tank wall temperature, and hence the liquid adjacent to the wall, exceed the existing saturation temperature by some arbitrary amount, this excess is eliminated by the evaporation of the appropriate amount of liquid directly into the ullage space. In effect, then, a portion of the vapor by passes the liquid-vapor interface. The arbitrary amount referred to above, the symbol for which is given as ΔT_{wmax} might be considered as the incipient boiling point, and no longer is arbitrary when sufficient information on its behavior is available.

They physical phenomena described above is simulated in the computer program as follows:

(1) The container wall temperature is calculated using Eq. (4).

(2) The liquid temperature is obtained using Eq. (51).

(3) The calculated wall temperature in the liquid region is examined. If it exceeds the saturation temperature by more than the prescribed temperature difference ΔT_{wmax} , it then is reduced such that it equals the saturation temperature plus the prescribed temperature difference.

(4) Part of the heat added to the liquid region appears as enthalpy in the wall and liquid and the rest is used for evaporating some of the liquid. The portion of the heat transferred to the liquid and resulting in evaporation is determined by setting an energy balance according to

$$\begin{aligned} & \int_0^X 2\pi a q_w(x,t) dx dt + \int_0^a 2\pi r q_{il} dr \\ &= \int_0^a \int_0^X 2\rho_l c_{pl} \pi r \frac{\partial T_l}{\partial t} dx dr + \int_0^X 2\pi a \delta \rho_w c_{pw} \frac{\partial T_w}{\partial t} dx + w_i h_{fg} \end{aligned} \quad (134)$$

where q_{il} is the rate of heat flow from the interface to the liquid and is given by,

$$q_{il} = k_l \left(\frac{\partial T_l}{\partial x} \right)_{x=X} \quad (135)$$

Equations (134) and (135) are used to determine the rate of evaporation from the interface, w_i .

If the difference between the wall temperature and the saturation temperature is less than the specified maximum, ΔT_{wmax} , then the procedure above is bypassed and computations proceed as described earlier. An implicit assumption in the use of this procedure is that the laminar flow conditions described by the momentum and energy equations are not affected. This may be reasonable if the container is relatively large compared to the "bubble boundary layer" region next to the wall. In other words, if the vapor bubbles remain in the vicinity of the wall, the major bulk laminar motion of the liquid will not be influenced by their movement to the ullage space. An accurate physical description of this behavior requires additional analytical and experimental investigation in incipient boiling and the departure and motion of vapor bubbles under low gravity fields with various patterns of subcooling.

D. COMPUTER PROGRAM

The computer program listing with the assumption of ideal gas behavior is given in Appendix A and a simplified flow sheet is shown in Appendix B. The MAD (Michigan Algorithmic Decoder) language is used here. In Appendix C are listed the meanings of the symbols employed, and Appendix D lists the

required program inputs. Appendix E presents the results for a single time step during the course of computations of a typical run, and includes the input conditions used.

VI. COMPUTATIONS

Computations were carried out using the program listing of Appendix A, varying several different parameters so as to demonstrate general trends. As a review, the general assumptions incorporated into this particular program are listed below.

A. GENERAL ASSUMPTIONS

1. Cylindrical tank having flat ends.
2. Acceleration or body forces act along the axis.
3. Two dimensional conditions prevail, with variations only along the axis and radially.
4. Laminar flow conditions within the entire container.
5. The vapor behaves as an ideal gas.
6. The liquid has constant properties except in the body force terms.
7. The tank side-wall is uniform in thickness and has constant properties. The wall is lumped in the radial direction but axial conduction is taken into consideration.
8. The imposed heat flux on the outside of the tank wall is uniform, but may differ in those portions in contact with the liquid and vapor.
9. The ends of the tank are adiabatic, and the heat capacity of the ends is neglected.
10. The grid size varies in the liquid and vapor region as liquid fraction changes, in order that a nodal point always exist at the liquid-vapor interface.
11. Initial conditions of uniform temperature and zero velocity exists within the container.
12. The Bond number is sufficiently large that a reasonable approximation to a flat liquid-vapor interface exists.

B. VARIATIONS POSSIBLE IN PROGRAM

By relatively minor modifications to the program, some of the above listed general assumptions can be relaxed, providing additional flexibility. In any case, however, axial symmetry must be maintained.

1. The imposed heat flux can be varied axially and with time.
2. Specified initial conditions of temperature and velocity can be utilized.
3. Specified heat flux to the tank ends, including variations with radius and time, and including heat capacity can be incorporated.
4. If the description of the physical process warrants, imposed temperatures of the container walls can be utilized, with variation axially and with time.

5. Axial variation of tank side wall thickness and variation of specific heat with temperature can be accounted for.

6. Radial variations in the tank wall temperature can be taken into consideration. This may be particularly desirable if the wall is of composite construction.

Although the influence of variations in liquid properties with temperature and pressure can be incorporated with minor changes, the use of real gas properties in the vapor space will require major modifications to the program.

Major modifications also are necessary to handle the spacewise variation of grid size in either the liquid or vapor domains.

C. VARIABLES

The variables listed below were maintained constant for the computations presented here:

1. Grid size: 21 Radial x 31 Axial Nodel Points
2. Tank Diameter: 5 feet
3. Tank Height: 10 feet
4. Tank Wall: Aluminum—0.01 feet thickness
5. Fluid: Liquid and Gaseous Oxygen, initially saturated at 15 psia, with zero velocity.

The grid size was made as small as possible for reasonable computational times on the IBM 7090 computer. It might be noted that decreasing the grid size by one-half would result in an increase in computational time by a factor of approximately 16.

The relation between real physical system time and computational time depends on a number of factors, but primarily on a/g level and heat flux. This arises from the stability requirement on the computational time interval—the higher the fluid velocity the smaller the time steps, hence the greater computer time required to cover a given amount of real time. For example, at $a/g = 10^{-5}$ and $q/A = 1$ BTU/hr-ft², 30 minutes of computational time results in 200 minutes of real time, for a ratio of approximately 7 to 1. On the other hand, at $a/g = 10^{-1}$ and $q/A = 1$ BTU/hr-ft², this ratio was 1 to 3.

The parameters listed below were varied in order to demonstrate their influence on the pressure rise and the mass of liquid evaporated:

1. ΔT_{wmax} : 0 to 4°F. This is the maximum permissible wall superheat. The value of zero corresponds to neglecting the the heat capacity of the container walls.
2. q/A : 1 to 72 BTU/hr-ft² imposed on wall. The heat flux to the liquid and vapor portions of the tank was made the same.
3. Ullage Fraction: 33% to 67%.
4. a/g : 10^{-1} to 10^{-5} .

D. RESULTS

1. Influence of ΔT_{wmax}

To demonstrate the influence of the specified maximum wall superheat, ΔT_{wmax} , on the computed pressure, computations were carried on for several values of this parameter at a relatively high and low heat flux.

Figure 7 shows the pressure rise and total mass evaporated for the heat flux of $q/A = 72 \text{ BTU/hr-ft}^2$. A continuing effect of ΔT_{wmax} up to 4°F is noted. The computer output listed finite nonzero values of the quantity designated DMB, indicating that evaporation was by-passing the liquid-vapor interface. It is anticipated that a sufficiently large value of ΔT_{wmax} exists such that a further change in it would produce no change in the pressure-time behavior. This resulting wall temperature would probably be considerably above the incipient boiling point, so that the results would have no physical significance.

Figure 8 shows the corresponding results with a relatively low heat flux $q/A = 1 \text{ BTU/hr-ft}^2$. No differences accrue when ΔT_{wmax} is changed from 1°F to 2°F , indicating that the "natural" wall superheat is less than 1°F for the given conditions. This is also demonstrated by the fact that the quantity DMB is zero for ΔT_{wmax} of 1°F and 2°F . The results for $\Delta T_{wmax} = 0$ correspond to the case where the heat capacity of the wall is neglected. After 120 minutes, it is noted that the rate of pressure rise is approximately the same for both cases where the wall heat capacity is considered and neglected, although the pressure level is somewhat different. It is also noted in the lower part of Figure 8 that the total mass evaporated levels off for $\Delta T_{wmax} = 0$. This also occurs with the high heat flux shown in Figure 7, and it is believed will occur with the low heat flux case for $\Delta T_{wmax} = 1^\circ\text{F}$, in Figure 8, at longer periods of time. Even though the rate of evaporation levels off, the rate of pressure rise continues. This is attributed to the increasing effect on pressure rise of the heat transfer to the ullage space as compared to the heat transfer to the liquid.

2. INFLUENCE OF HEAT FLUX

Figure 9 shows the influence of heat flux on pressure and mass evaporated for the case with $\Delta T_{wmax} = 0^\circ\text{F}$, which corresponds to neglecting the wall heat capacity. An additional heat flux of $q/A = 1 \text{ BTU/hr-ft}^2$ was used, but the effects were too small to be shown on Figure 9 because of the scale. A cross-plot of Figure 9 is shown on a log-log scale in Figure 10 for various time periods, with this additional data showing the effect of heat flux. It is noted that the pressure rise is approximately a linear function of heat flux. Whether this would hold for other values of initial ullage cannot be stated at this time. It might be anticipated that these results would be modified at the early periods of time with values of ΔT_{wmax} other than zero.

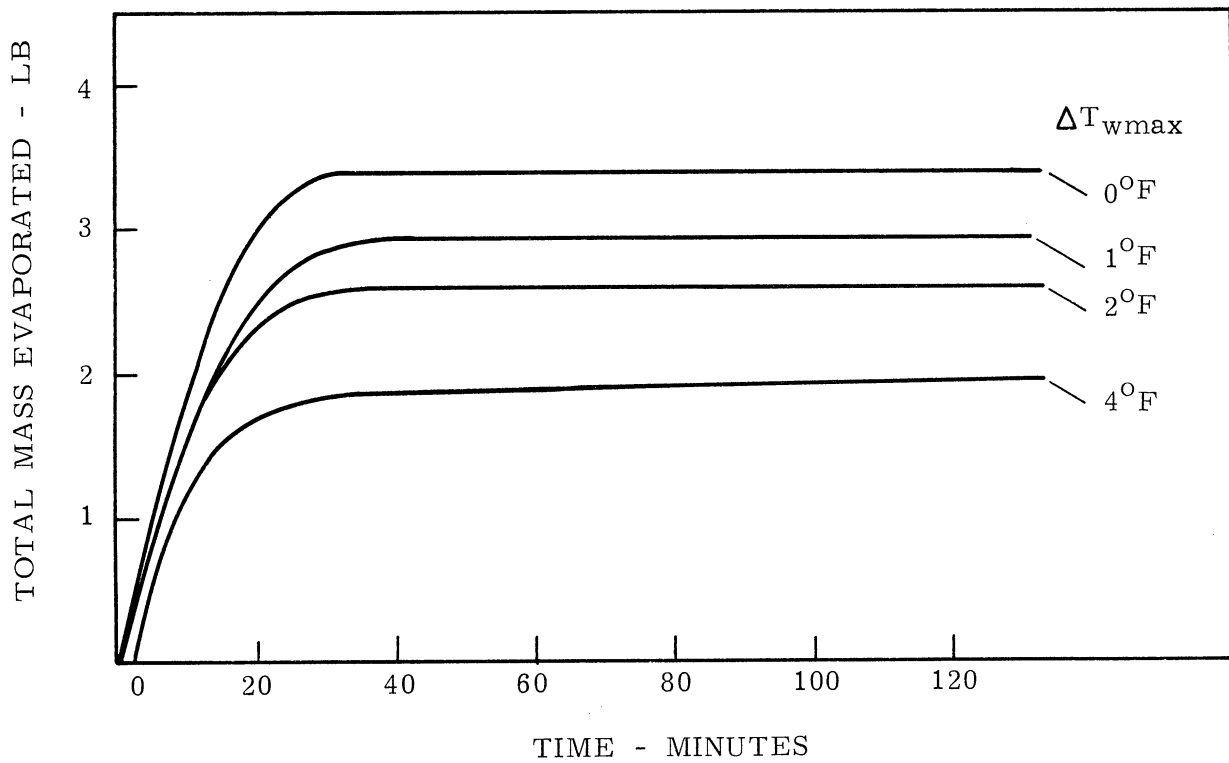
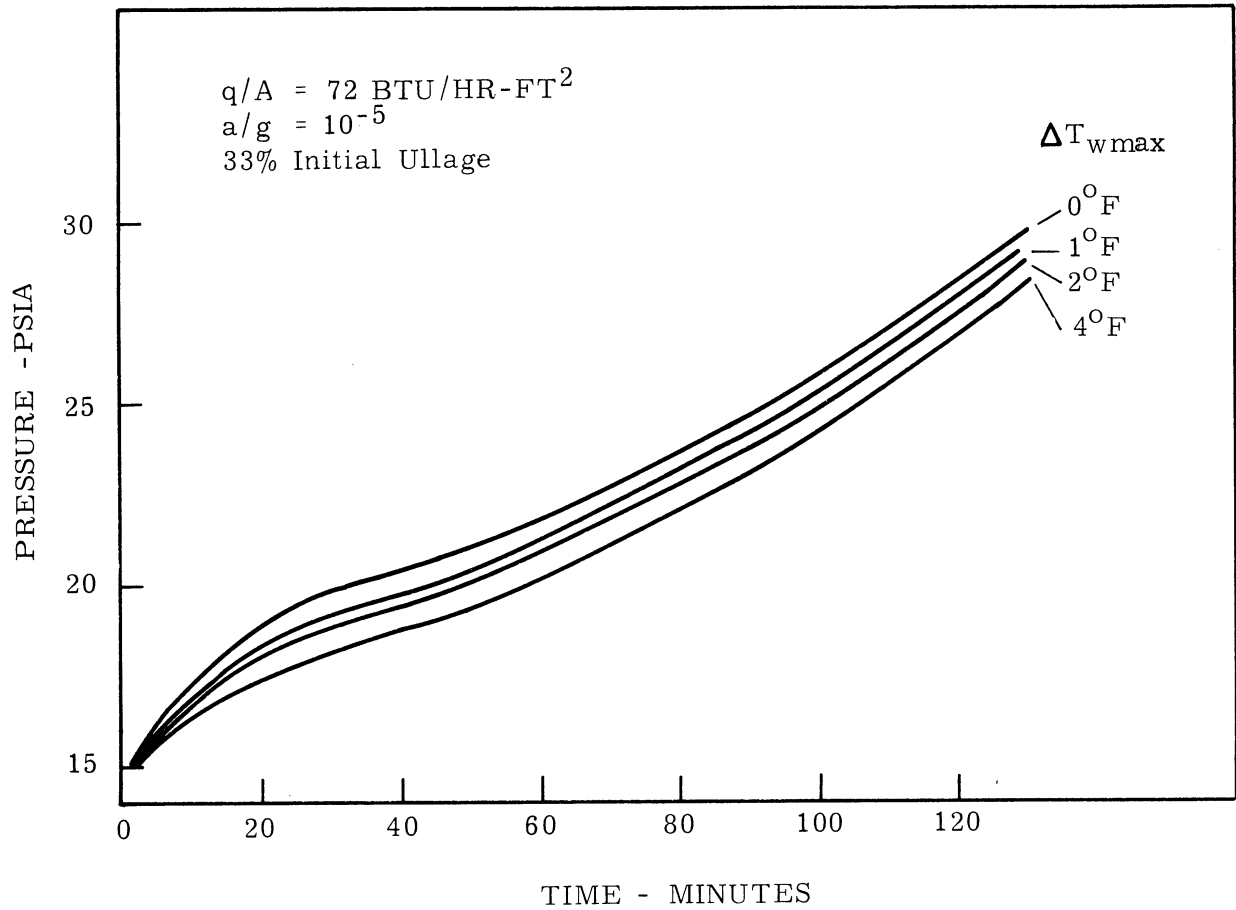


Figure 7. Total mass evaporated and pressure rise under high heat flux.

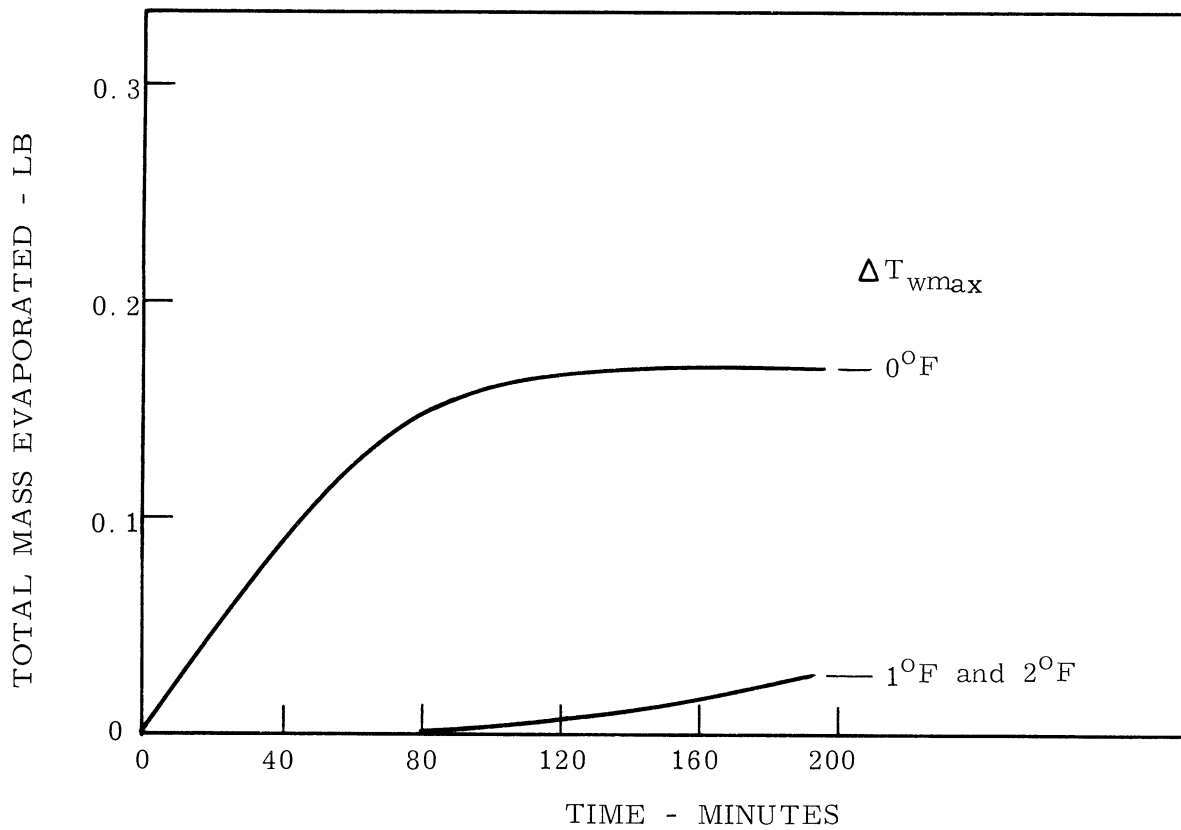
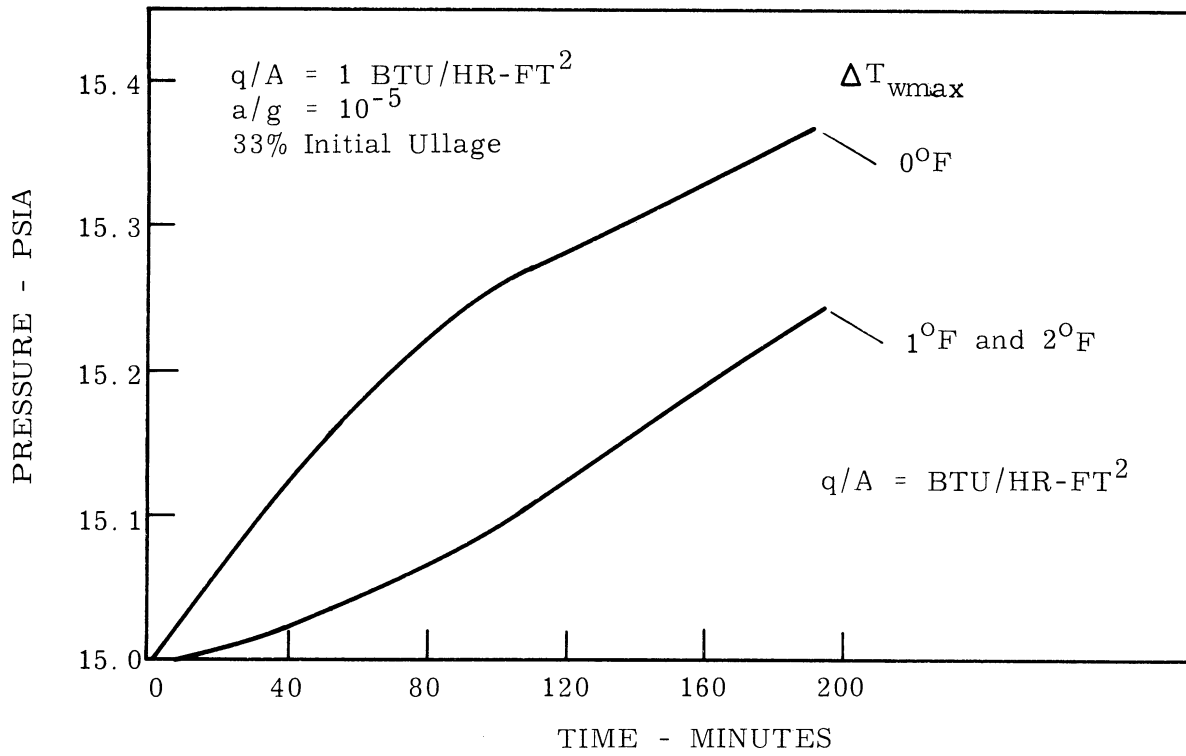


Figure 8. Total mass evaporated and pressure rise under low heat flux.

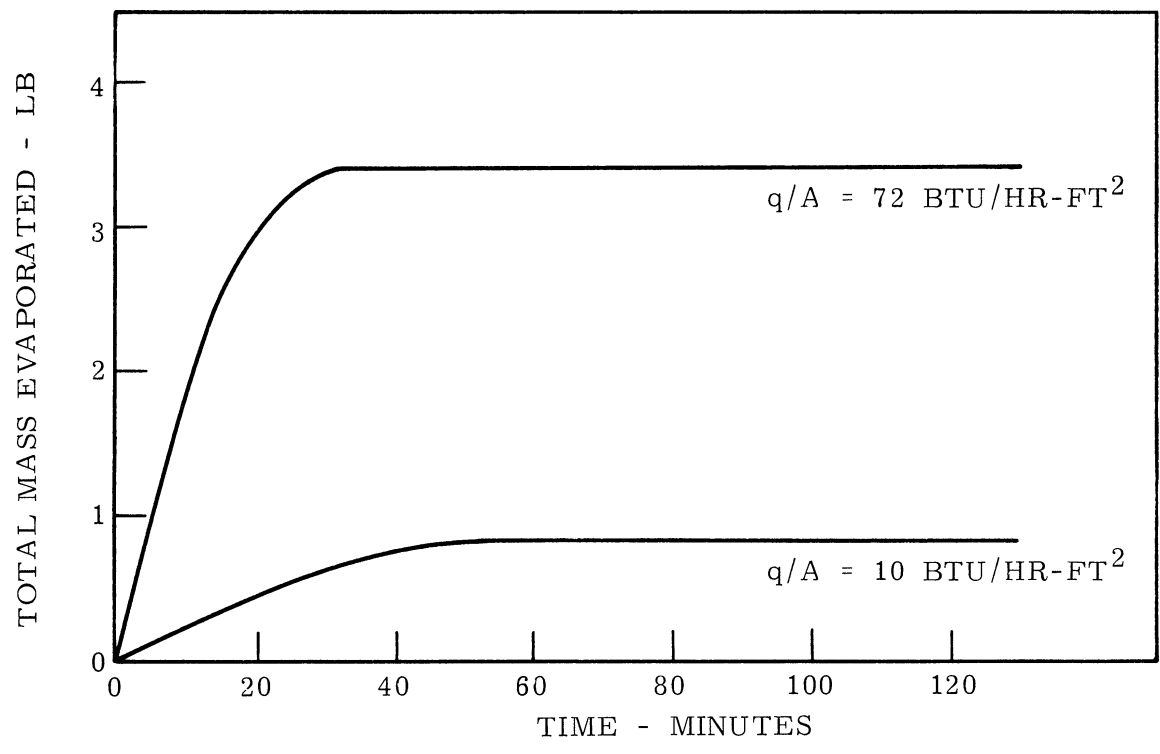
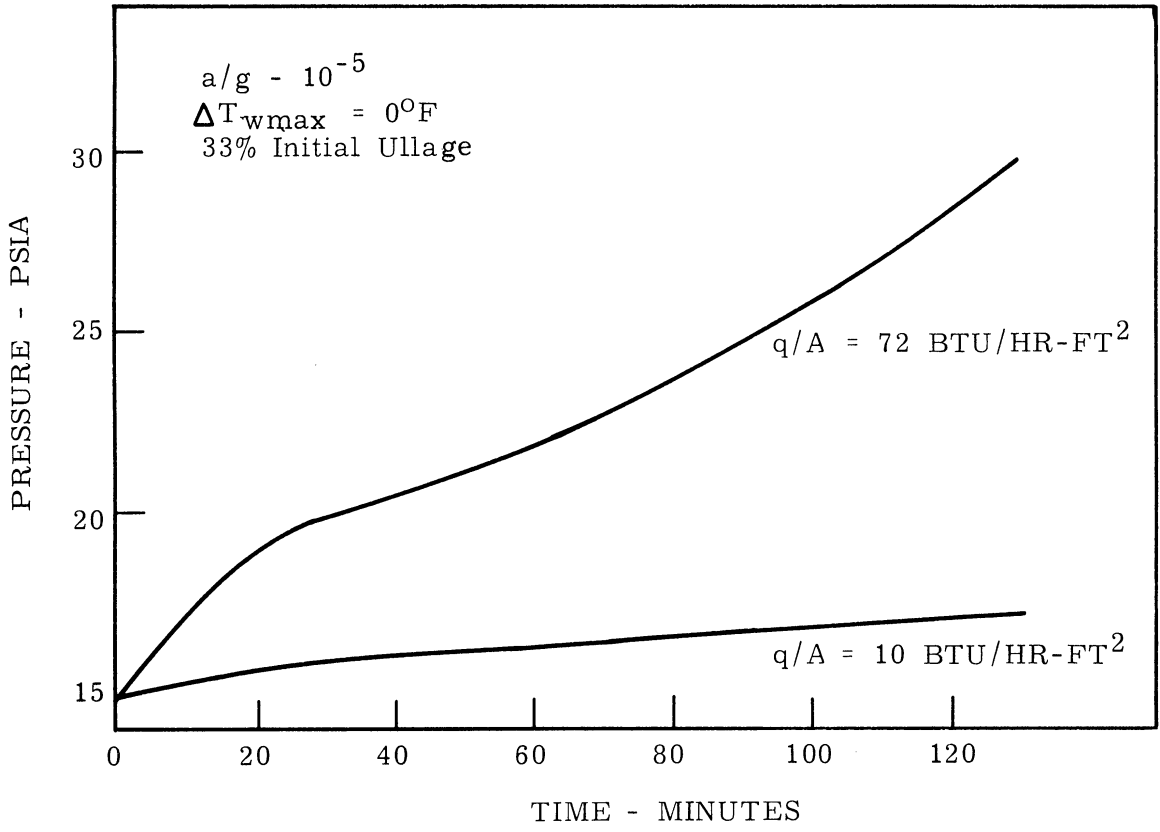


Figure 9. Effect of heat flux on pressure rise and mass evaporated.

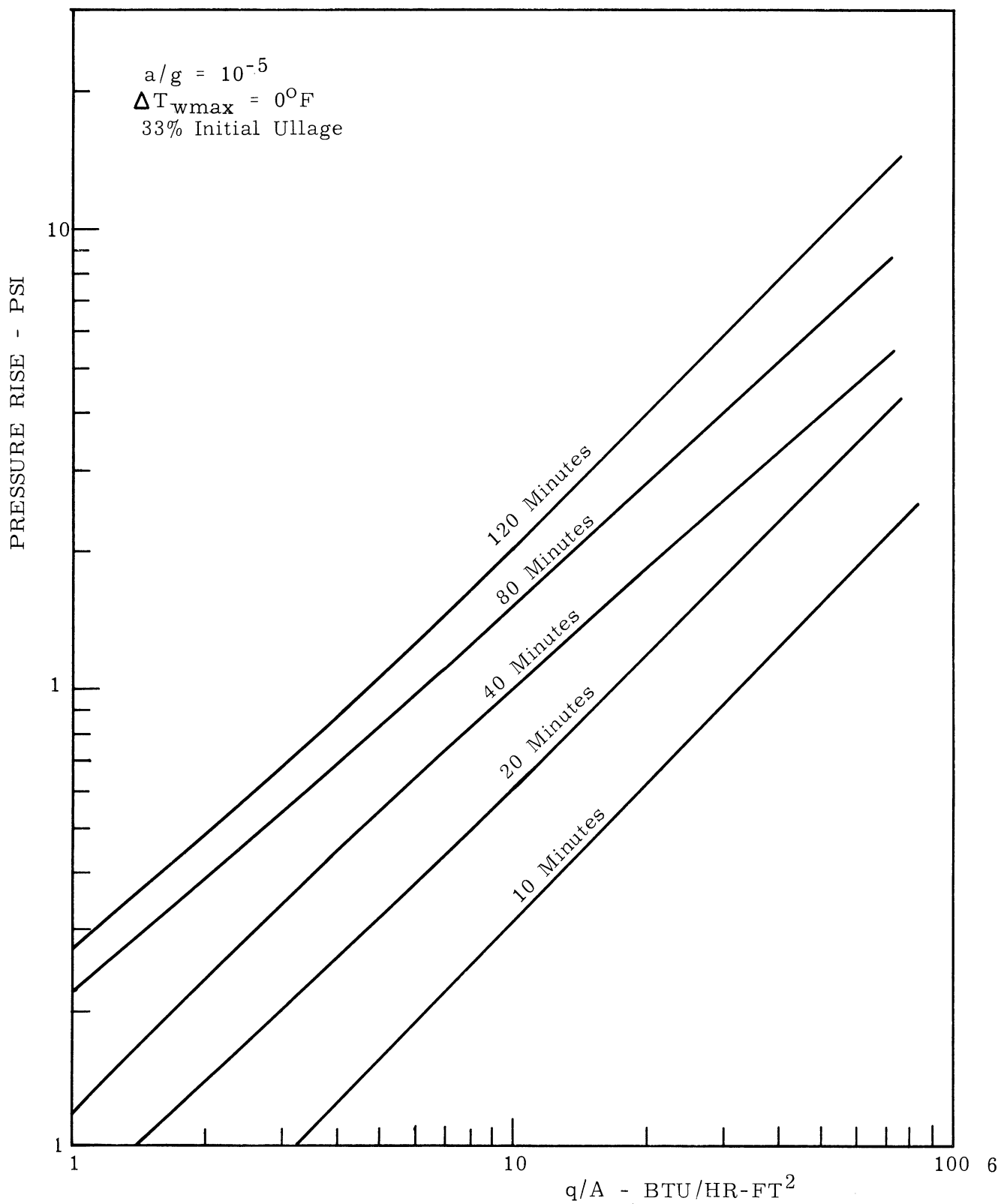


Figure 10. Effect of heat flux on pressure rise.

3. INFLUENCE OF ULLAGE FRACTION

Figure 11 shows that the influence of initial ullage volume on pressure rise and mass evaporated for the case where $q/A = 1 \text{ BTU/hr-ft}^2$, $a/g = 10^{-5}$, and $\Delta T_{wmax} = 1^\circ\text{F}$. In this case the wall superheat never reaches the specified maximum value of $\Delta T_{wmax} = 1^\circ\text{F}$, and hence all of the evaporation takes place at the liquid-vapor interface. In terms of the computer program the quantity DMP is always zero.

Figure 12 is a crossplot of Figure 11 for three levels of time. It is noted that the rate of pressure rise increases as the initial ullage fraction increases. This is contrary to the trend observed in an experimental study (9), and may indicate that the level of heat flux is an additional factor governing the effect of ullage volume. Added to the upper part of Figure 11 are the cases for 100% ullage, as computed from Eq. (83), and 0% ullage consistent with the assumption of an incompressible liquid. The behavior of the intermediate values of ullage is consistent with these limits.

It is further noted from Figure 11 that after an initial starting transient of approximately 100 minutes that both the pressure and mass evaporated become essentially linear functions of time.

4. INFLUENCE OF ACCELERATION LEVEL

The effect of acceleration or body force level on the pressure rise and mass evaporated is shown in Figure 13. Again, the wall superheat never reaches the specified maximum value of $\Delta T_{wmax} = 1^\circ\text{F}$. As might be anticipated, increasing the acceleration level increases both the pressure rise rate and the interface evaporation rate, owing to the increasing convective velocities induced in both the liquid and vapor.

Figure 13 also demonstrates, as discussed earlier, the relation between computational time and real time. In each of the three cases shown the computational time was 30 minutes. The increased fluid velocities associated with the larger body forces result in smaller incremental time steps from the stability requirements. If the body forces present in a particular physical application are considerably smaller than $a/g = 10^{-5}$, as in deep space probes, it can be anticipated that the behavior for long periods of real time can be described with reasonably small amounts of total computer time.

5. REPRESENTATIVE TEMPERATURE PROFILES

In Figure 14 a-e are plotted the axial temperature distribution for several levels of time, for five different radial locations from the center-line to the wall. All temperatures are expressed as the temperature increase above the initial temperature.

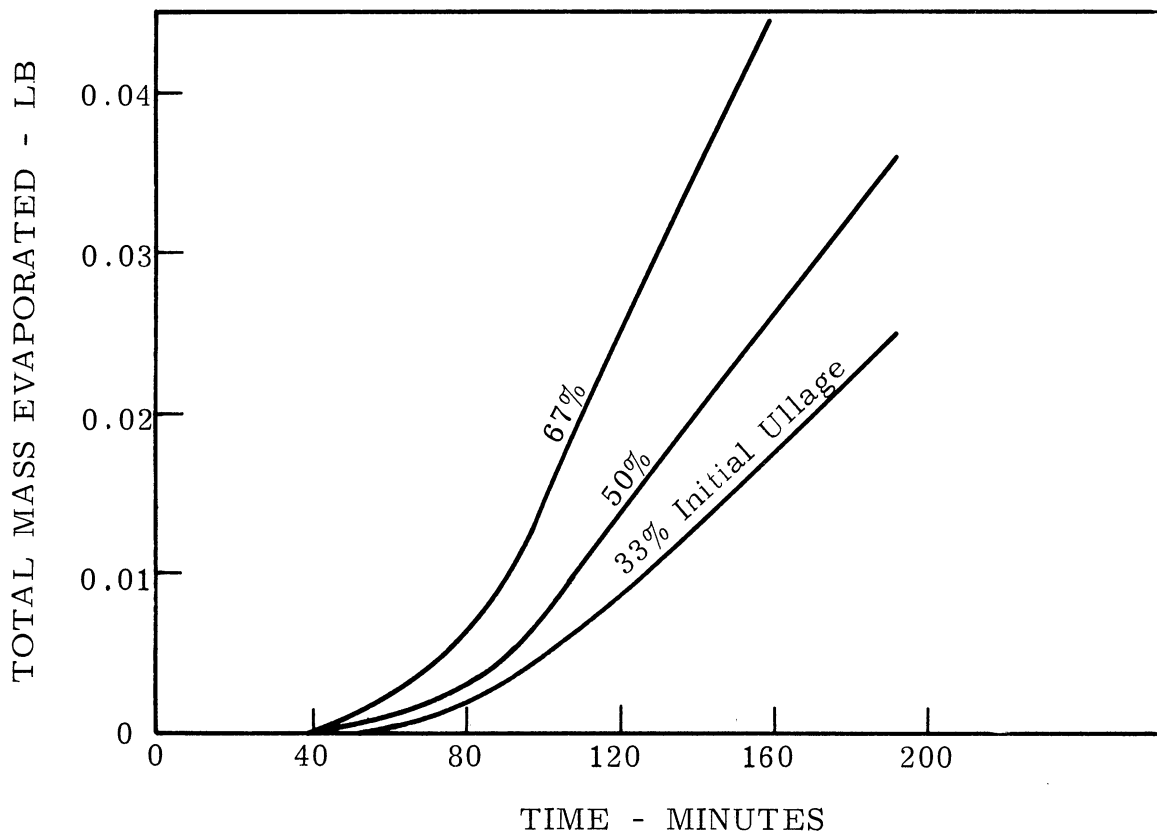
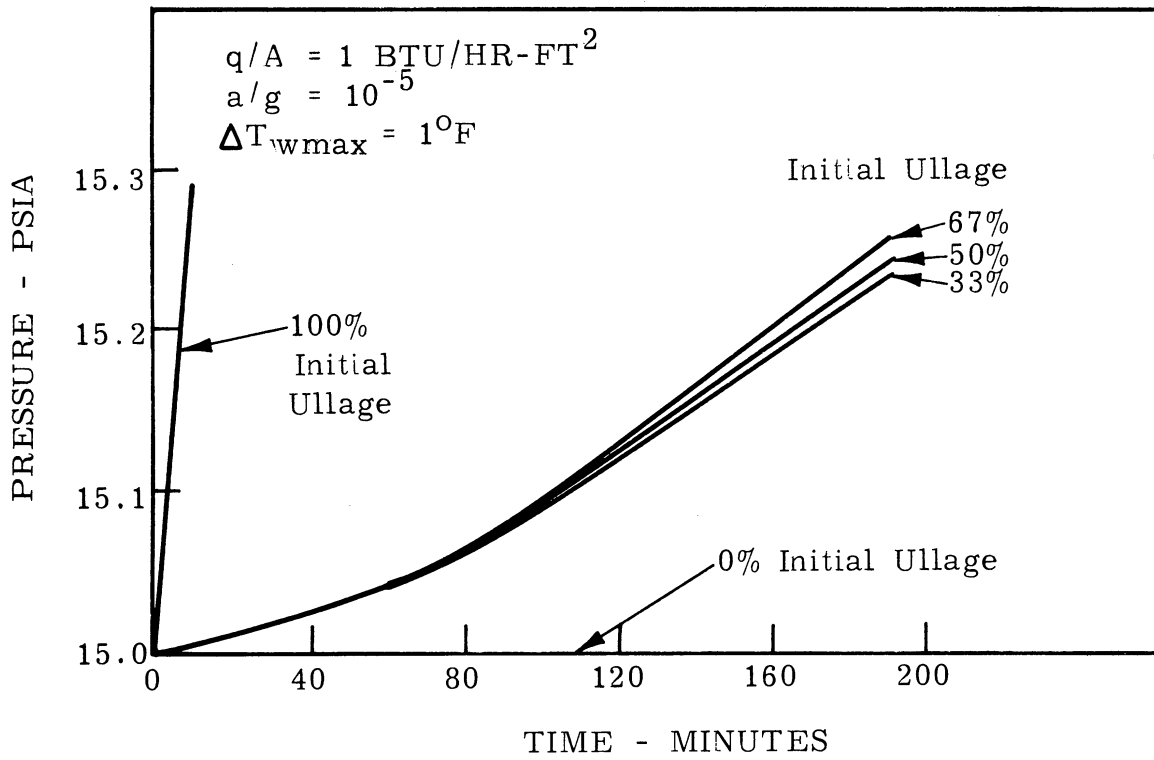


Figure 11. Effect of initial ullage on pressure rise and mass evaporated.

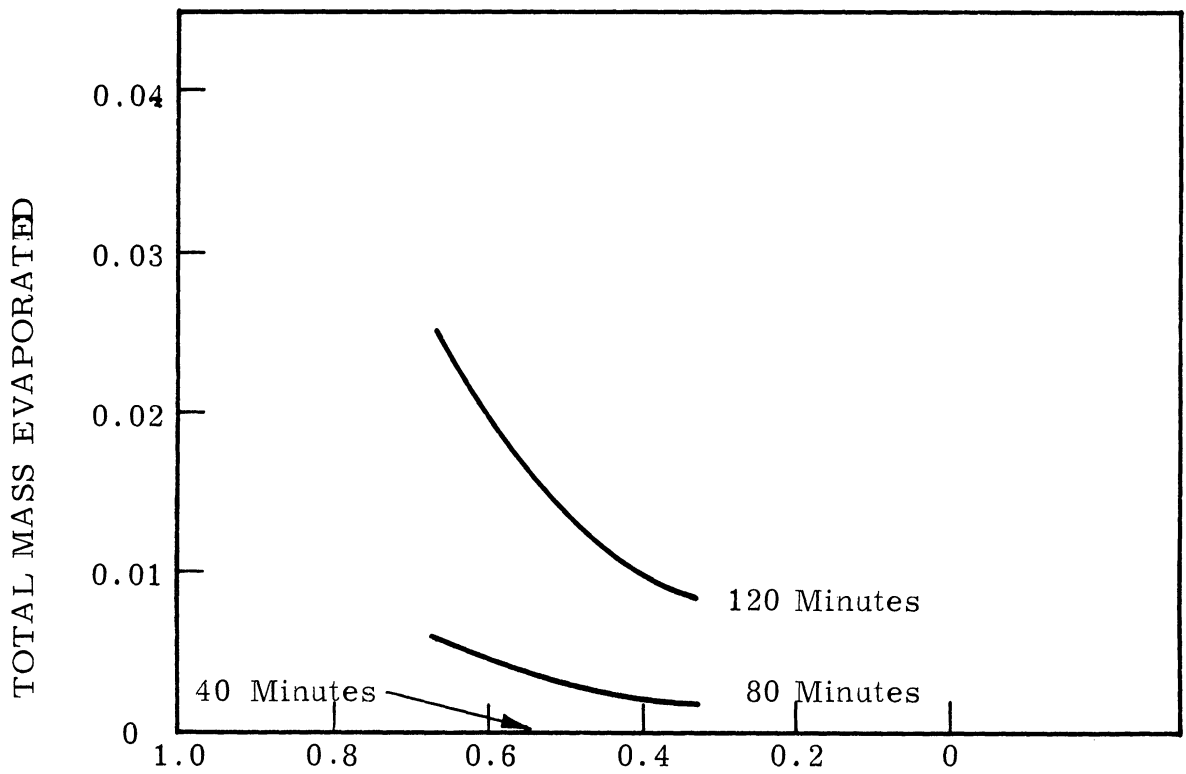
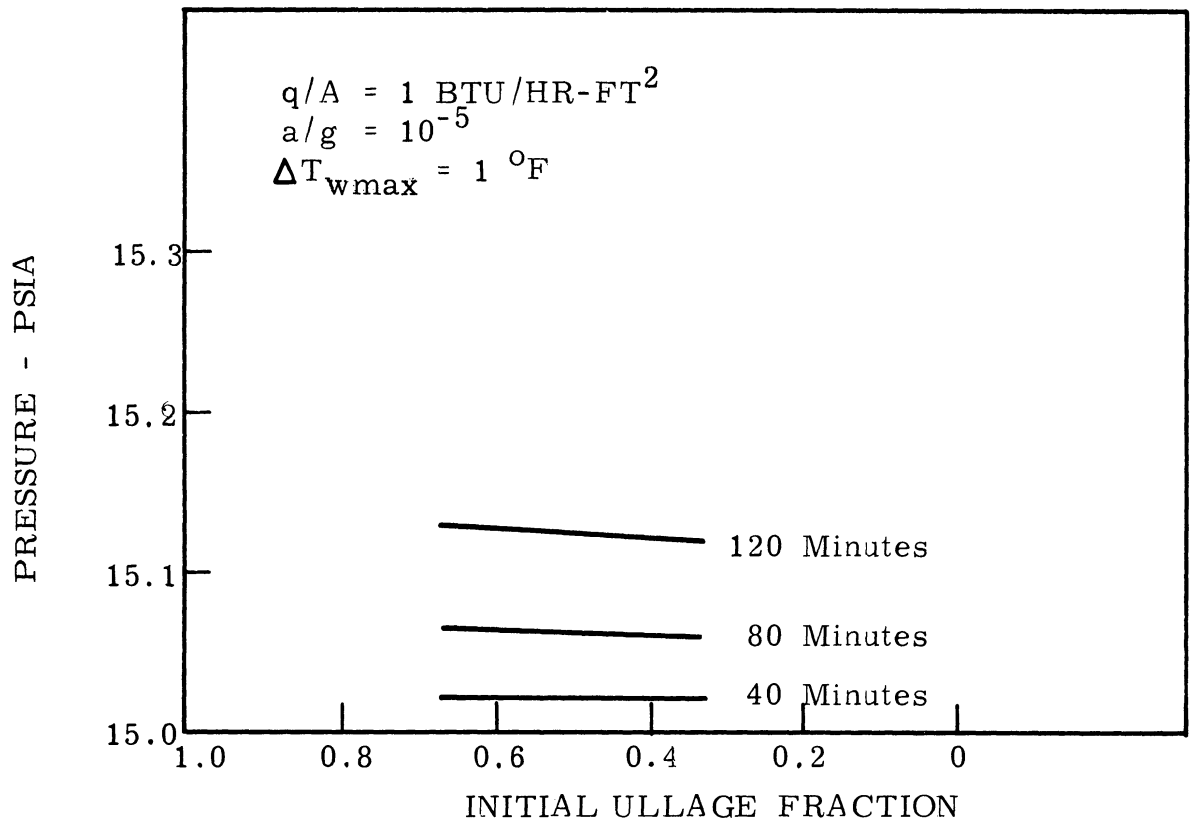


Figure 12. Effect of initial ullage on pressure rise and mass evaporated.

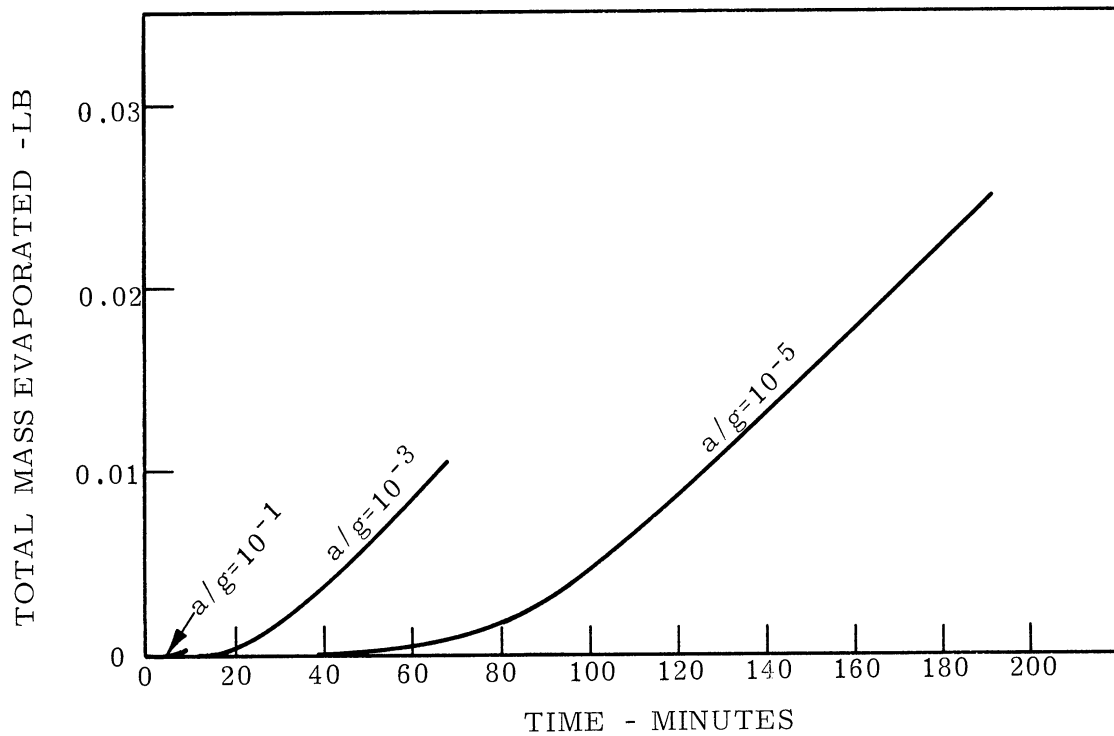
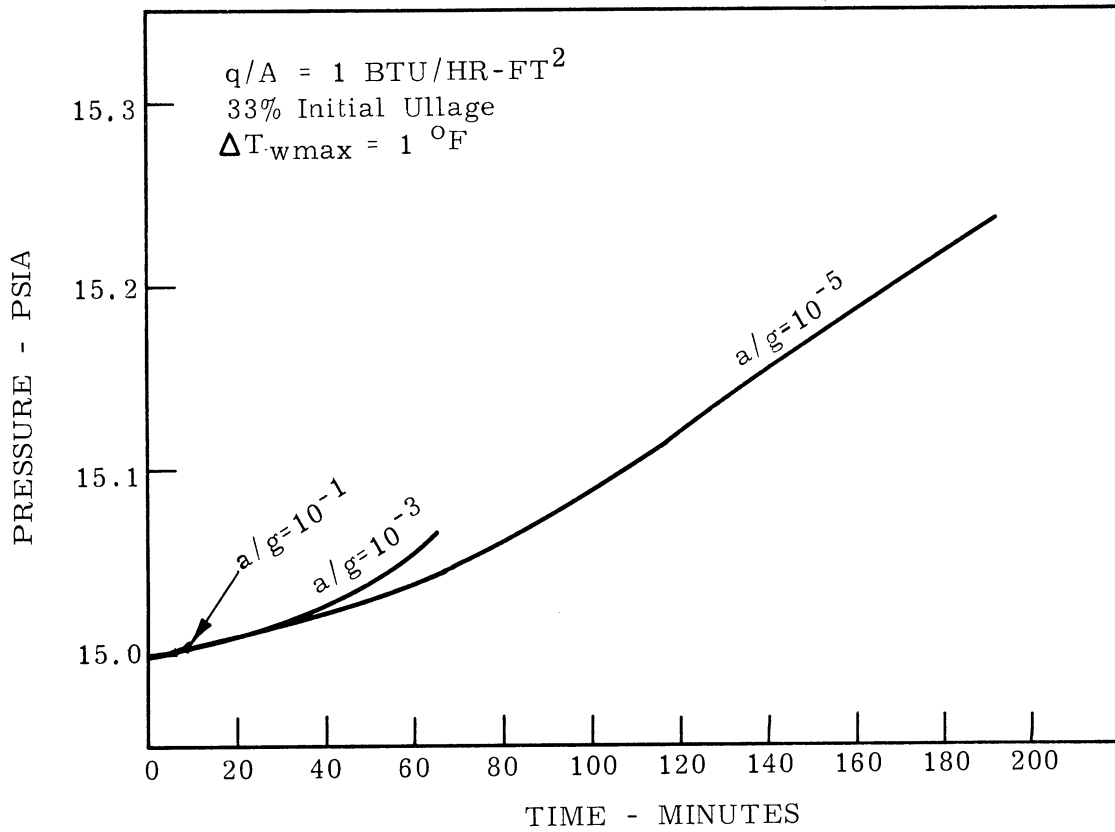


Figure 13. Effect of acceleration on pressure rise and mass evaporated.

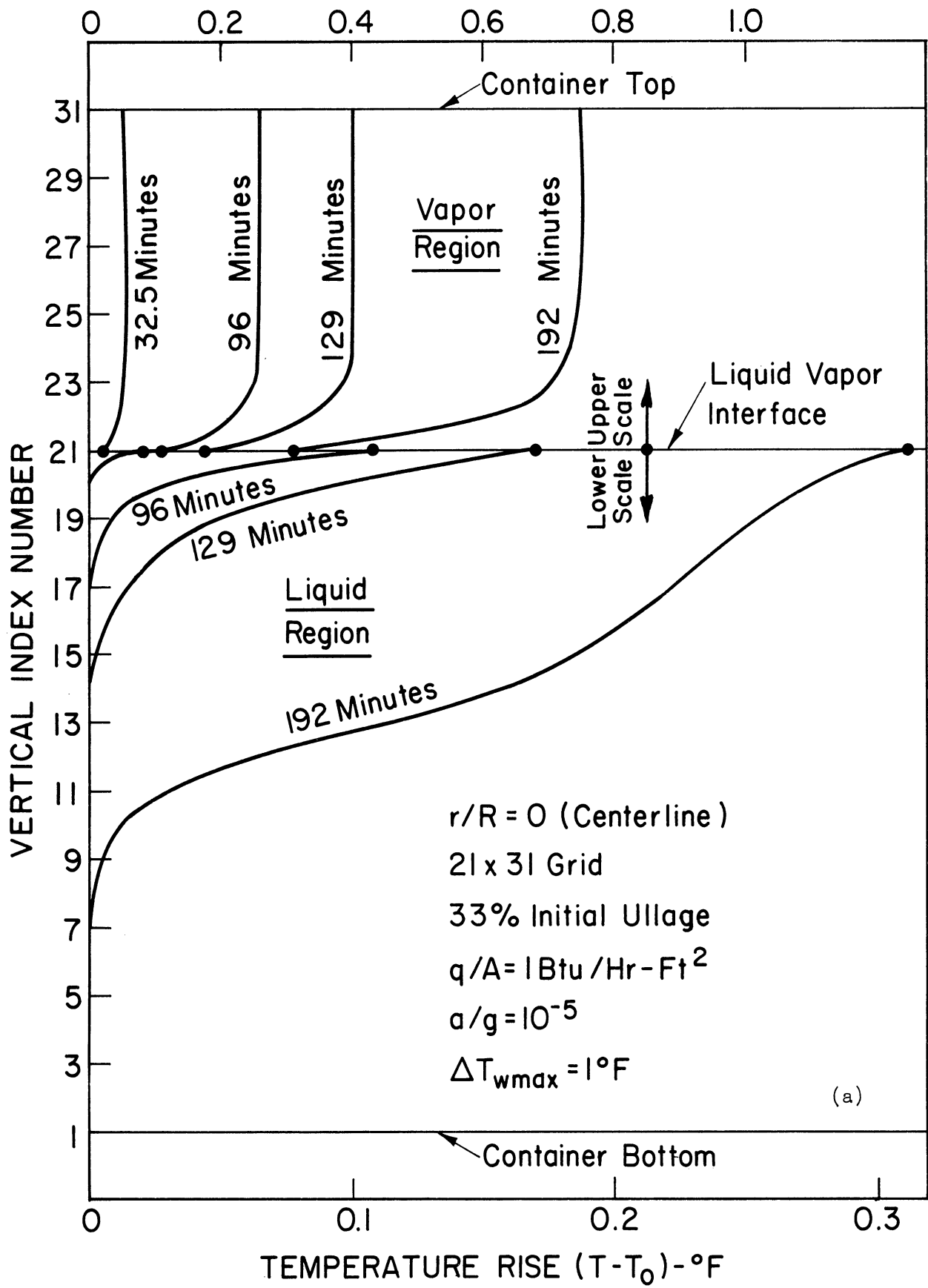


Figure 14. Axial temperature distribution.

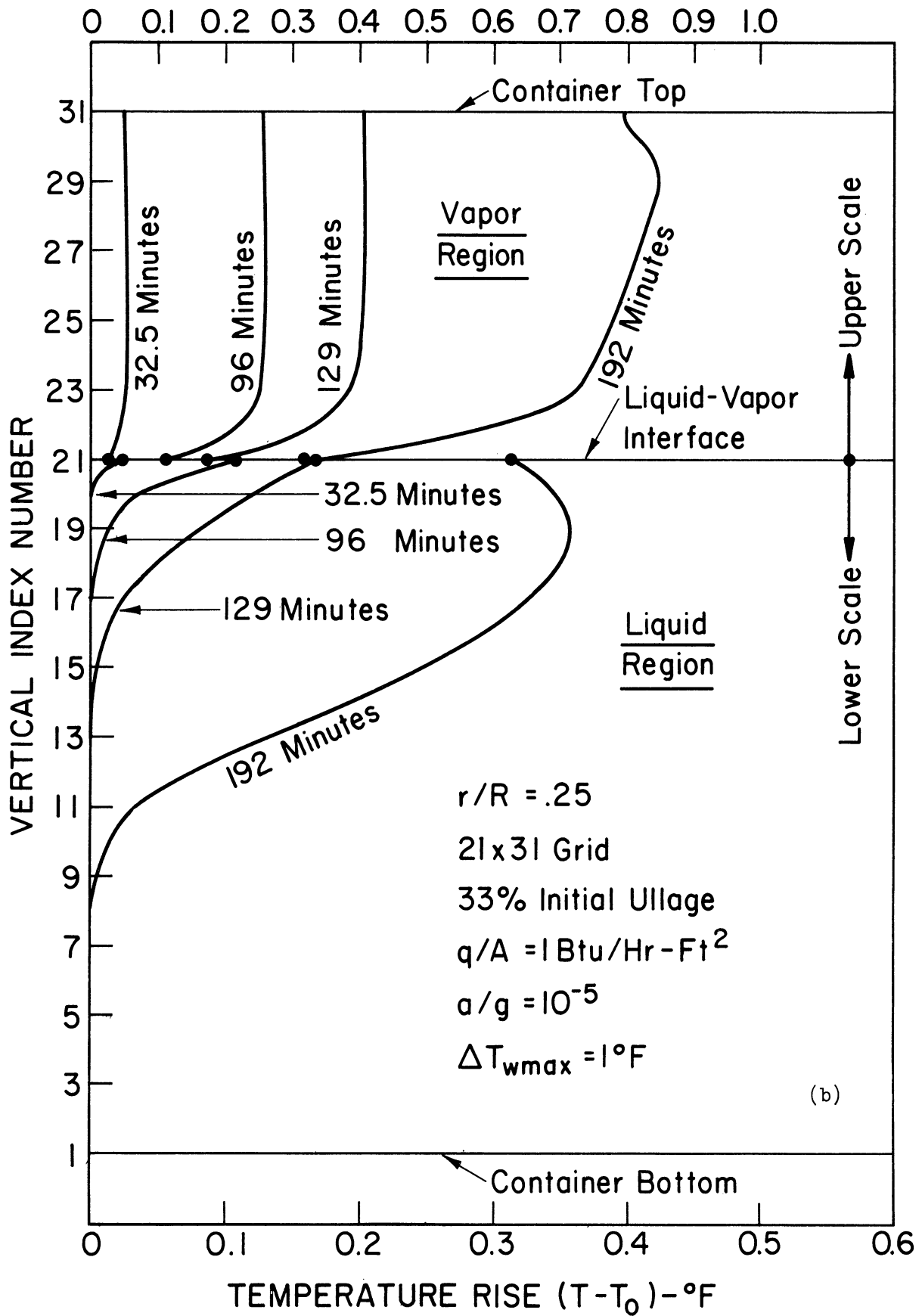


Figure 14. (Continued).

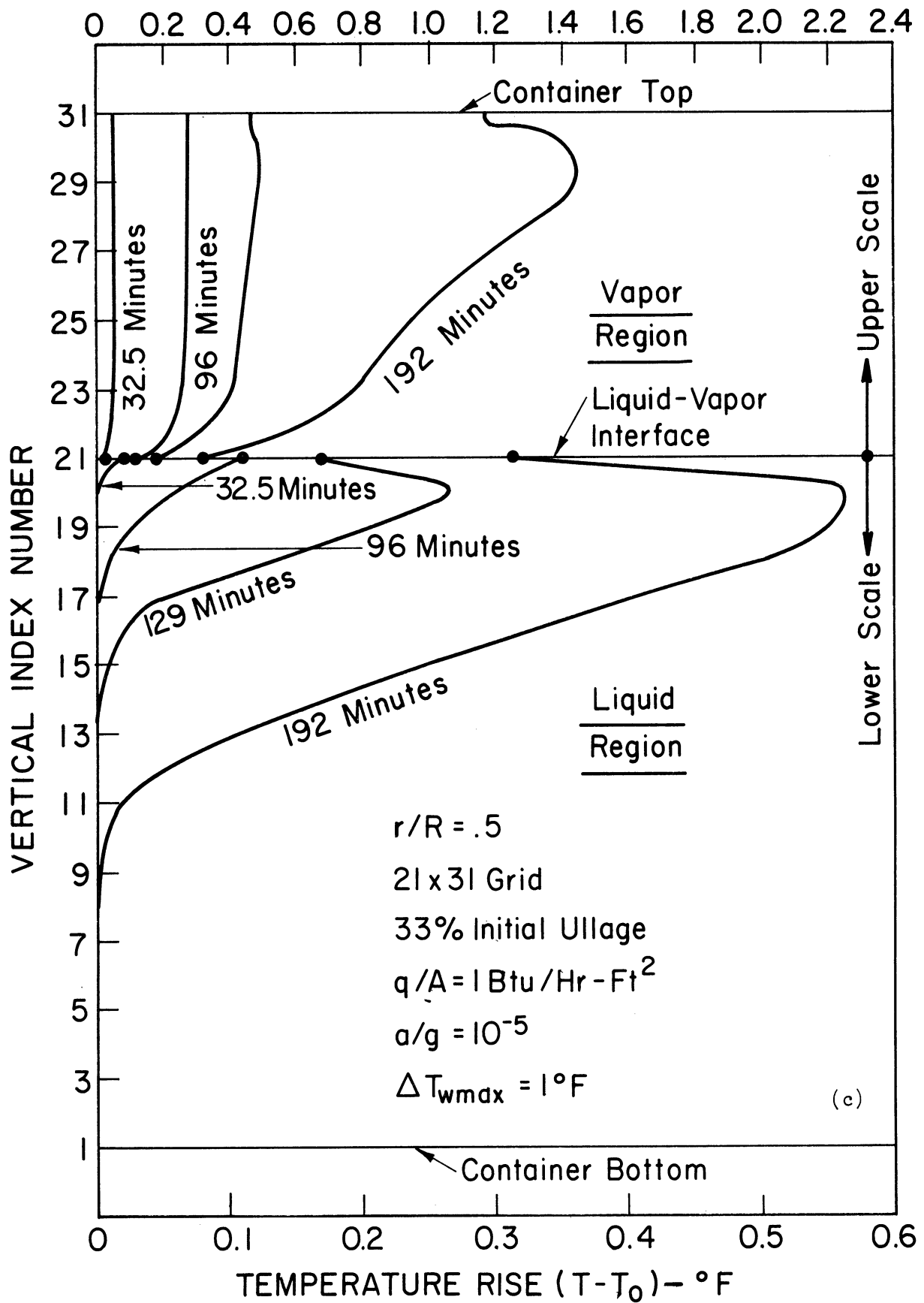


Figure 14. (Continued).

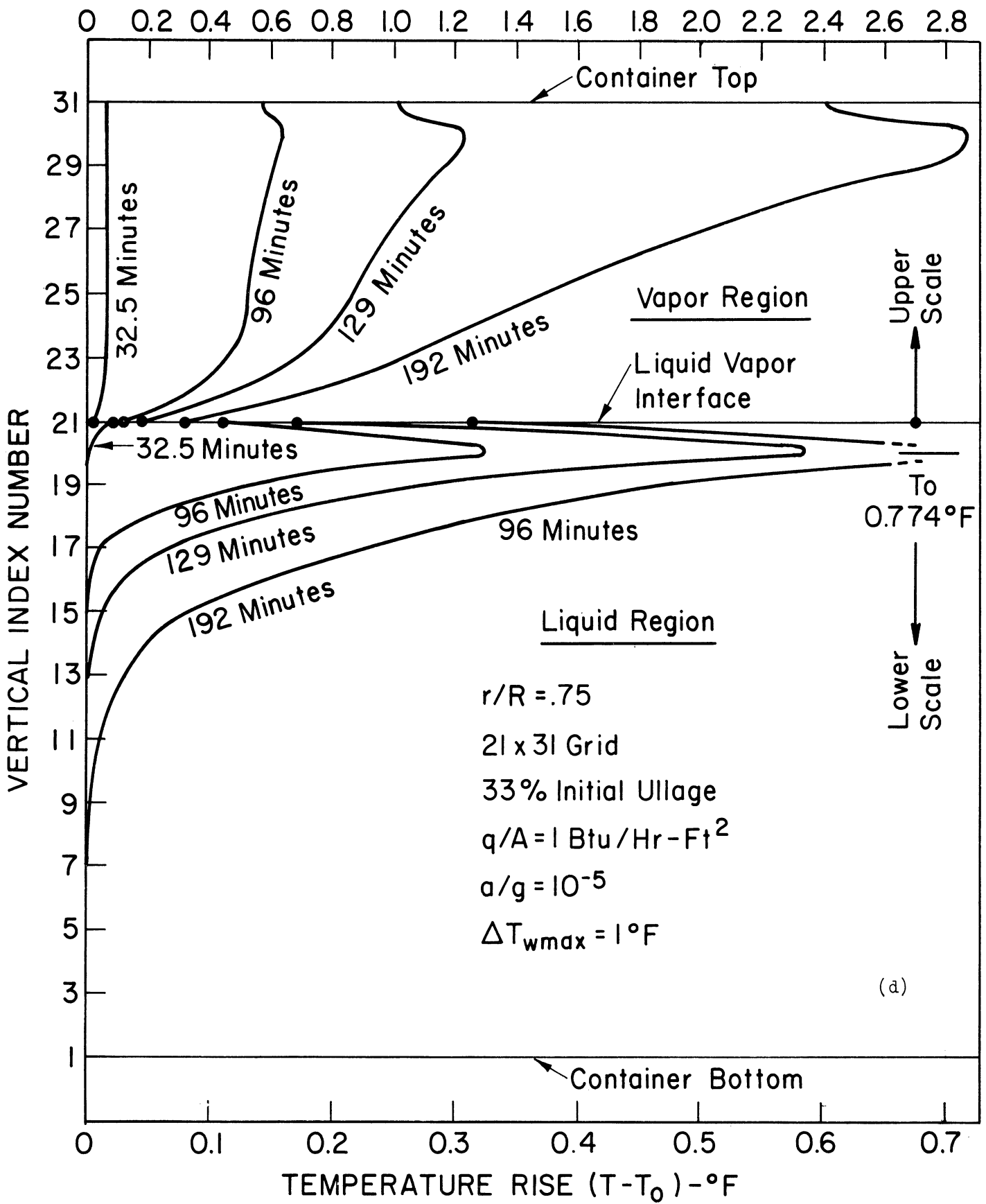


Figure 14. (Continued).

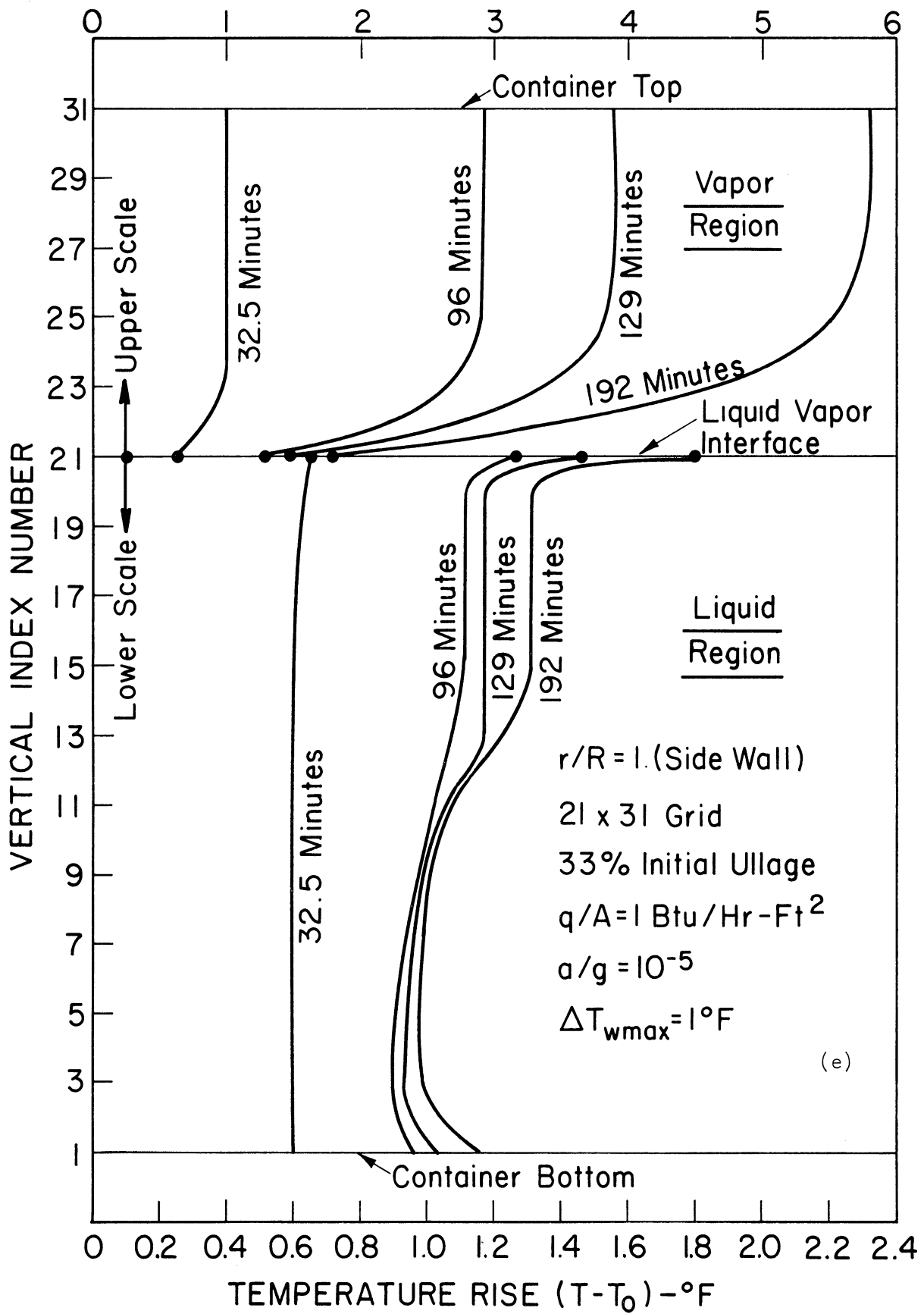


Figure 14. (Concluded).

The relatively rapid increase in temperature of the ullage space as compared to the liquid region is noted. In fact, about one half of the liquid undergoes no change in temperature at all during this period of time. The temperature gradients near the centerline are such that condensation may be taking place there simultaneously with evaporation toward the walls. Of particular interest is the superheated layer of liquid existing just below the liquid-vapor interface at the later time periods in Figures 14 b-d.

The influence of the stagnation region in the tank is observed in the lower part of Figure 14e.

In Appendix E the computer input and output are reproduced for the case represented in Figures 14 a-e, for computational step number 154, which corresponds to a total elapsed real time of 192 minutes.

APPENDIX A
COMPUTER PROGRAM LISTING

MAD (17 MAY 1967 VERSION) PROGRAM LISTING

```

DIMENSION U( 980,DIM),V( 980,DIM),T( 980,DIM),SF( 980,DIM),
1 W( 980,DIM),IO( 980,DIM),WC( 980,DIM),SEI(31),
2 EJ(31),F(31),DI(31),DR1(31),DR2(31),CR3(31),DR4(31),RI(31),R
3 2(31),R3(31),R4(31),R5(31),A1(31),A2(31),A3(31),C2(31
4 ),C1( 980,DIM),C3( 980,DIM),EJL(31),D1(31),D2(31),R6(31),CR6
5 (31),UL(31),DR5(31),DR6(31),DR7(31),DR8(31),R6(31),A4(31)
6 ,VG(31),RG( 980,DIM) , DTCRW(46) , DTCXG(31),UO( 980,DIM),VC( 5
7 80,DIM),DIDX(31),HL(31),HG(31),C4( 980,DIM)
VECTOR VALUES DIM=2,I,0
INTEGER I,J,M,N,NT,NE,NE1,NE2, L ,NR,NC,H,P,J1,J2,I1,I4,NP,
1 N1,N2,N3,IAUL,NMAX
EXECUTE FTTRAP.
READ AND PRINT DATA
DIM(2)=N+1
EXECUTE ZERO.(U(I,1)..U(P+1,N+1),V(I,1)..V(P+1,N+1),T(1,1)
1 ..T(P+1,N+1), SF(1,1)..SF(P+1,N+1), W(1,1)..W(P+1,N+1),
2 TO(1,1)..TO(P+1,N+1),NT,TIME,NE1,NE2,N2,U,TAU,
3 UL(0)..UL(N+1),DTCXG(0)..DTCXG(N+1),DTCRW(0)..DTCRW(N+1),
4 RO(1,1)..RO(P+1,N+1),PI,UO(1,1)..UG(P+1,N+1),VG(1,1)..VC
5 (P+1,N+1),DMT,DMB,DM,AC,MC,C4(I,1)..C4(N+1,N+1),NP1,DMB )
I1=M/2+1
Y=AOVERB
PR=NEW/ALPHA
PRV=NEWV/ALPHAV
RNEW=NEWV/NEW
RALPHA=ALPPAV/ALPHA
DR=1.0/N
DR2=DR*DR
GAM=CPV/CV
DYY=2.0*DR2
DR6=DR2/2.0
PRESS=PC
TSAT=C5*(PRESS.P.C6)
TINIT=C5*(PO.P.C6)
CONST = A*/ALPHA
CONST1=Y*PR*G*BEITA*(A.P.3)/NEW/NEW
CONST2=1.0/CONST
CONST3=1.0/CONST1
PRINT RESULTS CONST , CCNST2 , CCNST1 , CCNST3,PR,PRV
M1=AOVERB*QSURFL*(A.P.5)*BEITA*G/ALPHA/ALPHA/NEW/ROW/CPW
1 /DELTA
M2=KL*A/ALPHA/ROW/CPW/DELTA
M3=KG*A/ALPHA/ROW/CPW/DELTA
M7=AOVERB*QSURFG*(A.P.5)*BEITA*G/ALPHA/ALPHA/NEW/ROW/CPW
1 /DELTA
M5=CONST1*TINIT
D2R=DR/2.0
AOVRB2=AOVERB*AOVERB
THROUGH CC,FOR J=2,I,J.G.N+1
A1(J)=DR2*DR2*(J-1.)*(J-1.)
C2(J)=1.+(2.*(J-1.))
A4(J)=1.0/(J-1.0)/DR/4.0
R1(J)=12*(J-1.0)*DR2

```

*CC1
*C01
*CC1
*C01
*CC1
*C01
*C02
*C03
*C04
*C05
*C06
*C07
*C07
*C07
*C07
*C07
*C08
*C09
*C10
*C11
*C12
*C13
*C14
*C15
*C16
*C17
*C18
*C19
*C20
*C21
*C22
*C23
*C24
*C25
*C26
*C27
*C27
*C28
*C29
*C30
*C30
*C31
*C32
*C33
*C34
*C35
*C36
*C37
*C38

01
01
01
01

CC

```

*039
*040
*041
*042
*043
*044
*045
*046
*047
*048
*049
*050
*051
*051
*051
*051
*052
*053
*054
*055
*056
*057
*058
*059
*060
*061
*062
*063
*064
*065
*066
*067
*068
*069
*070
*071
*072
*073
*074
*075
*076
*077
*078
*079
*080
*081
*082
*083
*084
*085
*086
*087
*088
*089
*090
*091
*091
*091
*091
*092
*093

```

```

THROUGH GAST, FOR I=M+1, I, I.G.P+1
THROUGH GAST, FOR J=1, I, J.G.N
T(I, J)=0
WHENEVER CODE .E. 1
READ FORMAT INPUT, A, PRESS, PC, X, NI, TIME, U,
T(I, I)...T(P+1, N+1), SF(1, I)...SF(P+1, N+1)
THROUGH HUSS, FOR I=1, I, I.G.P+1
THROUGH HUSS, FOR J=1, I, J.G. N+1
T(I, J)=T(I, J)
END OF CONDITIONAL
N3=1
PI=PRESS
NT=NT+1
HFC=.00745*(-1.1383*(TSAT-180)*(TSAT-198)*(TSAT-216)+3.238*
1 (TSAT-162)*(TSAT-158)*(TSAT-216)-3.025*(TSAT-162)*(TSAT-180)
2 *(TSAT-216)+.925*(TSAT-162)*(TSAT-180)*(TSAT-198))
I=(P+M)/2+1
J=N/2+1
BEITAG = 1./((TINIT+T(I, J))/CCNSTI1)
M4=(GAM-1)/GAM
DX=X/M
CX2=DX*DX
DZ=(1-X)/(P-M)
DZ2=DZ*DZ
DRZ=DR2/DZ2
A3=DRZ*Y*Y
BJ1=2.*(1+A3)
CXR=DX2/DR2
DRX=CR2/DX2
A1=DRX*Y*Y
A2=DXR/Y*Y
DZ2=.5
ZVDR2=Z/2+.0
BJ=2.*(1.+A1)
BO=2.0*PR*Y*Y/DR2+2.C*PR/DRZ
EJ(I)=0
EJ(1)=0
THROUGH JE, FOR J = 2, I, J .G. N+1
A2(J)=DX2*DR2*(J-1.)*(J-1.)/Y/Y
A3(J)=DX2/Y/Y/(J-1.)/DR2/2.
D1(J)=BJ-C2(J)*EJ(J-1)
R2(J)=12*(J-1.)*DR*DX
D2(J)=BJ-C2(J)*EJ(J-1)
EJ1(J)=(1-1/(2.C*(J-1.C)))/D2(J)
R4(J)=Y*Y/(J-1.)/(J-1.)/DR2/EX2/2.
R5(J)=Y*Y/(J-1.)/(J-1.)/DR2/DZ2/2.
R6(J)=12*(J-1.)*DR*DX
EJ(J)=(1-1/(2.0*(J-1.0)))/D1(J)
WHENEVER CODE .E. 1
THROUGH FOUR, FOR J=2, I, J.G.N
SF(M+1, J)=0
THROUGH MMM, FOR I=2, I, I.G.M
THROUGH MMM, FOR J=2, I, J.G.N
W(I, J)=(SF(I+1, J)-2.*SF(I, J)+SF(I-1, J))*Y*Y/DX2-(SF(I, J+1)-
1 SF(I, J-1))/DR2/(J-1.0)/2+(SF(I, J+1)-2.C*SF(I, J)+SF(I, J-1))/
2 DR2)/DR2/(J-1.0)/(J-1.0)
THROUGH QQQ, FOR I=2, I, I.G.M
W(I, N+1) = (8.*SF(I, N)-SF(I, N-1)-7.*SF(I, N+1))/DY

```

```

THROUGH QQQQ, FOR I=M+1,1,I.G.P+1
THROUGH QQQQ, FOR J=1,1,J.G.N+1
RD(I,J)=CONST1*PRESS#144./RGAS/(I(I,J)+M5)
THROUGH QQQQ, FOR I=M+2,1,I.G.P
W(I,N+1)=(8*SF(I,N)-SF(I,N-1)-7*SF(I,N+1))/DYV/RC(I,N+1)
UG=-U*(ROL/RO(M+1,1)-1.0)
THROUGH FIVE, FOR J=2,1,J.G.N+1
SF(M+1,J)=RO(M+1,J)*UG*DR2*(J-1.0)*(J-1.0)/2.0
THROUGH WWW, FOR I=M+1,1,I.G.P
U(I,N)=2.*(3*SF(I,N)-6*SF(I,N-1)+SF(I,N-2))/RI(N)/RC(I,N)
U(I,1)=SF(I,2)/DR6/RO(I,1)
U(I,2)=2.*(6*SF(I,3)-SF(I,4)-3.*SF(I,2))/R1(2)/RO(I,2)
THROUGH WWW, FOR I=M+1,1,I.G.P
THROUGH WWW, FOR J=3,1,J.G.N-1
U(I,J)=(SF(I,J-2)-8*SF(I,J-1)+8*SF(I,J+1)-SF(I,J-2))/R1(J)
1 /RO(I,J)
THROUGH EFF, FOR J=2,1,J.G.N
V(M+2,J)=2.*(3.*SF(M+2,J)+SF(M+4,J)-6.*SF(M+3,J)+2.*SF(M+1,J)
1 )/R6(J)/RO(M+2,J)
1 V6(J)=2.*(SF(M+3,J)-8.*SF(M+2,J)+7.*SF(M+1,J))/R6(J)/RC(M+1,J)
1 )
V(P,J)=2.*(6.*SF(P-1,J)-3.*SF(P,J)-SF(P-2,J))/R6(J)/RC(P,J)
THROUGH EFFF, FOR J=2,1,J.G.N
THROUGH EFFF, FOR I=M+3,1,I.G.P
V(I,J)=(SF(I+2,J)-8*SF(I+1,J)+8*SF(I-1,J)-SF(I-2,J))/R1(J)/RC
1 (I,J)
THROUGH SSS, FOR I=M+2,1,I.G.P
THROUGH SSS, FOR J=2,1,J.G.N
W(I,J)=((SF(I+1,J)-2.*SF(I,J)+SF(I-1,J))*Y*Y/DZ2-(SF(I,J+1)-
1 SF(I,J-1))/DR2/(J-1.0)/2+(SF(I,J+1)-2*SF(I,J)+SF(I,J-1))/DR2)/
2 DR2/(J-1.0)/(J-1.0)/RO(I,J)-(U(I,J)*RC(I,J+1)-
3 RO(I,J-1))/DZ2R-V(I,J)*(RC(I+1,J)-RC(I-1,J))/DZ2)*A4(J)/RO(I,J)
4 )
THROUGH PPP, FOR J=2,1,J.G.N
W(P+1,J)=(-SF(P-1,J)+8.*SF(P,J)-7.*SF(P+1,J))
1 *R5(J)/RO(P+1,J)
W(1,J)=(-SF(3,J)+8.*SF(2,J))*R4(J)
CODE=2
TRANSFER TO ML
END OF CONDITIONAL
SMAX=0
THROUGH CDD, FOR I=2,1,I.G.M+1
THROUGH CDD, FOR J=1,1,J.G.N
S=BO+.ABS.U(I,J)/DX+.ABS.V(I,J)/DR
WHENEVER SMAX .L. S, SMAX=S
WHENEVER PRV.G.1.
BOO=4.*PRV/DR2+2.*PRV*Y/DZ2
BO=2.*PRV*(Y*Y/DZ2+1./CR2)
C THERWISE
BOO=4./DR2+2.*Y*Y/DZ2
BO=2.*(Y*Y/DZ2+1./DR2)
END OF CONDITIONAL
THROUGH DCC, FOR I=M+2,1,I.G.P
THROUGH DCC, FOR J=2,1,J.G.N
S=BO+.ABS.U(I,J)/DZ+.ABS.V(I,J)/DR
WHENEVER SMAX .L. S, SMAX=S
THROUGH MAXS, FOR I=M+2,1,I.G.P
S=BOO+.ABS.U(I,1)/DZ
WHENEVER (SMAX*DT) .G. 0.8,DT=0.8/SMAX
WHENEVER SMAX .L. S, SMAX=S

```

```

*094 01
*095 01 01
*096 01 02
*097 01
*098 01 01
*099 01
*100 01
*101 01 01
*102 01
*103 01 01
*104 01 01
*105 01 01
*106 01
*107 01 01
*108 01 02
*109 01
*110 01
*110 01
*111 01 01
*112 01 01
*113 01
*114 01 01
*115 01 02
*115 01
*116 01
*117 01 01
*118 01 02
*118 01
*118 01
*118 01
*119 01 01
*120 01
*120 01
*121 01 01
*122 01
*123 01
*124 01
*125 01
*126 01
*127 01 01
*128 01 02
*129 01
*130 01
*131 01
*132 01
*133 01
*134 01
*135 01
*136 01
*137 01
*138 01
*139 02 02
*140 02
*141 01
*142 01
*143 01
*144 01

```



```

1 6 DTDXG(J)=(-1)*T(M+1,J)+18*T(M+2,J)-9*T(M+3,J)+2*T(M+4,J))/DZ/
CRAD 1 6 UL(J)=(LDTDXL(J)-DTDG(J)*KG/KL)*CP*NEW*NEW*ACVERB/PR/
1 BEITA/G/HFG/(A.P.3)
U=0
THROUGH AVER, FOR J = 1,1, J .G. N
U=U+(UL(J+1)+UL(J))*(2.C*J-1.C)*DR2/2.C
THROUGH ACAA, FOR I = 1,1, I .G. P+1
DTRW(I)=(11*(I,N+1)-18* T(I,N)+9*T(I,N-1)-2*T(I,N-2))/6/CR
QM=0
THROUGH CAAA, FOR I=M+1,1, I.G.P
QM=QM+(DTRW(I)+DTRW(I+1))*DZ/2.
QI=0
DQIL = 0
THROUGH DAAA, FOR J=1,1, J.G.N
DQIL = DQIL+(DQIL(J)+DQIL(J+1))*(2.0*J-1.C)*DR2/2.0
CI=QI+(LDTDXG(J)+DTDG(J+1))*(2.C*J-1.C)*DR2/2.C
DQWDT=QM*KG*6.28*NEW*ALPHA/BEITA/G/A/A/ADVERB/ADVERB
RGIN=DQWCT*ADVERB/6.28/A/A/CSURFG/(1-X)
DQILDT = 3.14*DQIL*KL*NEW*ALPHA/BEITA/G/A/A
DQIDT=3.14*CI*KG*NEW*ALPHA/BEITA/G/A/A
DME = DT*U*ROL*(A.P.3) * 3.14/ADVERB
DMT=DMT+DME
DM=-DMB+DME
PRESS=PRESS+RGAS*ACVERB/(3.14*144.*A.P.3.* (1.-X))*((LQWDT-
1 DQIDT)*DT*A.P.2/(CV*ALPHA)-DM*GAM*TSAT)
A6=(PRESS-P1)/PRESS
N6=(PRESS-P1)/P1
P1=PRESS
TSAT=C5*(PRESS.P.C6)
A5=2.*DT*ADVERB*G*(A.P.3.)/ALPHA/ALPHA
THROUGH INTERF, FOR J=1,1, J.G.N
T(M+1,J)=(TSAT-TINIT)*CONST1
T(1,1)=TG(1,1)*CI+TG(1,2)*EX5+TG(2,1)*CR5
THROUGH DD, FOR I=2,1, I.G.M
WHENEVER U(I,1) .G. 0
C=(TO(I-1,1)-TO(I,1))*CI(I,1)
OTHERWISE
C=(TG(I,1)-TO(I+1,1))*CI(I,1)
END OF CONDITIONAL
T(I,1)=TO(I,1)*CI+TO(I,2)*DR5+(TO(I+1,1)+TC(I-1,1))*DX3 +C
THROUGH EE, FOR J=2,1, J.G.N
T(1,J)=TO(1,J)*C2+TG(2,J)*DX5+TG(1,J-1)*CR1(J)
+TO(1,J+1)*DR2(J)
1 THROUGH FF, FOR J=2,1, J.G.N
THROUGH FF, FOR I=2,1, I.G.M
WHENEVER U(I,J) .G. C
C=(TG(I-1,J)-TO(I,J))*CI(I,J)
OTHERWISE
C=(TO(I,J)-TO(I+1,J))*CI(I,J)
END OF CONDITIONAL
WHENEVER V(I,J) .G. 0
D=(TO(I,J-1)-TO(I,J))*C3(I,J)
OTHERWISE
D=(TO(I,J)-TO(I,J+1))*C3(I,J)
END OF CONDITIONAL
T(I,J)= TO(I,J)*C2+(TO(I+1,J)+TO(I-1,J))*DX3+
1 TO(I,J-1)*DR1(J)+TO(I,J+1)*DR2(J)+C+D
THROUGH GGG, FOR I=2,1, I.G.M
THROUGH GGG, FOR J=2,1, J.G.N

```

```

*254 FI=R3(J)*(T(I,J+1)-T(I,J-1))
*255 WHENEVER U(I,J) .G. 0
*256 C=(WO(I-1,J)-WO(I,J))*C1(I,J)
*257 OTHERWISE
*258 C=(WO(I,J)-WO(I+1,J))*C1(I,J)
*259 END OF CONDITIONAL
*260 WHENEVER V(I,J) .G. 0
*261 D=(WO(I,J-1)-WO(I,J))*C3(I,J)
*262 OTHERWISE
*263 D=(WO(I,J)-WO(I,J+1))*C3(I,J)
*264 END OF CONDITIONAL
*265 W(I,J)=WO(I,J)*C3+(WO(I+1,J)+WO(I-1,J))*DX7+C+D+
1 WO(I,J-1)*DR3(J)+WO(I,J+1)*DR4(J)+FI
*266 THROUGH MMMM, FCR J=2,1,J,G.N+1
*267 SF(M+1,J)=0
*268 NEI=0
*269 NEI=NEI+1
*270 WHENEVER NEI .G. NE, TRANSFER TO PRINT
*271 THROUGH LL, FCR I=1,1,I,G.N+1
*272 THROUGH LL, FCR J=1,1,J,G.N+1
*273 C3(I,J)=SF(I,J)
*274 I=1
*275 I=I+1
*276 F(I)=0
*277 THROUGH LM, FCR J=2,1,J,G.N
*278 DI(J)=(C3(I+1,J)+C3(I-1,J))*AI-W(I,J)*AI(J)
*279 F(I,J)=(DI(J)+F(I-1)*C2(J))/CI(J)
*280 THROUGH LN, FCR J=1,1,J,G.N-1
*281 H=N+1-J
*282 SF(I,H)=EJ(H)*SF(I,H+1)+F(H)
*283 WHENEVER I.L.M, TRANSFER TO II
*284 RMAX=0
*285 THROUGH AAA, FCR I=2, NR, I, G, M
*286 THROUGH AAA, FCR J=2, NR, J, G, N
*287 R3=.ABS.((SF(I,J)-C3(I,J))/(C3(I,J)+1.CE-20))
*288 WHENEVER RMAX .L. R3, RMAX=R3
*289 WHENEVER RMAX .G. EPSLCN, TRANSFER TO JJ
*290 THROUGH GFH, FCR I=1,1,I,G.M
*291 WHENEVER T(I,N+1) .G. (T(M+1,N)+DTM*CCNST1), T(I,N+1)=T(M+1,N)+DTM
1 *CONST1
*292 WHENEVER T(I,N).G.(T(M+1,N)+DTS*CCNST1), T(I,N)=T(M+1,N)+DTS*CCNST1
*293 DQS = 0
*294 DQL = 0
*295 DMB=0
*296 CT2=6-.28*AA*DX*RCM*CPW*DELTA/ADVERB/2.0/CCNST1
*297 THROUGH SQD, FCR I=1,1,I,G.M
*298 C=T(I,N+1)+T(I+1,N+1)
*299 DQS=DQS+(C-C4(I,N+1))*CT2
*300 C4(I,N+1)=C
*301 THROUGH GHF, FCR J=1,1,J,G.N+1
*302 DR1(J)=5.14*RQL*CP*(A.P.3)*DX*DR2*(2.0*J-1.0)/ADVERB
*303 THROUGH FHG, FCR I=1,1,I,G.M
*304 THROUGH FHG, FCR J=1,1,J,G.N
*305 C = (T(I,J)+T(I,J+1)+T(I+1,J)+T(I+1,J+1))/4.C/CONST1
*306 DQL = DQL +(C-C4(I,J))*DR1(J)
*307 C4(I,J) = C
*308 DOI={6.28*AA*XXQSURL/ACVERB+CQILD(T)*DT*CONST
*309 DMB = (CQI-DQL-DQS)/HFG
*310 WHENEVER DMB .L. 0.0, DMB=C.0
*311 DMBT=DMBT+DMB

```



```

SF(M+1,J)=RO(M+1,J)*UG*DR2*(J-1.01)*(J-1.C)/2.0
SFI(J)=SF(M+1,J)
NNN THROUGH DAAA, FOR I=M+2,1,I.G.P
DAAA SF(I,N+1)=SF(M+1,N+1)
NE2=0
JJJ NE2=NE2+1
WHENEVER NE2 .G.NE,TRANSFER TO PRINT
THROUGH LNL, FOR I = M+1,1, I .G. P + 1
LNL THROUGH LNL, FOR J=1,1,J .G. N+1
C3(I,J)=SF(I,J)
I=M+1
III I=I+1
THROUGH LLM, FOR J = 2,1, J .G. N
DI(J)=(C3(I+1,J)+C3(I-1,J))*A3-(M(I,J)*RC(I,J)+A4(J)*U(I,J))*
1 (RO(I,J+1)-RO(I,J-1))/D2R-V(I,J)*(RO(I+1,J)-RO(I-1,J))/D2Z)*
2 AI(J)
LLM F(J)=(DI(J)+F(J-1)*C2(J))/D2(J)
THROUGH LLN, FOR J = N,1, J .L. 2
LLN SF(I,J)=EJ(I)*SF(I,J+1)+F(J)
WHENEVER I .L. P, TRANSFER TO III
WHENEVER NT .E. 1 .AND. NE2 .E. 1, TRANSFER TO JJJ
RMAXX=0
THROUGH AAAA, FOR I=M+2,NR,I .G. P
AAAA THROUGH AAAA, FOR J = 2,NR, J .G. N
R3=.ABS.(SF(I,J)-C3(I,J))/(C3(I,J)+1.CE-2C)
WHENEVER RMAXX .L. R3, RMAXX= R3
WHENEVER RMAXX .G. EPSILON, TRANSFER TO JJJ
THROUGH BEE, FOR I=2,1,I.G.M
BEE W(I,N+1)=(8.*SF(I,N)-SF(I,N-1)-7.*SF(I,N+1))/DYY
THROUGH UUUU, FOR I= M+2,1,I.G.P
UUUU W(I,N+1)=(8.*SF(I,N)-SF(I,N-1)-7.*SF(I,N+1))/DYY/RC(I,N+1)
THROUGH CEE, FOR J=2,1,J .G. N
CEE W(P+1,J)=(-SF(P-1,J)+8.*SF(P,J)-7.*SF(P+1,J))*R5(J)/RC(P+1,J)
ML W(1,J)=(-SF(3,J)+8.*SF(2,J))*R4(J)
THROUGH UUU, FOR I=M+1, 1, I.G.P+1
UUU VO(I,J)=V(I,J)
UD(I,J)=U(I,J)
THROUGH BE, FOR I=2,1,I.G.M
BE U(I,N)=2.0*(3.*SF(I,N)-6.*SF(I,N-1)+SF(I,N-2))/R1(N)
U(I,1)=SF(I,2)/DR6
U(I,2)=2.0*(6.*SF(I,3)-3.*SF(I,2)-SF(I,4))/R1(2)
THROUGH VVV, FOR I=M+1,1,I.G.P
VVV U(I,N)=2.*(3.*SF(I,N)-6.*SF(I,N-1)+SF(I,N-2))/R1(N)/RO(I,N)
U(I,1)=SF(I,2)/DR6/RC(I,1)
U(I,2)=2.*(6.*SF(I,3)-SF(I,4)-3.*SF(I,2))/R1(2)/RO(I,2)
THROUGH BBETA, FOR I=2,1,I.G.M
BBETA THROUGH BBETA, FOR J=3,1,J.G.N-1
U(I,J)=(SF(I,J-2)-8.*SF(I,J-1)+8.*SF(I,J+1)-SF(I,J+2))/R1(J)
U(M+1,N)=U(M+1,N-1)
THROUGH VVVV, FOR I=M+1,1,I.G.P
VVVV THROUGH VVVV, FOR J=3,1,J.G.N-1
U(I,J)=(SF(I,J-2)-8.*SF(I,J-1)+8.*SF(I,J+1)-SF(I,J-2))/R1(J)
1 /RO(I,J)
THROUGH BFF, FOR J=2,1,J.G.N
BFF V(M+2,J)=2.*(3.*SF(M+2,J)+SF(M+4,J)-6.*SF(M+3,J)+2.*SF(M+1,J))
1 /R6(J)/RO(M+2,J)
V(P,J)=2.*(6.*SF(P-1,J)-3.*SF(P,J)-SF(P-2,J))/R6(J)/RO(P,J)
V(G,J)=2.*(SF(M+3,J)-8.*SF(M+2,J)+7.*SF(M+1,J))/R6(J)/RO(M+1,J)
1 )

```

```

*361 01
*362 01
*363
*364 01
*365
*366
*367
*368
*369 01
*370 02
*371
*372
*373
*374 01
*374
*374
*375 01
*376
*377 01
*378
*379
*380
*381
*382
*383 01
*384 02
*385
*386
*387 01
*388
*389 01
*390
*391 01
*392 01
*393
*394 01
*395 02
*396 02
*397
*398
*399 01
*400 01
*401
*402 01
*403 01
*404 01
*405
*406 01
*407 02
*408
*409
*410 01
*411 02
*411
*412
*413
*413
*414 01
*415 01
*415

```

THROUGH BFFF, FOR I=M+3, I, I.G.P-1	
THROUGH BFFF, FOR J=2, I, J.G.N	
BFFF V(I, J)=(SF(I+2, J)-8*SF(I+1, J))+8*SF(I-1, J)-SF(I-2, J))/R6(I, J)/RC	01
1 (I, J)	02
THROUGH FBF, FOR J=2, I, J.G.N+1	
SF(I+1, J)=0	
THROUGH BF, FOR J=2, I, J.G.N	
V(2, J)=2.0*(SF(I, J)-6.0*SF(I+1, J)+3.0*SF(I+2, J))/R2(J)	01
V(M, J)=2.0*(6.0*SF(M-1, J)-3.0*SF(M, J)-SF(M-2, J))/R2(J)	01
V(N+1, J)=2.0*(8*SF(M, J)-SF(M-1, J))/R2(J)	01
THROUGH BETA, FOR I=3, I, I.G.N-1	
THROUGH BETA, FOR J=2, I, J.G.N	
BETA V(I, J)=(SF(I+2, J)-8*SF(I+1, J))+8*SF(I-1, J)-SF(I-2, J))/R2(J)	01
WHENEVER NT.L.N1, TRANSFER TO PRINT	02
WHENEVER NT.E.NMAX	
PUNCH FORMAT DDATA, A, PRESS, PC, X, NT, TIME, U,	01
1 T(I, I)..T(P+1, N+1), SF(I, I)..SF(P+1, N+1)	
TRANSFER TO PRINT	01
END OF CONDITIONAL	01
NP=NPI	
NP1=TAU/(TAU*N3)	
WHENEVER NP1-NP-1.G.0, TRANSFER TO PRINT	
TRANSFER TO BACK	
WHENEVER NT.L.NC, TRANSFER TO NEXT	
R1=0	
THROUGH YZ, FOR I=2, I, I.G.M	
THROUGH YZ, FOR J=2, I, J.G.N+1	
R2=.ABS.(T(I, J)-TG(I, J))/TC(I, J)	01
WHENEVER R1.L.R2, RI=R2	02
NUG=0	02
NUL=0	
RAL=0	
RAG=0	
THROUGH CLH, FOR I=1, I, I.G.M+1	
HL(I)=.ABS.(KL*DTDRM(I)/A/(T(I, N+1)-T(I, 1)))	01
RAL=RAL+DX*T(I, N+1)	01
NUL=NUL+DX*HL(I)*A*X/ACVERB/KL	01
RAL=RAL*(X.P.3)/(ACVERB.P.4)	
THROUGH GLH, FOR I=M+1, I, I.G.P+1	
J=I-M	
HG(J)=.ABS.(KG*DTDRM(I)/A/(T(I, N+1)-T(I, 1)))	01
RAG=RAG+DZ*T(I, N+1)	01
NUG=NUG+DZ*HG(J)*A*(1-X)/ACVERB/KG	01
RAG=RAG*(1-X).P.3)*BEITAG/RALPHA/RNEM/BEITA/	
1 (ACVERB.P.4)	
CL=NUL/(RAL.P.0.25)	
CG=NUG/(RAG.P.0.25)	
UR=U(I, 1)*R1(I)/2.0	
THROUGH DAL, FOR J=2, I, J.G.N+1	
UR=(UR+U(I, J)*R1(J))/I2.C	
PRINT RESULTS NT, TIME, IAU, DT, UR, U, PRESS, Z, X, DX,	
1 DME, DMT, DMB, DMBI, DM, DMTI,	
2 RQIN, DQIDT, DWDI, DQDWT, PFG, U(I, 1)..U(P+1, N+1), V(I, 1)..V(I	
3 P+1, N+1), T(I, 1)..T(P+1, N+1), SF(I, 1)..SF(P+1, N+1), VG(I)...	
4 VG(N+1), UL(I).....UL(N+1), HL(I)....HL(M+1), HG(I)....HG(P+1-N),	
5 NUL, NUG, RMAX, RI, NE1, NE2, RAL, RAG, CL, CG, RP, RI,	
6 SF(I)....SFI(N+1), CQILCT	
WHENEVER NE1.G.NE, TRANSFER TO END	
WHENEVER NT.E.NMAX, TRANSFER TO END	
WHENEVER N2.E.1	

*467 01
*468 01
*469 01
*470 01
*471 01

N3=2.*N3
N2=0
OTHERWISE
N2=1
END OF CONDITIONAL
TRANSFER TO BACK
CONTINUE
TRANSFER TO START
VECTOR VALUES INPUT=\$3F12.4,F12.8,I 4,F12.8,E16.8/(5E16.8)*\$
VECTOR VALUES DDATA=\$3F12.4,F12.8,I 4,F12.8,E16.8/(5E16.8)*\$
END OF PROGRAM

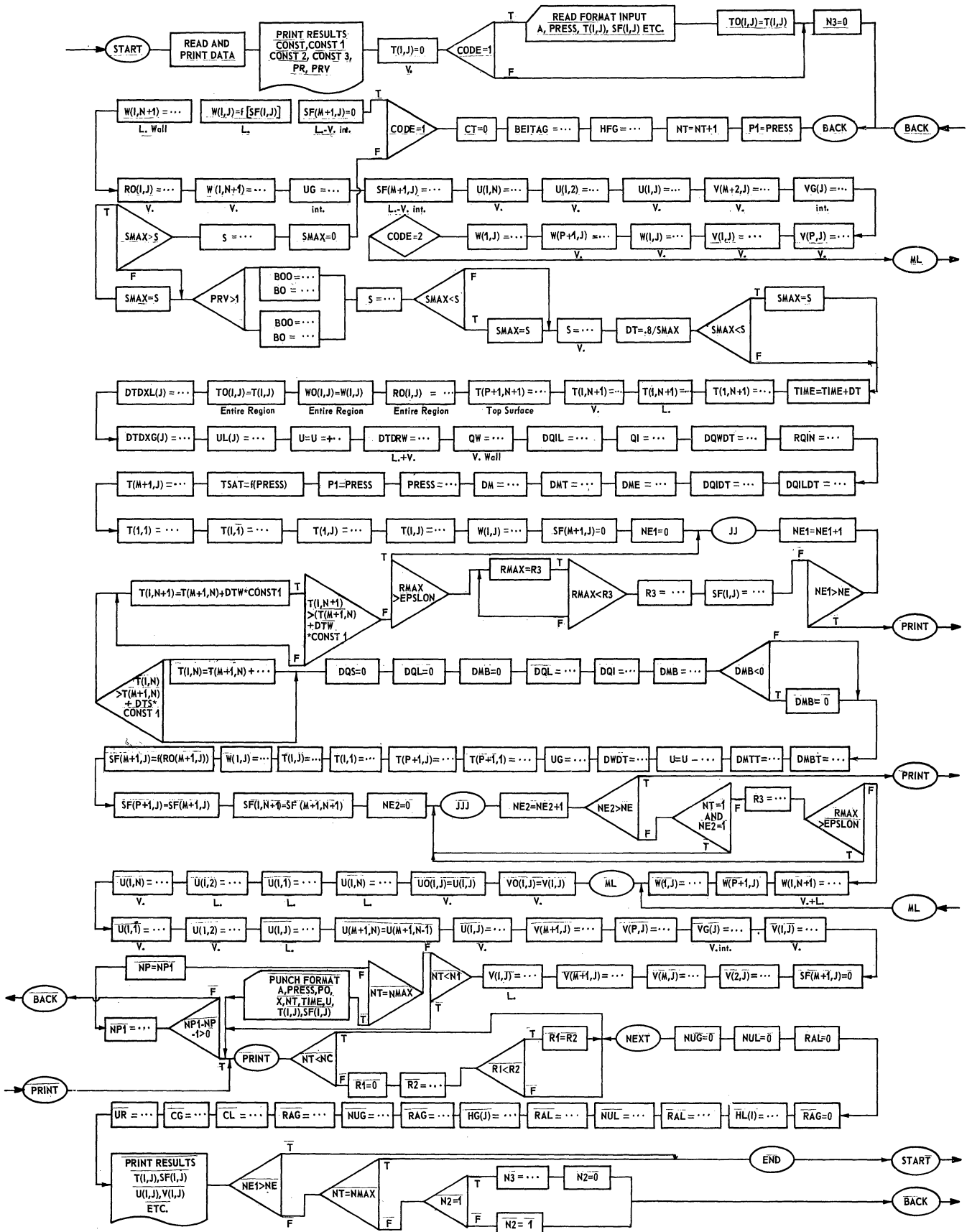
END

THE FOLLOWING NAMES HAVE OCCURRED ONLY ONCE IN THIS PROGRAM.
COMPIATION WILL CONTINUE.

CPV *016
N1 *428
NC *437
TAU1 *434

APPENDIX B

FLOW CHART



APPENDIX C

PROGRAM NOTATION AND NOMENCLATURE

Symbols preceding the expression indicate the following:

* - Input data
** - Printout

Symbols following the expression indicate the following:

[0] - Integer
[1] - Dimensionless or units
(150) - e.g., - This expression appears in statement number 150 in the program of Appendix A.

A

*A - [ft] - Tank radius
*AOVERB - [1] - A/B
AOVERB2 - [1] - (A/B)²
A1 - [1] - (67)
A2 - [1] - (68)
A3 - [1] - (63)
A5 - [1] - (226,359)
A6 - [1] - (222,348)
A1(J) - [1] - (35)
A2(J) - [1] - (76)
A3(J) - [1] - (77)
A4(J) - [1] - (37)
ALPHA - [ft²/sec] - Thermal diffusivity of liquid
ALPJAW - [ft²/sec] - Thermal diffusivity of wall
ALPHAV - [ft²/sec] - Thermal diffusivity of vapor

B

B - [ft] - Total tank height
BJ - [1] - (71)
BJ1 - [1] - (64)
BO - [1] - (72,132,135)
BOO - [1] - (131,134)
BEITA - [°F⁻¹] - Volumetric coeff. of expansion-liquid
BEITAG - [°F⁻¹] - (55) - Volumetric coeff. of expansion-vapor

C

C - [1] - Temporary storage
C1 - [1] - (167,316)
C2 - [1] - (317)
C3 - [1] - (318)

C

*C5	- [°F]	- (20,225)	- Coefficient for computing TSAT as function of pressure
*C6	- [1]	- (20,225)	- Exponent for computing TSAT as function of pressure
C1(I,J)	- [1]	- (184,242,321)	- Temporary storage
C2(J)	- [1]	- (36)	
C3(I,J)	- [1]		- Temporary storage
C4(I,J)	- [1]		- Temporary storage
**CL	- [1]	- (458)	- Coefficient of Rayleigh number correlation-liquid
**CG	- [1]	- (459)	- Coefficient of Rayleigh number correlation-vapor
*CP	- [BTU/lbm-°F]		- specific heat-liquid
*CPV	- [BTU/lbm-°F]		- specific heat-vapor-constant pressure
*CV	- [BTU/lbm-°F]		- specific heat-vapor-constant volume
*CPW	- [BTU/lbm-°F]		- specific heat-wall
CT	- [1]	- (57)	- Property term for vapor (=1 for ideal gas)
CT2	- [BTU]	- (296)	- Property term for wall
*CODE	- [0]	- (86)	- = 2 for a new run = 1 for continuation of prior run vs READ FORMAT INPUT
**CONST	- [SECONDS]	- (22)	- conversion constant for dimensionless time
**CONST1	- [°F ⁻¹]	- (23)	- conversion constant for dimensionless temperature
**CONST2	- [SECONDS ⁻¹]		- = 1/CONST
**CONST3	- [°F]		- = 1/CONST1

D

D	- [1]		- Temporary storage
D1(J)	- [1]	- (78)	
D2(J)	- [1]	- (80)	
DI(J)	- [1]	- (278,374)	
DR1(J)	- [1]	- (173,302)	
DR2(J)	- [1]	- (174)	
DR3(J)	- [1]	- (175)	
DR4(J)	- [1]	- (176)	
DR5(J)	- [1]	- (178)	
DR6(J)	- [1]	- (179)	
DR7(J)	- [1]	- (180)	
DR8(J)	- [1]	- (181)	
DI	- [1]	- (172)	

D

DR - [1] - (14) - Radial grid space
D2R - [1] - (32) - DR/2
DR1 - [1] - (163) -
DR2 - [1] - (15) - DR²
DR3 - [1] - (159)
DR4 - [1] - (160)
DR5 - [1] - (161)
DR6 - [1] - (18)
DR7 - [1] - (166)
DRZ - [1] - (62) - (DR/DZ)²
**DX - [1] - (58) - Axial grid space-liquid
DX1 - [1] - (148) - DT/DX
DX2 - [1] - (59) - DX²
DX3 - [1] - (158)
DX5 - [1] - (162)
DX7 - [1] - (164)
DX8 - [1] - (165)
DXR - [1] - (65) - (DX/DR)²
DRX - [1] - (66) - 1/DXR
DYY - [1] - (17) - 2(DR)²
DY1 - [1] - (155)
DY3 - [1] - (154)
DY5 - [1] - (157)
DY7 - [1] - (156)
DZ - [1] - (60) - Axial grid space-vapor
DZ1 - [1] - (149) - DT/DZ
DZ2 - [1] - (61) - DZ²
D2Z - [1] - (69) - DZ/2
DZ3 - [1] - (150)
DZ5 - [1] - (151)
DZ7 - [1] - (152)
DZ8 - [1] - (153)
**DM - [lbm] - (220) - Net phase change in time DT. (minus sign for evaporation)
**DMB - [lbm] - (309) - Phase change in time DT from energy balance on tank wall and liquid system (plus sign for evaporation)
**DME - [lbm] - (218) - Phase change at L-V interface in time DT (minus sign for evaporation)
**DMT - [lbm] - (219) - Cumulative total of DME (minus sign for evaporation)
**DMBT - [lbm] - (311) - Cumulative total of DMB
**DMTT - [lbm] - (312) - Cumulative total of DM (minus sign for evaporation)

D

***DT	- [1]		Time step interval
*DTS	- [°F]	- (292)	Max. permissible liquid superheat at node adjacent to wall
*DTW	- [°F]	- (291)	Max. permissible superheat of wall in contact with liquid
DTDRW(I)	- [1]	- (205,448,454)	Temperature gradient in fluid at wall
DTDYG(J)	- [1]	- (199)	Temperature gradient in vapor at liquid-vapor interface
DTDYL(J)	- [1]	- (198)	Temperature gradient in liquid at liquid-vapor interface
DQIL	- [1]	- (212)	Mean temperature gradient in liquid at L-V interface
DQILDT	- [BTU/sec]	- (216)	Heat transfer rate in liquid at L-V interface (plus for heat transfer to liquid)
**DQIDT	- [BTU/sec]	- (217)	Heat transfer rate in vapor at L-V interface (plus for heat transfer out of vapor)
**DQWDT	- [BTU/sec]	- (214)	Heat transfer rate to vapor from wall (plus for heat transfer to vapor)
**DWDT	- [BTU/sec]	- (314)	Work rate by vapor control volume
DQI	- [BTU]	- (308)	Sum of heat transfer to wall in contact with liquid and to liquid at L-V interface in DT (plus for heat transfer in)
DQL	- [BTU]	- (306)	Enthalpy rise of liquid in DT
DQS	- [BTU]	- (299)	Enthalpy rise of wall in contact with liquid in DT
*DELTA	- [feet]		Wall thickness

E

EJ(J)	- [1]	- (85,282)	
EJL(J)	- [1]	- (81)	
*EPSLON	- [1]	- (289,385)	Maximum fractional change in stream function between iterations before iteration is terminated

F

F(J)	- [1]	- (279,375)	Temporary storage
FI	- [1]	- (171,254,348)	Temporary storage

G
 *G - [ft/sec²] - Acceleration corresponding to effective body force acting on container
 GAM - [1] - Ratio of specific heats-vapor

H
 H - [0] - (281) - Index
 **HFG - [BTU/lbm] - (51) - Latent heat of vaporization corresponding to TSAT
 **HG(I) - [BTU/sec-ft²-°F] - (454) - Local heat transfer coefficient of vapor based on ΔT between wall and centerline
 **HL(I) - [BTU/sec-ft²-°F] - (448) - Local heat transfer coefficient of liquid based on ΔT between wall and centerline

I
 I - [0] - Axial nodel index number
 I1 - [0] - Mid vertical height of liquid

J
 J - [0] - Radial nodel index number

K
 *KG - [BTU/sec-ft-°F] - Thermal conductivity-vapor
 *KL - [BTU/sec-ft-°F] - Thermal conductivity-liquid

M
 *M - [0] - Number of vertical divisions in liquid (M+1 = L-V interface)
 M1 - [1] - (27) - Liquid-wall property
 M2 - [1] - (28) - Liquid-wall property
 M3 - [1] - (29) - Vapor-wall property
 M4 - [1] - (56) - Vapor property
 M5 - [1] - (31) - Initial temperature
 M6 - [1] - (223) - Pressure rise ratio in DT
 M7 - [1] - (30) - Vapor-wall property

N
 *N - [0] - Number of radial divisions (N+1 = wall)
 *N1 - [1] - (428) - Minimum number of time steps before punch is permitted

N

N2	- [0]	(466,468)	Control number for establishing time steps between printouts.
N3	- [0]	(48,467)	Control number for establishing time steps between printouts
*NC	- [0]	(437)	Minimum number of time steps NT before fractional temperature changes between time steps is computed
*NE	- [0]	(270,367)	Maximum number of iterations permitted in computations of stream function
**NE1	- [0]	(269,270)	counter on iterations on stream function-liquid
**NE2	- [0]	(366,367)	counter on iterations on stream function-vapor
NP	- [0]	(433,435)	control for printout instruction
NP1	- [1]	(433,434,435)	control for printout instruction
*NR	- [0]	(285,381)	Index steps of grid spaces for which fractional change in stream function with iterations is computed
**NT	- [0]	(50)	Time step number
*NMAX	-	(465)	Maximum number of time steps NT permitted before program is terminated
*NEW	- [ft ² /sec]		kinematic viscosity-liquid
*NEWV	- [ft ² /sec]		kinematic viscosity-vapor
**NUG	- [1]		Mean Nusselt number-vapor
**NUL	- [1]		Mean Nusselt number-liquid

P

*P	- [0]		Total number of vertical divisions
*PO	- [lb _f /in ²]		Initial system pressure
P1	- [lb _f /in ²]	(49,224)	Pressure previous time step
**PRESS	- [lb _f /in ²]	(221)	Current system pressure
**PR	- [1]	(10)	Prandtl number-liquid
**PRV	- [1]	(11)	Prandtl number-vapor

Q

QI	- [1]	(213)	Mean temperature gradient in vapor at L-V interface
QW	- [1]	(208)	Mean temperature gradient in vapor at wall
*QSURFG	- [BTU/sec-ft ²]		Imposed heat flux on container exterior on vapor portion
*QSURFL	- [BTU/sec-ft ²]		Imposed heat flux on container exterior on liquid portion

R

**R1	- [1]	- (442)	- Maximum value of R2
R2	- [1]	- (441)	- Fractional change in temperature between time steps
R3	- [1]	- (287,383)	- Fractional change in stream function with iteration
R1(J)	- [1]	- (38)	
R2(J)	- [1]	- (79)	
R3(J)	- [1]	- (177)	
R4(J)	- [1]	- (82)	
R5(J)	- [1]	- (83)	
R6(J)	- [1]	- (84)	
RO(I,J)	- [lbm/ft ³]	- (96)	- Local vapor density
*ROL	- [lbm/ft ³]		- Liquid density
*ROW	- [lbm/ft ³]		- Wall density
**RP	- [1]	- (52)	- Ratio of current pressure to initial
**RMAX	- [1]	- (289)	- Maximum value of change in stream function with iteration-liquid
RMAXX	- [1]	- (385)	- Maximum value of change in stream function with iteration-vapor
**RAG	- [1]	- (455)	- Mean Rayleigh number-vapor
**RAL	- [1]	- (451)	- Mean Rayleigh number-liquid
*RGAS	- [ft-lb _f /lbm-°R]		- Gas constant-vapor
**RQIN	- [1]	- (215)	- Fraction of total heat transfer rate to vapor part of tank going into vapor
RALPHA	- [1]	- (13)	- Ratio-thermal diffusivity of vapor to liquid
RNEW	- [1]	- (12)	- Ratio-kinematic viscosity of vapor to liquid

S

S	- [1]	- (139,142)	- stability criteria
SMAX	- [1]	- (143,144)	- Maximum value of S
**SF(I,J)	- [1]		- stream function
**SFI(J)	- [1]		- vapor stream function at L-V interface

T

**T(I,J)	- [1]		- Current temperature
TO(I,J)	- [1]		- Temperature of prior time step
**TAU	- [seconds]	- (146)	- Current time
*TAUL	- [seconds]	- (434)	- Basic multiple of time for which printout occurs
**TIME	- [1]	- (145)	- Current time
TINIT	- [°F]	- (21)	- Initial saturation temperature corresponding to initial pressure

T
 TSAT - [°F] - (20,225) - Current saturation temperature corresponding to current pressure

U
 **U(I,J) - [1] - Axial component of velocity
 **U - [1] - (147,203,313) - Mean velocity of liquid-vapor interface
 UG - [1] - (99,315) - Mean velocity of vapor at liquid-vapor interface
 **UL(J) - [1] - (200) - Local L-V interface velocity due to interface phase change
 UO(I,J) - [1] - (396) - Temporary storage of U(I,J)
 **UR - [1] - (460,462) - Mean axial velocity at mid-point of liquid (serves as check on continuity)

V
 **V(I,J) - [1] - Radial component of velocity
 VO(I,J) - [1] - (395) - Temporary storage of V(I,J)
 **VG(J) - [1] - (111,415) - Radial velocity of vapor at L-V at interface

W
 W(I,J) - [1] - Vorticity
 WO(I,J) - [1] - Vorticity of prior time step

X
 ***X - [1] - (147) - Liquid fraction in container

Y
 Y - [1] - (9) - A/B

Z
 Z - [1] - Compressibility factor
 ZOVRZ - [1] - (70) - = Z/2, = 0.5 for ideal gas

APPENDIX D

COMPUTER PROGRAM DATA INPUTS

P - Total number of vertical grid spaces
 M - Number of vertical grid spaces in liquid
 N - Number of radial grid spaces
 CODE - = 2 for a new run
 = 1 for continuation of prior run via READ FORMAT INPUT
 N1 - Minimum number of time steps NT before PUNCH FORMAT DDATA is permitted
 NC - Minimum number of time steps NT before fractional temperature changes
 between time steps is computed
 NMAX - Maximum number of time steps NT permitted before program is terminated
 NE - Maximum number of iterations permitted in computations of stream function
 EPSLON - Maximum fractional change in stream function between iterations be-
 fore iteration is terminated
 NR - Index steps of grid spaces for which fractional change in stream function
 with iterations is computed
 DT - Initial estimate of dimensionless time step
 TAU1 - seconds - Basic multiple of real time for which printout occurs

A - feet - Tank radius
 APVERB - Ratio of tank radius to height
 X - Initial fraction of liquid in tank
 QSURFG - BTU/sec-ft²-Imposed heat flux on container exterior on vapor por-
 tion
 QSURFL - BTU/sec-ft² - Imposed heat flux on container exterior on liquid
 portion
 G - ft/sec² - Acceleration corresponding to effective body force acting on
 container
 PO - lb_f/in² - Initial system pressure
 DTW - °F - Imposed maximum permissible temperature difference between con-
 tainer wall and saturation
 DTS - °F - Imposed maximum permissible temperature difference between liquid
 nodes adjacent to container wall and saturation
 CPW - BTU/lbm-°F - specific heat of container wall
 ROW - lbm/ft³ - Density of container wall
 ALPHAW - ft²/sec - Thermal diffusivity of container wall
 DELTA - ft - container wall thickness
 ALPHA - ft²/sec - Thermal diffusivity of liquid
 ROL - lbm/ft³ - Liquid density
 CP - BTU/lbm - °F - Specific heat of liquid
 KL - BTU/sec - ft - °F - Thermal conductivity of liquid
 BEITA - °F⁻¹ - Volumetric coefficient of expansion of liquid
 C5 - Coefficient for computing TSAT
 C6 - Exponent for computing TSAT
 NEW - ft²/sec - kinematic viscosity of liquid
 ALPHAV - ft²/sec - Thermal diffusivity of vapor
 CPV - BTU/lbm - °F - Specific heat of vapor, constant pressure
 CV - BTU/lbm - °F - Specific heat of vapor, constant volume
 KG - BTU/sec - ft - °F - Thermal conductivity of vapor
 RGAS - ft-lb_f/lbm - °R Gas constant of vapor
 Z - Compressibility factor

APPENDIX E
TYPICAL OUTPUT

\$ DATA

MAP

ACCEPT 00000* DPUNCH 00000* SPRINT 00000* ERROR 00000* SKIP6 00000* SPEEK 00000*
 SCARDS 00000* FTRAP 00000* SYSTEM 00000* (PGCM) 10000 (MAIN) 10000
 .IOH 64412* VER.87 64412* .LINK 64412* .IR1 64412* .IR2 64412*
 .SCOM. 71135* DFMIOH 71466* .DFDIOH 71466* .ERR 71541* .RTN 71541*
 ATLOC 71666* .03311 71714* .ICSET 71733* .IOFMT 71751* .RST4 71751*
 .WR. 72025* .READ 72041* .RD. 72056* .RDSW 72056* GICTLW 72140*
 .EOF7 72153* .PUNCH 72211* .PC. 72222* .LBUFF 72236* .PRSLT 72367*
 USQRT 74423* SQRT 74473* .EXIT 74515* ELUG 74572* .RPDTA 73207*
 EXP 75071* ZERO 75204* (PROG) 75240 (ERAS) 77741
 .CL301 74773*

EXECUTION BEGINS WITH ROUTINE (MAIN)
 02501 LOCS. CAN BE SAFELY USED IN EXPANDING PROG. (OCTAL)
 FULL CORE LOADING PROCEDURE USED
 LGADER OVERLAPPED BY 05416 LOCS. (OCTAL), FULL CCRE LOADING PROCEDURE USED

A=2.5, AOVERB=.25, P=30, M=20, N=20, X=.67, CCDE=2, DT=10. E-6,

NMAX=500, PO=15., G=32.2E-5, QSURFG=2.78E-4, CSURFL=2.78E-4,

DTW=1., DTS=1., C5=116., C6=.123, ALPHA=8.35E-7, NEW=1.63E-6,

KL=2.33E-5, BEITA=.49E-2, ROL=70., CP=.4, ALPHAV=2.14E-5,

NEWV=2.11E-5, KG=1.4E-6, CPV=.216, CV=.153, RGAS=48.3,

ALPHAW=4.16E-5, CPW=.11, RQW=488., DELTA=.C1, TAU1=30, NI=6,

NE=50, EPSLON=.01, NC=5, NR=4, Z=1.0*

CONST = 7.485030E+06, CONST2 = 1.336000E-07, CONST3 = 2.208320E-07
 PR = 1.952096, PRV = .985981
 NT = 154, TIME = 1.539999E-03, TAU = 1.152694E+04, DT = 1.000000E-05
 UR = 2.329724, U(1,0) = -2.198956E-03, PRESS = 15.235658, Z = 1.000000
 X = .665998, DX = .033500, DME = -3.020815E-04, DMT = -.024537
 DMB = .000000, DMBT = .000000, DM = -3.020815E-04, DMTT = -.024537
 RQIN = .058085, DQIDT = 6.577250E-05, DWDT = 1.6253330E-07, DQWDT = 8.366078E-04
 HFG = 296.621334

U(1,1) ... U(31,21)

.CCCC000E+00 .000000E+00 .000000E+00 .000000E+00 .000000E+00 .000000E+00 .000000E+00
 .000000E+00 .000000E+00 .000000E+00 .000000E+00 .000000E+00 .000000E+00 .000000E+00
 .CCCC000E+00 .000000E+00 .000000E+00 .000000E+00 .000000E+00 .000000E+00 .000000E+00

-2.211137E+01	-2.211628E+01	-2.225188E+01	-2.244571E+01	-2.272659E+01	-2.310834E+01	-2.361043E+01	-2.425556E+01
-2.509219E+01	-2.615838E+01	-2.752779E+01	-2.929880E+01	-3.161301E+01	-3.467842E+01	-3.880801E+01	-4.449614E+01
-5.269644E+01	-6.635545E+01	-5.981325E+01	1.179201E+02	.000000E+00			
-4.683610E+01	-4.685800E+01	-4.708505E+01	-4.740008E+01	-4.785116E+01	-4.845818E+01	-4.574635E+01	-5.024781E+01
-5.150318E+01	-5.306329E+01	-5.499125E+01	-5.736472E+01	-6.027796E+01	-6.384294E+01	-6.818893E+01	-7.346853E+01
-7.595209E+01	-8.827012E+01	-7.033406E+01	2.037808E+02	.000000E+00			
-7.013079E+01	-7.015323E+01	-7.037743E+01	-7.068790E+01	-7.113194E+01	-7.172829E+01	-7.249926E+01	-7.347136E+01
-7.467518E+01	-7.614510E+01	-7.791836E+01	-8.003371E+01	-8.252880E+01	-8.543651E+01	-8.878148E+01	-9.258206E+01
-9.682913E+01	-1.003642E+02	-6.765599E+01	2.721730E+02	.000000E+00			
-9.198101E+01	-9.199214E+01	-9.211884E+01	-9.229820E+01	-9.256296E+01	-9.293085E+01	-9.342255E+01	-9.406132E+01
-9.487201E+01	-9.587981E+01	-9.710866E+01	-9.857919E+01	-1.003064E+02	-1.022977E+02	-1.045527E+02	-1.070612E+02
-1.096186E+02	-1.092829E+02	-6.147666E+01	3.257831E+02	.000000E+00			
-1.132106E+02	-1.131973E+02	-1.131234E+02	-1.130357E+02	-1.129417E+02	-1.128624E+02	-1.128279E+02	-1.128651E+02
-1.130063E+02	-1.132824E+02	-1.137217E+02	-1.143478E+02	-1.151781E+02	-1.1622229E+02	-1.174879E+02	-1.189573E+02
-1.202147E+02	-1.165049E+02	-5.393336E+01	3.804950E+02	.000000E+00			
-1.355505E+02	-1.354936E+02	-1.350659E+02	-1.345101E+02	-1.337946E+02	-1.329568E+02	-1.320439E+02	-1.311056E+02
-1.302104E+02	-1.294025E+02	-1.287380E+02	-1.282618E+02	-1.280097E+02	-1.280079E+02	-1.282771E+02	-1.287985E+02
-1.289337E+02	-1.222121E+02	-4.553632E+01	4.266123E+02	.000000E+00			
-1.619037E+02	-1.617711E+02	-1.607155E+02	-1.593285E+02	-1.575151E+02	-1.553476E+02	-1.539197E+02	-1.503402E+02
-1.477259E+02	-1.451929E+02	-1.428477E+02	-1.407794E+02	-1.390547E+02	-1.377175E+02	-1.367927E+02	-1.362332E+02
-1.351375E+02	-1.253352E+02	-3.255222E+01	4.690483E+02	.000000E+00			
-1.971351E+02	-1.968796E+02	-1.946884E+02	-1.917840E+02	-1.879560E+02	-1.833471E+02	-1.781493E+02	-1.725956E+02
-1.669441E+02	-1.614516E+02	-1.563457E+02	-1.518035E+02	-1.479428E+02	-1.448252E+02	-1.424738E+02	-1.408340E+02
-1.388662E+02	-1.271841E+02	-2.547719E+01	5.101930E+02	.000000E+00			
-2.483274E+02	-2.479085E+02	-2.437584E+02	-2.381751E+02	-2.300716E+02	-2.216422E+02	-2.113332E+02	-2.003016E+02
-1.891394E+02	-1.784355E+02	-1.686878E+02	-1.602406E+02	-1.532615E+02	-1.477534E+02	-1.435848E+02	-1.404458E+02
-1.367071E+02	-1.201905E+02	-8.311547E+00	5.455704E+02	.000000E+00			
-3.232453E+02	-3.226866E+02	-3.155704E+02	-3.057719E+02	-2.923645E+02	-2.757001E+02	-2.564844E+02	-2.358041E+02
-2.149971E+02	-1.954091E+02	-1.781428E+02	-1.638970E+02	-1.529398E+02	-1.451973E+02	-1.404146E+02	-1.382898E+02
-1.374097E+02	-1.230529E+02	-6.175006E-01	5.894478E+02	.000000E+00			
-4.241774E+02	-4.235865E+02	-4.128358E+02	-3.975921E+02	-3.759794E+02	-3.482250E+02	-3.156311E+02	-2.756627E+02
-2.436424E+02	-2.101698E+02	-1.815030E+02	-1.589480E+02	-1.427801E+02	-1.324584E+02	-1.269832E+02	-1.252167E+02
-1.248605E+02	-1.050002E+02	9.428528E+01	6.517009E+02	.000000E+00			
-5.405803E+02	-5.400068E+02	-5.257460E+02	-5.049056E+02	-4.741055E+02	-4.330652E+02	-3.832464E+02	-3.280022E+02
-2.720399E+02	-2.203770E+02	-1.771503E+02	-1.44378E+02	-1.235249E+02	-1.123189E+02	-1.091181E+02	-1.118555E+02
-1.175967E+02	-9.864233E+01	1.462055E+02	6.995412E+02	.000000E+00			
-6.497908E+02	-6.491102E+02	-6.320017E+02	-6.063197E+02	-5.668796E+02	-5.127497E+02	-4.457560E+02	-3.705795E+02
-2.940208E+02	-2.235700E+02	-1.656213E+02	-1.239646E+02	-9.921260E+01	-8.937681E+01	-9.114832E+01	-1.011170E+02
-1.145081E+02	-9.488580E+01	2.227802E+02	7.536559E+02	.000000E+00			
-7.280661E+02	-7.271375E+02	-7.079985E+02	-6.786406E+02	-6.323588E+02	-5.679241E+02	-4.876210E+02	-3.971589E+02
-3.048780E+02	-2.202081E+02	-1.515213E+02	-1.040198E+02	-7.861821E+01	-7.256481E+01	-8.132342E+01	-1.002501E+02
-1.232050E+02	-9.917574E+01	2.966782E+02	8.065073E+02	.000000E+00			
-7.595894E+02	-7.584945E+02	-7.385789E+02	-7.075731E+02	-6.582059E+02	-5.895087E+02	-5.041374E+02	-4.081042E+02
-3.100772E+02	-2.200262E+02	-1.471928E+02	-9.783018E+01	-7.337138E+01	-7.058148E+01	-8.382255E+01	-1.073184E+02
-1.316758E+02	-7.827946E+01	3.904505E+02	8.410642E+02	.000000E+00			

-7.365917E+02	-7.357071E+02	-7.171696E+02	-6.880736E+02	-6.418908E+02	-5.781857E+02	-4.996360E+02	-4.116660E+02
-3.218854E+02	-2.389192E+02	-1.708284E+02	-1.235208E+02	-9.871720E+01	-9.338325E+01	-1.014688E+02	-1.169637E+02
-1.201232E+02	1.846268E+01	5.12594E+02	8.235279E+02	.000000E+00			
-6.536520E+02	-6.531456E+02	-6.389111E+02	-6.163503E+02	-5.805661E+02	-5.314536E+02	-4.711419E+02	-4.037703E+02
-3.350413E+02	-2.712689E+02	-2.180214E+02	-1.787402E+02	-1.537808E+02	-1.401121E+02	-1.308327E+02	-1.261681E+02
-3.878747E+01	2.141488E+02	6.078245E+02	7.137864E+02	.000000E+00			
-5.023515E+02	-5.024320E+02	-4.944684E+02	-4.814649E+02	-4.604321E+02	-4.312205E+02	-3.549327E+02	-3.538452E+02
-3.111886E+02	-2.705911E+02	-2.351936E+02	-2.064891E+02	-1.827778E+02	-1.568788E+02	-1.131325E+02	-2.789796E+01
1.138102E+02	3.117109E+02	5.186524E+02	4.901771E+02	.000000E+00			
-2.020124E+02	-2.789231E+02	-2.764831E+02	-2.721145E+02	-2.645342E+02	-2.534676E+02	-2.350216E+02	-2.216443E+02
1.126064E+02	-1.808089E+02	-1.583320E+02	-1.341289E+02	-1.065836E+02	-7.265148E+01	-2.794357E+01	3.272106E+01
5.473984E-01	2.041811E+02	2.735157E+02	2.315450E+02	.000000E+00			
7.298645E-01	5.473984E-01	7.298645E-01	7.298645E-01	7.298645E-01	7.298645E-01	7.298645E-01	7.298645E-01
7.298645E-01	7.298645E-01	7.298645E-01	7.298645E-01	7.298645E-01	7.298645E-01	7.298645E-01	7.298645E-01
7.298645E-01	7.298645E-01	7.298645E-01	7.298645E-01	7.298645E-01	7.298645E-01	7.298645E-01	7.298645E-01
-5.388525E+01	-5.387820E+01	-7.230521E+01	-7.278958E+01	-7.333054E+01	-7.373435E+01	-7.373837E+01	-7.300918E+01
-7.114455E+01	-6.768447E+01	-6.213350E+01	-5.399423E+01	-4.280847E+01	-2.819807E+01	-9.858295E+00	1.219124E+01
3.776487E+01	6.496241E+01	8.625551E+01	6.400463E+01	.000000E+00			
-1.032714E+02	-1.032316E+02	-1.388776E+02	-1.395729E+02	-1.411530E+02	-1.420267E+02	-1.420608E+02	-1.405781E+02
-1.367669E+02	-1.297086E+02	-1.184231E+02	-1.019304E+02	-7.932722E+01	-4.988296E+01	-1.318201E+01	3.056650E+01
7.976737E+01	1.289958E+02	1.615013E+02	1.132115E+02	.000000E+00			
-1.435387E+02	-1.436568E+02	-1.934623E+02	-1.953036E+02	-1.972830E+02	-1.987956E+02	-1.990207E+02	-1.969252E+02
-1.912928E+02	-1.807804E+02	-1.639973E+02	-1.395962E+02	-1.063793E+02	-6.345126E+01	-1.051333E+01	5.146846E+01
1.189829E+02	1.826529E+02	2.185738E+02	1.464104E+02	.000000E+00			
-1.706188E+02	-1.708263E+02	-2.306679E+02	-2.334531E+02	-2.365116E+02	-2.350278E+02	-2.398944E+02	-2.377286E+02
-2.309281E+02	-2.177695E+02	-1.965354E+02	-1.656456E+02	-1.237893E+02	-7.011673E+01	-4.667783E+00	7.060270E+01
1.501719E+02	2.212577E+02	2.557183E+02	1.650289E+02	.000000E+00			
-1.803302E+02	-1.806508E+02	-2.449155E+02	-2.488407E+02	-2.532572E+02	-2.573056E+02	-2.595247E+02	-2.582754E+02
-2.516187E+02	-2.374921E+02	-2.138921E+02	-1.790706E+02	-1.317248E+02	-7.122623E+01	1.876205E+00	8.452577E+01
1.693558E+02	2.413482E+02	2.703626E+02	1.692162E+02	.000000E+00			
-1.650696E+02	-1.695218E+02	-2.311775E+02	-2.362296E+02	-2.421800E+02	-2.480008E+02	-2.522555E+02	-2.531150E+02
-2.484290E+02	-2.358650E+02	-2.131226E+02	-1.782149E+02	-1.297996E+02	-6.757025E+01	7.124181E+00	9.002655E+01
1.725239E+02	2.386885E+02	2.600340E+02	1.584337E+02	.000000E+00			
-1.355081E+02	-1.360790E+02	-1.871253E+02	-1.927695E+02	-1.996694E+02	-2.069481E+02	-2.133281E+02	-2.171215E+02
-2.162533E+02	-2.083408E+02	-1.908680E+02	-1.615086E+02	-1.186343E+02	-6.200152E+01	6.426422E+00	8.152475E+01
1.543793E+02	2.102805E+02	2.250899E+02	1.348011E+02	.000000E+00			
-8.387775E+01	-8.452203E+01	-1.176191E+02	-1.225290E+02	-1.287539E+02	-1.357908E+02	-1.428391E+02	-1.487704E+02
-1.520871E+02	-1.508894E+02	-1.428922E+02	-1.256437E+02	-9.693591E+01	-5.575205E+01	-3.438022E+00	5.509378E+01
1.117539E+02	1.548514E+02	1.665842E+02	1.000982E+02	.000000E+00			
-2.873880E+01	-2.936403E+01	-4.163849E+01	-4.404742E+01	-4.720672E+01	-5.102794E+01	-5.530838E+01	-5.972610E+01
-6.379774E+01	-6.679627E+01	-6.763685E+01	-6.478414E+01	-5.630510E+01	-4.027421E+01	-1.578596E+01	1.528582E+01
4.768112E+01	7.417348E+01	8.506414E+01	5.398312E+01	.000000E+00			
.000000E+00	.000000E+00	.000000E+00	.000000E+00	.000000E+00	.000000E+00	.000000E+00	.000000E+00
.000000E+00	.000000E+00	.000000E+00	.000000E+00	.000000E+00	.000000E+00	.000000E+00	.000000E+00
.000000E+00	.000000E+00	.000000E+00	.000000E+00	.000000E+00	.000000E+00	.000000E+00	.000000E+00

4.447415E+01	5.365844E+01	1.585166E+01	-1.289977E+02	.000000E+00	1.594337E+C1	2.419991E+01	2.558566E+01
.000000E+00	4.001483E+00	8.087498E+CC	1.229838E+01	1.619074E+C1	7.447852E+C1	8.341156E+01	9.161104E+01
3.629777E+01	4.393424E+01	5.168775E+01	5.900409E+01	6.635274E+01			
9.408867E+01	7.317708E+01	-6.125195E+01	-1.816710E+02	.000000E+00			
.000000E+00	-3.868078E+01	-7.508905E+00	-1.079223E+02	-1.344901E+02	-1.512252E+C2	-1.545498E+C2	-1.418101E+02
-1.120631E+02	-6.667315E+01	-9.568711E+00	5.308745E+01	1.139443E+02	1.661068E+02	2.037071E+02	2.202396E+02
2.079497E+02	5.676240E+01	-2.094771E+C2	-2.392325E+C2	.000000E+00			
.000000E+00	-8.654335E+01	-1.689059E+02	-2.441496E+02	-3.071017E+02	-3.520374E+C2	-3.738814E+02	-3.692818E+02
-3.374649E+02	-2.807693E+02	-2.047398E+02	-1.178885E+02	-3.147351E+01	4.073254E+01	7.551935E+01	5.433086E+01
-7.572167E+01	-3.089484E+02	-4.758461E+02	-2.976958E+02	.000000E+00			
.000000E+00	-1.406700E+02	-2.767917E+02	-4.047851E+02	-5.188198E+02	-6.128597E+C2	-6.818697E+02	-7.229282E+02
-7.362085E+02	-7.255982E+02	-6.986833E+02	-6.660067E+02	-6.398136E+02	-6.327979E+02	-6.567641E+02	-7.201281E+02
-8.251856E+02	-8.501942E+02	-6.861803E+02	-2.517352E+02	.000000E+00			
.000000E+00	-1.896571E+02	-3.763765E+02	-5.572607E+02	-7.276717E+02	-8.826922E+C2	-1.017989E+C3	-1.130626E+03
-1.219845E+03	-1.287602E+03	-1.338571E+03	-1.379340E+03	-1.416343E+03	-1.451701E+C3	-1.475672E+03	-1.456473E+03
-1.337459E+03	-1.091213E+03	-7.011010E+C2	-2.404403E+02	.000000E+00			
.000000E+00	-2.149394E+02	-4.286857E+02	-6.396252E+02	-8.445816E+02	-1.035877E+C3	-1.221690E+03	-1.386375E+03
-1.530739E+03	-1.652030E+03	-1.747620E+03	-1.814185E+03	-1.846498E+03	-1.836060E+03	-1.770140E+03	-1.632076E+03
-1.402658E+03	-1.066051E+C3	-6.395190E+02	-2.160580E+C2	.000000E+00			
.000000E+00	3.980614E+01	7.986476E+01	1.203395E+02	1.613177E+C2	2.027352E+C2	2.443104E+02	2.854742E+02
3.253002E+02	3.624434E+02	3.950967E+02	4.209737E+02	4.373268E+02	4.410090E+C2	4.285964E+02	3.966111E+02
3.420188E+02	2.633540E+02	1.639575E+02	6.080399E+01	.000000E+00			
.000000E+00	3.444746E+01	6.925409E+01	1.045782E+C2	1.405059E+02	1.769641E+C2	2.136455E+02	2.495956E+02
2.849144E+02	3.171420E+02	3.448324E+02	3.657638E+02	3.773385E+02	3.766593E+02	3.669266E+02	3.266378E+02
2.727866E+02	2.000551E+02	1.151421E+02	3.637832E+01	.000000E+00			
.000000E+00	2.602231E+01	5.248262E+01	7.957383E+01	1.074341E+02	1.260316E+C2	1.650905E+02	1.546211E+02
2.218672E+02	2.472875E+02	2.685802E+02	2.837467E+02	2.905806E+02	2.867782E+C2	2.701239E+02	2.389229E+02
1.929744E+02	1.349641E+02	7.265779E+01	2.102769E+01	.000000E+00			
.000000E+00	1.442435E+01	2.938584E+01	4.511662E+01	6.184262E+01	7.563665E+01	9.834560E+01	1.175219E+02
1.363748E+02	1.537600E+02	1.682225E+02	1.780979E+02	1.816580E+02	1.772745E+C2	1.636082E+02	1.399774E+02
1.073195E+02	6.909727E+01	3.235465E+01	7.129430E+00	.000000E+00			
.000000E+00	-2.775363E-01	5.090634E-02	1.212859E+00	3.522747E+00	7.204759E+00	1.233589E+01	1.878632E+01
2.616520E+01	3.378378E+01	4.065572E+01	4.556467E+01	4.722914E+01	4.456714E+C1	3.702926E+01	2.502154E+01
1.049882E+01	-2.815433E+00	-9.726333E+00	-6.659998E+00	.000000E+00			
.000000E+00	-1.716295E+01	-3.381292E+01	-4.983201E+01	-6.489109E+01	-7.862297E+C1	-9.063675E+C1	-1.005472E+02
-1.080282E+02	-1.128973E+02	-1.152216E+02	-1.153902E+02	-1.140525E+02	-1.118095E+C2	-1.086485E+02	-1.033523E+02
-9.353255E+01	-7.633154E+01	-5.007075E+01	-1.883813E+C1	.000000E+00			
.000000E+00	-3.345687E+01	-6.679347E+01	-1.002028E+02	-1.335400E+02	-1.664423E+C2	-1.982659E+02	-2.280391E+02
-2.544612E+02	-2.759855E+02	-2.910132E+02	-2.981810E+02	-2.966315E+02	-2.860587E+02	-2.663245E+02	-2.367891E+02
-1.561341E+02	-1.441409E+02	-8.426626E+01	-2.803569E+01	.000000E+00			
.000000E+00	-4.325045E+01	-8.705460E+01	-1.321944E+02	-1.790024E+02	-2.274900E+C2	-2.771912E+02	-3.265973E+02
-3.750058E+02	-4.184328E+02	-4.536587E+02	-4.764983E+02	-4.827701E+02	-4.691332E+C2	-4.339582E+02	-3.777586E+02
-3.027076E+02	-2.127670E+02	-1.176122E+02	-3.644418E+01	.000000E+00			
.000000E+00	-3.554796E+01	-7.242999E+01	-1.112670E+02	-1.527822E+02	-1.574746E+C2	-2.454674E+02	-2.963295E+02
-3.488698E+02	-4.009089E+02	-4.490613E+02	-4.886143E+02	-5.136775E+02	-5.178313E+02	-4.954398E+02	-4.434598E+02

-3.63C791E+02
.CCCCCE+00
.000000E+00
.000000E+00
.000000E+00
.000000E+00
.000000E+00
-2.597532E+02
.000000E+00
.000000E+00
.000000E+00
.000000E+00
.000000E+00
-1.462572E+C2
.000000E+00
.000000E+00
.000000E+00
.000000E+00
.000000E+00
-4.685714E+01
.000000E+00
.000000E+00
.000000E+00
.000000E+00
.000000E+00
T(1,1)...T(31,21)
3.495397E-06
7.695154E-05
5.177224E+04
7.783252E-04
1.955269E-03
1.506630E+02
2.87184CE-02
6.122528E-02
2.202270E+02
5.248538E-01
9.264603E-01
3.955206E+02
6.422473E+00
4.98847E+00
6.177296E+02
5.97374E+01
7.439723E+01
9.353266E+02
4.406950E+02
4.73346E+02
1.536939E+C3
2.664961E+03
2.510136E+03
2.967320E+03
1.306714E+C4
1.117195E+04
6.544982E+03
5.054096E+04
4.138460E+04
1.485732E+C4
1.484046E+05
1.252014E+05
3.228273E+04
3.227506E+05
3.033176E+05
6.311366E+C4
5.307542E+05
5.873684E+05
1.131305E+05
3.406996E-06
1.271062E-C3
3.235763E+05
8.193104E-04
3.420809E-03
3.025189E+C4
2.908460E-02
7.421677E-02
2.545403E+03
1.512554E+03
2.908460E-02
7.421677E-02
2.545403E+03
5.306073E-01
1.066175E+00
3.865630E+03
6.481852E+00
1.041438E+01
5.335430E+03
5.993047E+01
7.813045E+01
6.930285E+C3
4.434953E+02
4.768606E+02
8.768130E+03
2.679380E+03
2.433354E+03
1.117732E+04
1.313308E+04
1.047359E+04
1.511582E+C4
5.081729E+04
3.783737E+04
2.199654E+04
1.494066E+05
1.130617E+05
3.576850E+C4
3.255672E+05
2.747695E+05
5.832360E+04
3.255672E+05
2.747695E+05
5.832360E+04
5.366651E+C5
5.410229E+05
9.221266E+04
3.707045E-06
2.216198E-02
1.546724E+06
8.853089E-04
5.094375E-03
6.188326E+05
3.225529E-02
1.166033E-01
4.775746E+05
5.738845E-01
1.470293E+00
4.576776E+05
6.843161E+00
1.283687E+01
4.700313E+05
6.184987E+01
8.688036E+01
4.936915E+05
4.484357E+02
4.809604E+02
5.223042E+05
2.664593E+03
2.237381E+03
5.505611E+05
1.292740E+04
8.851478E+03
5.852914E+05
4.998930E+04
2.981866E+04
6.006047E+05
1.486647E+05
8.497587E+04
6.882082E+05
3.313884E+05
2.026592E+05
1.082424E+06
3.313884E+05
2.026592E+05
1.082424E+06
5.624808E+05
4.028932E+05
1.345909E+06
4.161366E-06
3.537634E-01
5.189355E+06
9.833987E-C4
1.329515E-02
4.690227E+06
3.509364E-02
1.592966E-01
4.453294E+C6
6.119075E-01
1.777847E+00
4.385143E+C6
7.156796E+00
1.443739E+01
4.388604E+C6
6.352008E+01
9.205595E+01
4.420132E+06
4.530376E+C2
4.822134E+02
4.462839E+06
2.655959E+03
2.127870E+03
4.510352E+C6
1.276979E+04
8.012171E+03
4.564790E+06
4.929865E+04
2.584144E+04
4.631771E+06
1.477733E+05
7.117965E+04
4.786670E+C6
3.352458E+05
1.660939E+05
5.167368E+C6
5.829203E+C5
3.277559E+05
5.58392E+C6
4.820190E-C6
5.063138E+C6
1.232178E-C1
3.503409E-C2
3.206734E-01
6.631308E-C1
2.411907E+C6
1.566233E+C6
1.676140E+C1
6.561487E+C1
9.849964E+01
4.582313E+C2
4.844659E+C2
2.638986E+C3
2.018793E+02
1.253650E+C4
7.205527E+03
4.822071E+C4
2.214681E+C4
1.456681E+C5
5.863324E+04
3.370738E+C5
1.328873E+C5
6.028320E+C5
2.584516E+C5
5.768783E-06
6.408640E+01
1.309884E+01
1.321699E-02
1.138668E+C6
4.438356E-02
1.936052E+00
1.985418E+01
5.157609E-02
1.985418E+01
8.164453E-01
4.155294E+01
8.718040E+00
8.310969E+01
7.106361E+01
2.010087E+02
4.688275E+02
6.075071E+02
2.569306E+03
1.956959E+03
1.175220E+04
5.931459E+03
4.433867E+04
1.609987E+04
1.348253E+05
3.864511E+04
3.232280E+05
8.090060E+04
3.339841E+05
1.043622E+05
6.150108E+05
1.504593E+05

7.090756E+05	7.188928E+05	7.402508E+05	7.769053E+05	8.263311E+05	8.807659E+05	9.272671E+05	5.505715E+05
9.378320E+05	8.834446E+05	7.917186E+05	6.755515E+05	5.515182E+05	4.341975E+05	3.326561E+05	2.502038E+05
1.858518E+05	1.385979E+05	2.354474E+05	1.766377E+06	5.934748E+06			
8.384305E+05	8.524022E+05	8.869792E+05	9.476352E+05	1.032020E+06	1.1256338E+06	1.221966E+06	1.286098E+06
1.300738E+06	1.253270E+06	1.145221E+06	9.927960E+05	8.210281E+05	6.545376E+05	5.096433E+05	3.922390E+05
2.559552E+05	2.035455E+05	2.935527E+05	2.178164E+06	5.935200E+06			
9.331344E+05	9.511018E+05	9.981679E+05	1.081479E+06	1.198567E+06	1.336762E+06	1.473957E+06	1.582509E+06
1.635404E+06	1.613903E+06	1.514521E+06	1.351832E+06	1.154685E+06	9.567557E+05	7.809468E+05	6.322913E+05
4.852531E+05	2.985756E+05	5.400638E+05	2.655721E+06	5.935200E+06			
1.010045E+06	1.031529E+06	1.088544E+06	1.188555E+06	1.328293E+06	1.494079E+06	1.663620E+06	1.809749E+06
1.905952E+06	1.932941E+06	1.884170E+06	1.766743E+06	1.601143E+06	1.417860E+06	1.233248E+06	1.043744E+06
7.851053E+05	3.939107E+05	1.116459E+06	3.193703E+06	5.935200E+06			
1.080623E+06	1.103551E+06	1.164412E+06	1.269827E+06	1.416635E+06	1.593233E+06	1.781239E+06	1.958066E+06
2.100835E+06	2.191275E+06	2.219856E+06	2.186750E+06	2.098170E+06	1.958723E+06	1.766119E+06	1.520481E+06
1.055600E+06	1.179014E+06	2.036500E+06	3.798874E+06	5.935200E+06			
1.154258E+06	1.175066E+06	1.225921E+06	1.324585E+06	1.458060E+06	1.624365E+06	1.813165E+06	2.010390E+06
2.199476E+06	2.363194E+06	2.485310E+06	2.551067E+06	2.546392E+06	2.459478E+06	2.256918E+06	2.131056E+06
2.142720E+06	2.422508E+06	3.136242E+06	4.410170E+06	5.935200E+06			
1.245637E+06	1.259120E+06	1.294602E+06	1.356641E+06	1.446475E+06	1.565582E+06	1.713427E+06	1.888371E+06
2.087346E+06	2.305938E+06	2.538417E+06	2.777359E+06	3.012465E+06	3.228357E+06	3.401934E+06	3.500320E+06
3.554831E+06	3.825617E+06	4.271677E+06	5.014033E+06	5.935200E+06			
1.406871E+06	1.406871E+06	1.406871E+06	1.406871E+06	1.406871E+06	1.406871E+06	1.406871E+06	1.406871E+06
1.406871E+06	1.406871E+06	1.406871E+06	1.406871E+06	1.406871E+06	1.406871E+06	1.406871E+06	1.406871E+06
2.757322E+06	2.761148E+06	2.773917E+06	2.782206E+06	2.790452E+06	2.800415E+06	2.813239E+06	2.825946E+06
2.851579E+06	2.879268E+06	2.914367E+06	2.958854E+06	3.016393E+06	3.054863E+06	3.212158E+06	3.408915E+06
3.798092E+06	4.640331E+06	6.451824E+06	1.013947E+07	1.626798E+07			
3.207775E+06	3.210762E+06	3.220469E+06	3.230277E+06	3.243468E+06	3.262375E+06	3.289392E+06	3.327132E+06
3.378359E+06	3.445959E+06	3.533255E+06	3.644864E+06	3.789244E+06	3.982990E+06	4.260600E+06	4.694864E+06
5.458455E+06	6.902468E+06	9.631520E+06	1.442168E+07	2.107286E+07			
3.327484E+06	3.330259E+06	3.339277E+06	3.353029E+06	3.374766E+06	3.406081E+06	3.457124E+06	3.526258E+06
3.619502E+06	3.740157E+06	3.891572E+06	4.078977E+06	4.314502E+06	4.624101E+06	5.059841E+06	5.722315E+06
6.808566E+06	8.683138E+06	1.150651E+07	1.704966E+07	2.369652E+07			
3.360504E+06	3.364249E+06	3.376527E+06	3.398260E+06	3.434321E+06	3.490326E+06	3.573344E+06	3.685745E+06
3.844240E+06	4.038626E+06	4.272488E+06	4.547213E+06	4.874233E+06	5.286579E+06	5.855696E+06	6.707394E+06
8.042191E+06	1.019902E+07	1.364171E+07	1.874366E+07	2.503187E+07			
3.375419E+06	3.380844E+06	3.398650E+06	3.431861E+06	3.487733E+06	3.575731E+06	3.706410E+06	3.889290E+06
4.129902E+06	4.427300E+06	4.774237E+06	5.162592E+06	5.595781E+06	6.107355E+06	6.782237E+06	7.777661E+06
5.282379E+06	1.159067E+07	1.505635E+07	1.999007E+07	2.566546E+07			
3.286461E+06	3.393946E+06	3.418422E+06	3.465975E+06	3.545480E+06	3.672663E+06	3.862455E+06	4.128682E+06
4.479012E+06	4.910935E+06	5.410870E+06	5.959756E+06	6.547943E+06	7.199447E+06	7.999509E+06	5.107521E+06
1.070154E+07	1.302065E+07	1.631730E+07	2.073170E+07	2.595989E+07			
3.394013E+06	3.403259E+06	3.433345E+06	3.492558E+06	3.594916E+06	3.759207E+06	4.006804E+06	4.357545E+06
4.824174E+06	5.406989E+06	6.091371E+06	6.851277E+06	7.661646E+06	8.521216E+06	9.482237E+06	1.067147E+07
1.226434E+07	1.446209E+07	1.746120E+07	2.139431E+07	2.609094E+07			

3.395665E+06	3.405487E+06	3.437397E+06	3.501316E+06	3.613208E+06	3.752333E+06	4.073756E+06	4.475427E+06
5.021635E+06	5.722715E+06	6.573977E+06	7.555459E+06	8.636866E+06	9.788871E+06	1.100162E+07	1.230784E+07
1.387508E+07	1.588638E+07	1.852366E+07	2.195796E+07	2.615204E+07	3.130777E+06	3.975563E+06	4.337209E+06
3.389088E+06	3.397350E+06	3.424282E+06	3.478352E+06	3.573698E+06	3.635669E+06	3.731401E+06	3.948686E+06
4.844132E+06	5.519400E+06	6.376798E+06	7.418684E+06	8.635669E+06	1.000723E+07	1.150276E+07	1.308518E+07
1.479170E+07	1.677615E+07	1.921145E+07	2.231454E+07	2.617683E+07	3.085548E+06	3.934601E+06	4.092369E+07
3.378047E+06	3.383307E+06	3.400382E+06	3.438399E+06	3.491631E+06	3.585548E+06	3.731401E+06	3.948686E+06
4.259613E+06	4.687600E+06	5.255606E+06	5.984868E+06	6.894636E+06	8.003653E+06	9.334601E+06	1.092369E+07
1.283851E+07	1.518814E+07	1.811242E+07	2.177403E+07	2.617446E+07	3.130777E+06	3.975563E+06	4.337209E+06
SF(1,1)...SF(31,21)							
.000000E+00	.000000E+00	.000000E+00	.000000E+00	.000000E+00	.000000E+00	.000000E+00	.000000E+00
.000000E+00	.000000E+00	.000000E+00	.000000E+00	.000000E+00	.000000E+00	.000000E+00	.000000E+00
.000000E+00	.000000E+00	.000000E+00	.000000E+00	.000000E+00	.000000E+00	.000000E+00	.000000E+00
.000000E+00	.000000E+00	.000000E+00	.000000E+00	.000000E+00	.000000E+00	.000000E+00	.000000E+00
-1.878569E+00	-2.763921E-02	-1.108687E-01	-2.505503E-01	-4.481759E-01	-7.055832E-01	-1.027141E+00	-1.416017E+00
-1.032565E+01	-2.422901E+00	-3.060085E+00	-3.805385E+00	-4.680109E+00	-5.714486E+00	-6.952208E+00	-8.457599E+00
-1.032565E+01	-1.267874E+01	-1.542704E+01	-1.542543E+01	.000000E+00	.000000E+00	.000000E+00	.000000E+00
-3.922210E+00	-5.854513E-02	-2.347553E-01	-5.300263E-01	-9.468746E-01	-1.488467E+00	-2.160139E+00	-2.968442E+00
-1.916731E+01	-5.032993E+00	-6.315781E+00	-7.789923E+00	-9.480276E+00	-1.141859E+01	-1.364505E+01	-1.620939E+01
.000000E+00	-2.253579E+01	-2.587929E+01	-2.488746E+01	.000000E+00	.000000E+00	.000000E+00	.000000E+00
.000000E+00	-8.766349E-02	-3.512246E-01	-7.920587E-01	-1.412516E+00	-2.316086E+00	-3.267607E+00	-4.353541E+00
-5.782291E+00	-7.384573E+00	-9.213820E+00	-1.128660E+01	-1.362300E+01	-1.624692E+01	-1.918603E+01	-2.247054E+01
-2.612373E+01	-3.008661E+01	-3.363662E+01	-3.138792E+01	.000000E+00	.000000E+00	.000000E+00	.000000E+00
.000000E+00	-1.149763E-01	-4.602233E-01	-1.036529E+00	-1.845290E+00	-2.888671E+00	-4.169807E+00	-5.653040E+00
-7.464178E+00	-9.490761E+00	-1.178230E+01	-1.435046E+01	-1.720916E+01	-2.037452E+01	-2.386446E+01	-2.765679E+01
-3.187520E+01	-3.628284E+01	-3.993589E+01	-3.644811E+01	.000000E+00	.000000E+00	.000000E+00	.000000E+00
.000000E+00	-1.415132E-01	-5.658488E-01	-1.272593E+00	-2.261230E+00	-3.531315E+00	-5.082917E+00	-6.916571E+00
-9.033966E+00	-1.143808E+01	-1.413350E+01	-1.712661E+01	-2.042570E+01	-2.404093E+01	-2.798392E+01	-3.226537E+01
-3.687636E+01	-4.164970E+01	-4.535546E+01	-4.068066E+01	.000000E+00	.000000E+00	.000000E+00	.000000E+00
.000000E+00	-1.654381E-01	-6.766260E-01	-1.519038E+00	-2.692842E+00	-4.193256E+00	-6.015022E+00	-8.152559E+00
-1.060258E+01	-1.336059E+01	-1.642554E+01	-1.979811E+01	-2.348138E+01	-2.748089E+01	-3.180431E+01	-3.645852E+01
-4.142600E+01	-4.645507E+01	-5.020852E+01	-4.439052E+01	.000000E+00	.000000E+00	.000000E+00	.000000E+00
.000000E+00	-2.023796E-01	-8.067628E-01	-1.806871E+00	-3.193003E+00	-4.552732E+00	-7.071844E+00	-9.535461E+00
-1.232928E+01	-1.544080E+01	-1.886034E+01	-2.258183E+01	-2.660318E+01	-3.092630E+01	-3.555648E+01	-4.049845E+01
-4.572743E+01	-5.098893E+01	-5.461434E+01	-4.767278E+01	.000000E+00	.000000E+00	.000000E+00	.000000E+00
.000000E+00	-2.464188E-01	-9.800253E-01	-2.187701E+00	-3.848957E+00	-5.537307E+00	-8.422153E+00	-1.127120E+01
-1.445323E+01	-1.794084E+01	-2.171267E+01	-2.575478E+01	-3.006106E+01	-3.463280E+01	-3.947742E+01	-4.460383E+01
-4.999032E+01	-5.536073E+01	-5.887678E+01	-5.083165E+01	.000000E+00	.000000E+00	.000000E+00	.000000E+00
.000000E+00	-3.104096E-01	-1.231168E+00	-2.737149E+00	-4.788409E+00	-7.322578E+00	-1.030850E+01	-1.365154E+01
-1.730011E+01	-2.120214E+01	-2.531988E+01	-2.963211E+01	-3.413350E+01	-3.883170E+01	-4.374248E+01	-4.888018E+01
-5.421573E+01	-5.941704E+01	-6.241799E+01	-5.320110E+01	.000000E+00	.000000E+00	.000000E+00	.000000E+00
.000000E+00	-4.040566E-01	-1.598828E+00	-3.540497E+00	-6.157300E+00	-9.352361E+00	-1.301001E+01	-1.700717E+01
-2.122856E+01	-2.558191E+01	-3.000868E+01	-3.448766E+01	-3.903170E+01	-4.368009E+01	-4.848979E+01	-5.352541E+01
-5.882017E+01	-6.409276E+01	-6.707186E+01	-5.678192E+01	.000000E+00	.000000E+00	.000000E+00	.000000E+00

.000000E+00	-5.903224E-02	-2.384484E-01	-5.433192E-01	-9.807094E-01	-1.557825E+00	-2.279108E+00	-3.142242E+00
-4.133248E+00	-5.221071E+00	-6.352386E+00	-7.447550E+00	-8.398859E+00	-9.072272E+00	-9.314318E+00	-8.568440E+00
-7.510605E+00	-6.105229E+00	-3.714757E+00	-1.286512E+00	.000000E+00			
.000000E+00	-4.731345E-02	-1.918993E-01	-4.393091E-01	-7.975822E-01	-1.275682E+00	-1.880929E+00	-2.615343E+00
-3.470928E+00	-4.424108E+00	-5.429822E+00	-6.416303E+00	-7.282268E+00	-7.899079E+00	-8.120812E+00	-7.805601E+00
-6.852285E+00	-5.248792E+00	-3.162845E+00	-1.083864E+00	.000000E+00			
.000000E+00	-2.928635E-02	-1.196112E-01	-2.756771E-01	-5.045935E-01	-8.149866E-01	-1.215407E+00	-1.711910E+00
-2.304654E+00	-2.983648E+00	-3.722815E+00	-4.474210E+00	-5.162557E+00	-5.684219E+00	-5.915314E+00	-5.734128E+00
-5.059507E+00	-3.887204E+00	-2.348073E+00	-8.091169E-01	.000000E+00			
.000000E+00	-1.003438E-02	-4.173250E-02	-9.726093E-02	-1.801322E-01	-2.950050E-01	-4.472661E-01	-6.423445E-01
-8.84650E-01	-1.175938E+00	-1.512600E+00	-1.881630E+00	-2.255088E+00	-2.584461E+00	-2.798708E+00	-2.813471E+00
-2.561618E+00	-2.026410E+00	-1.264174E+00	-4.560396E-01	.000000E+00			
.000000E+00	.000000E+00	.000000E+00	.000000E+00	.000000E+00	.000000E+00	.000000E+00	.000000E+00
.000000E+00	.000000E+00	.000000E+00	.000000E+00	.000000E+00	.000000E+00	.000000E+00	.000000E+00
.000000E+00	.000000E+00	.000000E+00	.000000E+00	.000000E+00	.000000E+00	.000000E+00	.000000E+00
VG(1)...VG(21)							
1.884517E-37	4.180647E+01	8.375581E+01	1.260429E+02	1.687858E+02	2.119452E+02	2.552647E+02	2.982064E+02
3.398825E+02	3.789929E+02	4.137776E+02	4.420003E+02	4.605725E+02	4.676224E+02	4.585959E+02	4.303634E+02
3.793518E+02	3.024777E+02	1.997301E+02	8.398052E+01	1.884517E-37			
UL(1)...UL(21)							
5.176800E-05	4.222789E-05	1.678685E-05	-2.725246E-05	-9.368162E-05	-1.868194E-04	-3.115143E-04	-4.727127E-04
-6.749414E-04	-9.217645E-04	-1.215196E-03	-1.584897E-03	-1.936269E-03	-2.344234E-03	-2.734328E-03	-2.992454E-03
-3.067164E-03	-3.275801E-03	-3.664573E-03	-4.355241E-03	.000000E+00			
HL(1)...HL(21)							
1.925877E-04	2.701233E-04	2.840120E-04	2.860186E-04	2.849335E-04	2.828131E-04	2.802910E-04	2.779480E-04
2.756607E-04	2.772220E-04	2.760033E-04	2.478657E-04	2.378216E-04	2.107919E-04	1.759380E-04	1.403507E-04
1.144092E-04	9.059505E-05	6.992228E-05	5.330813E-05	3.424333E-04			
HG(1)...HG(11)							
2.057539E-05	6.322576E-06	4.800074E-06	4.094149E-06	3.589955E-06	3.196971E-06	2.881997E-06	2.621537E-06
2.393444E-06	2.250477E-06	2.493679E-06					
NUL =	44.996140,	NUG =	4.295404,	RMAX =	9.006338E-03,	R1(C) =	.261686
NE1 =	2,	NE2 =	6,	RAL =	2.859151E+08,	RAG =	2.870898E+05
CL =	.346032,	CG =	.185567,	RP =	1.015559,	R1(C) =	.261686
SFI(1)...SFI(21)							
1.884517E-37	1.916388E-04	7.665551E-04	1.724749E-03	3.066220E-03	4.790369E-03	6.898996E-03	9.390300E-03
1.226488E-02	1.552274E-02	1.916388E-02	2.318829E-02	2.759598E-02	3.238695E-02	3.756120E-02	4.311872E-02
4.905553E-02	5.538361E-02	6.209096E-02	6.918160E-02	1.884517E-37			

REFERENCES

1. Clark, J. A. A Review of Pressurization, Stratification and Interfacial Phenomena: International Advances in Cryogenic Engineering, Vol. 10, pp. 259-284, 1966.
2. Thomas, P.D. and Morse, F.H. Analytical Solution for the Phase Change in a Suddenly Pressurized Liquid-Vapor System: Advances in Cryogenic Engineering, Vol. 8, pp. 550-562, 1964.
3. Knuth, E.L. Evaporation and Condensation of One Component Systems: Journal of the American Rocket Society: Vol. 32, pp. 1424-1426, 1962.
4. Yang, W.J. Phase Change of One-Component System in a Container: AIChE Paper No. 63-A48, presented at the 6th National Heat Transfer Conference, Boston, Mass., August 1963.
5. Yang, W.J. and Clark, J.A. On the Application of the Source Theory on Problems Involving Phase Change—Part 2: J. Heat Transfer, Trans. ASME, Ser. C. Vol. 86, pp. 443, 1964.
6. Yang, W.J., Larsen, P.S. and Clark, J.A. Interfacial Heat and Mass Transfer in a Suddenly Pressurized, Binary Liquid-Vapor System: Trans. ASME, J. Eng. for Ind., Vol. 87, pp. 413, 1965.
7. O'Loughlin, J.R. and Glenn, H. Bulk Liquid Mass Transfer with Variable Ullage Pressure: Proceedings of the Conference on Propellant Tank Pressurization and Stratification, NASA MSFC, Jan. 20-21, Vol. 1, 1965.
8. Epstein, M., Georgius, H.K. and Anderson, R.E. Generalized Propellant Tank Pressurization Analysis: International Advances in Cryogenic Engineering, Vol. 10, 1966.
9. Huntley, S.C. Temperature-Pressure-Time Relations in a Closed Cryogenic Container: Advances in Cryogenic Engineering, Vol. 3, p. 342, 1960.
10. Leibenberg, D.H. and Edescuty, F.J. Pressurization Analysis of a Large Scale Hydrogen Dewar: International Advances in Cryogenic Engineering, Vol. 10, 1966.
11. Van Wylen, G.J. Thermodynamics: John Wiley and Sons, Inc. pp. 425, 1960.
12. Barakat, H.Z. and Clark, J.A. Analytical and Experimental Studies of the Transient Laminar Natural Convection Flows in Partially Filled Liquid Containers: Proceedings, Third International Heat Transfer Conference, Vol. II, Chicago, Ill., Aug. 7-12, 1966.

REFERENCES (Concluded)

13. Jacob, M. Heat Transfer, Vol. I: John Wiley and Sons, Inc. Chap. 29.
14. Swim, R.T. Temperature Distribution in Liquid and Vapor Phases of Helium in Cylindrical Dewars: Advances in Cryogenic Engineering, Vol. 5, 1960.
15. Brenteri, E.G., Giarratano, P.J. and Smith, R.V.: Boiling Heat Transfer for Oxygen, Nitrogen, Hydrogen and Helium: NBS Technical Note No. 317, Sept. 1965.
16. Barakat, H.Z. and Clark, J.A. Transient Natural Convection Flows in Closed Containers: Technical Report 04268-10-T, Office of Research Administration, University of Michigan, Ann Arbor, Michigan, Contract NAS 8-825, Marshall Space Flight Center, Aug. 1965.

